

**RETENTION OF IODINE
AND OTHER AIRBORNE RADIONUCLIDES
IN NUCLEAR FACILITIES
DURING ABNORMAL AND ACCIDENT CONDITIONS**

FINAL REPORT
OF A CO-ORDINATED RESEARCH PROGRAMME
SPONSORED BY THE
INTERNATIONAL ATOMIC ENERGY AGENCY
FROM 1983 TO 1988



A TECHNICAL DOCUMENT ISSUED BY THE
INTERNATIONAL ATOMIC ENERGY AGENCY, VIENNA, 1989

The IAEA does not normally maintain stocks of reports in this series.
However, microfiche copies of these reports can be obtained from

INIS Clearinghouse
International Atomic Energy Agency
Wagramerstrasse 5
P.O. Box 100
A-1400 Vienna, Austria

Orders should be accompanied by prepayment of Austrian Schillings 100,—
in the form of a cheque or in the form of IAEA microfiche service coupons
which may be ordered separately from the INIS Clearinghouse.

**PLEASE BE AWARE THAT
ALL OF THE MISSING PAGES IN THIS DOCUMENT
WERE ORIGINALLY BLANK**

**RETENTION OF IODINE AND OTHER AIRBORNE RADIONUCLIDES
IN NUCLEAR FACILITIES
DURING ABNORMAL AND ACCIDENT CONDITIONS**
IAEA, VIENNA, 1989
IAEA-TECDOC-521
ISSN 1011-4289

Printed by the IAEA in Austria
September 1989

FOREWORD

The design of the ventilation and air cleaning systems to prevent radioactive contamination of working areas and surroundings under normal and accident conditions is a vital part in the general design of all nuclear facilities. Under the abnormal conditions arising in nuclear facilities, the gas-borne nuclides of main concern are radioiodine and radioactive particulates presenting a complex problem with concentration, chemical form and physical properties requiring retention technology different from normal operation.

Extensive research efforts have been undertaken in the world scientific community advancing the status of systems to maintain high air cleaning efficiency under the extreme abnormal conditions. The IAEA Co-ordinated Research Programme to upgrade technology in the area started in 1983 on the recommendations of a previous programme and the development covering a five year term is described in this document. Research laboratories from ten Member States participated, Belgium, German Democratic Republic, Hungary, India and Yugoslavia for three years with Austria, Canada , Federal Republic of Germany, Republic of Korea and UK for lesser periods. Research co-ordination meetings were held in Belgium (1984), Canada (1986) and Hungary (1988).

The IAEA wishes to express thanks to the participants in the programme. The IAEA officers responsible for the meetings in turn were S. Gorbunov, W. Bähr and V. Friedrich and the final report was the responsibility of G. Plumb, Division of Nuclear Fuel Cycle.

EDITORIAL NOTE

In preparing this material for the press, staff of the International Atomic Energy Agency have mounted and paginated the original manuscripts as submitted by the authors and given some attention to the presentation.

The views expressed in the papers, the statements made and the general style adopted are the responsibility of the named authors. The views do not necessarily reflect those of the governments of the Member States or organizations under whose auspices the manuscripts were produced.

The use in this book of particular designations of countries or territories does not imply any judgement by the publisher, the IAEA, as to the legal status of such countries or territories, of their authorities and institutions or of the delimitation of their boundaries.

The mention of specific companies or of their products or brand names does not imply any endorsement or recommendation on the part of the IAEA.

Authors are themselves responsible for obtaining the necessary permission to reproduce copyright material from other sources.

CONTENTS

1. INTRODUCTION	7
2. SCIENTIFIC BACKGROUND	10
3. SCOPE AND OUTLINE OF THE CO-ORDINATED RESEARCH PROGRAMME	13
4. CONCLUSIONS	18
4.1. HEPA filtration	18
4.2. Activated carbon adsorbers	18
5. RECOMMENDATIONS	21

CONTRIBUTIONS OF THE PARTICIPANTS

Application of a new technology for the quality assurance testing of ultra efficient particulate air filters	25
<i>J.P. Deworm, W. Slegers</i>	
Filter testing under special conditions	37
<i>W. Ullmann, P. Hamel, W. Schulz</i>	
Investigations on the ageing of activated carbons in the exhaust air of a pressurized water reactor (PWR 4)	63
<i>H. Deuber, K. Gerlach, R. Kaempffer</i>	
Investigation of the influence of accident conditions on the performance of HEPA filter and iodine trapping systems	75
<i>V. Friedrich</i>	
Evaluation of high efficiency particulate air (HEPA) and iodine filters under high temperature, humidity and radiation	113
<i>K. Ramarathinam, S. Kumar, K.G. Gandhi, S. Ramachandran</i>	
Experimental, analytical and numerical study on the removal efficiency of a charcoal bed for methyl-iodide under humid conditions (<i>Summary</i>)	143
<i>Soon Heung Chang</i>	
The ageing and poisoning of charcoal used in nuclear power plant air cleaning systems (<i>Abstract</i>)	149
<i>D. Broadbent</i>	
The effects of temperature and humidity on the ageing of TEDA impregnated charcoals	151
<i>B.H.M. Billinge, D. Broadbent</i>	
Removal of ^{131}I from off-gas stream at Krško nuclear power plant	169
<i>L. Vujišić</i>	
List of Participants	179

1. INTRODUCTION

All work involving the handling of radioactive material may cause the air to become contaminated. Releases from nuclear facilities to the atmosphere during normal operation are usually small and account for a very minor fraction of the total radiation exposure of the public. However without adequate design, in abnormal or accident conditions the release of airborne radioactive material - and hence the exposure of the local population and of workers - could be much higher.

The techniques adopted for reducing the quantity of radioactive airborne material discharged from nuclear facilities vary in detail, depending on the type of plant concerned; generally, they involve the use of particulate filtration systems and gaseous sorption systems. These cleaning systems must be properly designed and operated so that the prescribed release limits will not be exceeded. Radioactive off-gas cleaning technologies currently employed for normal conditions in the nuclear facilities have been developed to operate efficiently where the form and quantity of radionuclides and other contaminants are well known. The state-of-the-art of nuclear air cleaning technologies, the design, operation, testing and monitoring of air cleaning systems and the components have been described in detail in the IAEA Technical Reports Series (see refs. [1-10]).

Under abnormal and accident conditions in nuclear facilities (especially in nuclear power plants and fuel reprocessing facilities), the airborne radioactive materials of primary concern are iodine and radioactive particulates. These present a complex set of technological problems since the concentration, chemical form and physical characteristics may require recovery/retention technology different from those employed under normal operating conditions. Also the physico-chemical conditions (temperature, air humidity, pressure transient, and concentration) of other airborne contaminants can be very different from those which exist under normal operating conditions.

In the world scientific community, extensive research efforts are being directed to investigations on the behaviour of high efficiency filter materials and air cleaning devices under extreme conditions and on the development of advanced processes and technologies for iodine and particulate retention under abnormal and accident conditions. The participants of an IAEA

Co-ordinated Research programme on "Comparison of High Efficiency Particulate Filter Testing Methods" [11], which was terminated in 1982, recommended the sponsoring of basic filtration research to promote the development of more effective and reliable filtration units for accident conditions.

Recognizing the current status of this technology and the expanding base of nuclear power plants and reprocessing facilities, the IAEA, in accordance with the recommendations of the participants of the previous programme, initiated a new Co-ordinated Research Programme on "Retention of Iodine and Other Airborne Radionuclides in Nuclear Facilities During Abnormal and Accident Conditions". The programme started in 1983 and terminated in 1988. Research laboratories from 10 Member States were participating in the programme. Five laboratories (from Belgium, GDR, Hungary, India and Yugoslavia) had been participating for three years with five other laboratories (from Austria, Canada, FRG, Republic of Korea and UK) participating for one or two years. The chief scientific investigators met in three research co-ordination meetings (SCK/CEN Mol, Belgium 1984, Ontario Hydro, Toronto, Canada 1986, and the Institute of Isotopes of Hungarian Academy of Sciences, Budapest, Hungary, 1988) to discuss the results, to co-ordinate future work and finally, to draw up conclusions and recommendations.

This final report consists of a brief scientific background (Chapter 2), the scope of the Co-ordinated Research Programme including the scientific projects of the individual participants (Chapter 3), some conclusions (Chapter 4), and recommendations drawn up by the chief investigators during the final meeting (Chapter 5), and a collection of the scientific reports of the participants which represents the essential part of this document (Chapter 6).

References

- [1] Design and operation of off-gas cleaning and ventilation systems in facilities handling low- and intermediate- level radioactive material Technical Reports Series No. 292 (1988)
- [2] Treatment of off-gas from radioactive waste incinerators Technical Reports Series (in press)
- [3] Design and operation of off-gas cleaning systems at high level liquid waste conditioning facilities Technical Reports Series No. 291 (1988)

[4] Treatment, conditioning and disposal of iodine-129	Technical Reports Series No. 276	(1987)
[5] Design of off-gas and air cleaning systems at nuclear power plants	Technical Reports Series No. 274	(1987)
[6] Testing and monitoring of off-gas clean-up systems at nuclear facilities	Technical Reports Series No. 243	(1984)
[7] Control of semivolatile radionuclides in gaseous effluents at nuclear facilities	Technical Reports Series No. 220	(1982)
[8] Handling of tritium-bearing wastes	Technical Reports Series No. 203	(1981)
[9] Radioiodine removal in nuclear facilities: methods and techniques for normal and emergency situations	Technical Reports Series No. 201	(1980)
[10] Separation, storage and disposal of krypton-85	Technical Reports Series No. 201	(1980)
[11] Comparison of methods for testing of particulate filters	IAEA-TECDOC-355	(1985)

2. SCIENTIFIC BACKGROUND

Currently employed radioactive off-gas and air cleaning technologies for routine operating conditions for nuclear power plants and, to a lesser extent, fuel reprocessing facilities are fairly well developed since experience has been accumulated over many years of normal operation. For the range of normal operations occurring in the different nuclear facilities, reliable data has been obtained on source terms covering arisings, physical and chemical characteristics of the aerosols and volatile contaminants. The properties of the various filter materials and adsorption systems have been evaluated and there is a high degree of confidence in the design of the air cleaning systems for normal situations.

Any process involving radioactive materials may give rise to contamination in the form of radioactive gases, vapours and aerosols to an extent which will depend on the nature of the process and the radioactive materials involved. The most important volatile contaminants are fission product noble gases, fission product iodine isotopes in the form of elemental iodine or organic iodides and submicron aerosols which can bear a great variety of fission products (mainly iodine isotopes) and activated corrosion products (e.g. Co, Cs, Fe isotopes). For these contaminants the basic air cleaning processes are high efficiency particulate filtration (for aerosols) and adsorption (for iodine retention and noble gas delaying).

The basic component of the aerosol filtration train is the High Efficiency Particulate Air (HEPA) filter. It has a high performance efficiency for removing submicron particles. The service life of HEPA filters is determined by the pressure drop, and in particular cases by the radiation level on the filter, rather than by a fall-off in removal efficiency. Since HEPA filters have relatively low dust holding capacity, prefilters are often used upstream from HEPA filters to prolong service life. The filtering medium, or paper, consists of very fine fibres in a matrix of larger diameter fibres. The most widely used material is fibre-glass held together by an organic binder.

Adsorbers containing activated charcoal, which has a large specific surface area (of the order of $10^3 \text{ m}^2/\text{g}$), are used for removal of radioiodine from air or gas streams in nuclear power plants. The activated charcoal can be impregnated with chemicals to enhance the removal efficiency for organic iodides. These chemicals are usually either I_2 , KI or triethylenediamine (TEDA).

The base charcoal can be obtained from coconut or other nut shell, wood, bituminous coal, petroleum sludge or animal bones. Coconut and coal were preferred because they contain impurities which improve the adsorption efficiency.

The most important characteristics of HEPA filters are the removal efficiency and pressure drop. Both characteristics are strongly influenced by the operating conditions (temperature, air humidity, particle size distribution of the aerosols, air flow rate, pressure transients). In the case of the charcoal adsorbers, the removal efficiency and the break-through of different iodine species are significantly affected by the physical and chemical characteristics of the air stream to be filtered.

It is obvious that any changes in one or more of the airstream parameters occurring in abnormal operation of the nuclear facility can lead to efficiency loss of the air cleaning system causing unacceptable radioactive release. The proper set of technologies necessary to accommodate the postulated process abnormality or accident condition must be developed and integrated into the overall off-gas cleaning system so as to minimize efficiency losses and thereby to minimize radioactive releases. R & D investigations are required as follows:

- to characterize the radioactive materials expected to be released from the various classes of postulated accidents;
- to obtain the necessary technological data to adequately understand mechanisms of iodine retention for the specific chemical forms released under varying conditions;
- to determine the extent to which existing retention systems need to be modified to adequately handle off-gas releases from the wide range of abnormal and accident conditions;
- to develop special new technology particulate equipment capable of high efficiency operation under abnormal/accident conditions (high temperature and relative humidity, large volumes of off-gases and pressure transients); and
- to review and expand the scope of technical data on the use of inorganic and other sorbents for radioiodine and determine the effectiveness under varying conditions.

Since there has been far less field experience on the performance of air cleaning systems under abnormal or accident conditions, extensive research efforts are needed involving relevant laboratory experiments and theoretical investigations of the influence of various air stream parameters on the removal mechanism of particulate filters and adsorbers.

The development of filter testing methods which can be used reliably under high temperature and high humidity conditions is also necessary. Most of the test aerosols used for HEPA filter testing are either not stable at high temperatures or react with water vapour. The detection method can also be disturbed by a high moisture content in the air. In the case of charcoal adsorbers the long term effect of air humidity on the performance of the adsorbent can invalidate the test results through parallel vapour adsorption and chemical reaction with charcoal impregnants. Theoretical developments in this area are also necessary.

More detailed descriptions of the various existing nuclear air cleaning systems and components as well as filter testing methods can be found in the references given in Chapter 1.

3. SCOPE AND OUTLINE OF THE CO-ORDINATED RESEARCH PROGRAMME

The Co-ordinated Research Programme was intended to promote the exchange of information making results of current investigations in various laboratories available to each participant in a timely manner and to review the work in progress in the field of gaseous waste treatment technology with particular reference to iodine retention and collection of particulate matter under abnormal operating events. The main topics investigated by the participating laboratories were the following:

- Theoretical models and experimental studies of removal mechanism of organic and oxygenated iodine species by different sorbents;
- Studies of physical/mechanical/chemical properties of alternative adsorbents for radioactive iodine removal;
- Influence of different parameters (temperature, relative humidity, face velocity, etc) on removal efficiency of iodine trapping systems;
- Changes in performance of iodine trapping equipment due to the degradation of sorbent materials (ageing, weathering, poisoning of impregnated charcoals);
- Investigation of behaviour of HEPA filters subjected to simulated accident conditions and
- Development of new sensitive methods and equipment for testing off-gas cleaning system components, including methods capable of demonstrating compliance with more stringent criteria in terms of performance requirements under more severe in-plant conditions.

The summary record of the Research Coordination Meetings is as follows:

Meeting No. 1

Dates:	24 - 28 September 1984
Location:	SCK/CEN, Mol, Belgium
Hosts:	Government of Belgium
Responsible Officer:	Mr. S. Gorbunov
Visit:	Mol Laboratories
Attendees:	Mr. P. Patek, Austria Mr. J. Deworm, Belgium Mr. W. Ullmann, DDR Mr. H. Deuber, FRG Mr. V. Friedrich, Hungary Mr. K. Ramarathinam, India Mr. Soon Chang, S. Korea

Meeting No. 2

Dates: 2 - 6 June 1986
Location: Ontario Hydro, Toronto, Canada
Hosts: Government of Canada
Responsible Officer: Mr. W. Baehr
Visit: Bruce Power Station
Attendees:
Mr. J. Deworm, Belgium
Mr. W. Ullmann, DDR
Mr. V. Friedrich, Hungary
Mr. K. Gandhi, India
Mr. D. Broadbent, UK
Ms. L. Vujisic, Yugoslavia
Mr. M. Kabat, Canada
Mr. Soon Chang, S. Korea

Meeting No. 3

Dates: 25 - 29 April 1988
Location: Institute of Isotopes, Hungarian Academy of Sciences
Hosts: Government of Hungary
Responsible Officer: Mr. V. Friedrich
Visit: Paks Nuclear Power Station
Attendees:
Mr. W. Slegers, Belgium
Mr. W. Ullmann, DDR
Ms. Z. Koppány, Hungary
Mr. K. Ramarathinam, India
Mr. B. Billinge, UK
Ms. L. Vujisic, Yugoslavia
Mr. M. Kabat, Canada
Mr. Soon Chang, S. Korea

The scientific projects of the individual participants are listed below:

Austria

Peter R.M. Patek +

The behaviour of HEPA and ceramic filters during abnormal conditions in an incineration plant was investigated. The influence of pressure peaks, high temperature and the presence of acids in the off-gas were studied during the

+ Peter R. M. Patek died during the course of the programme.

operation of the incinerator plant. The service life of the electrostatic filters was observed to decrease. Abnormal behaviour of the ceramic filter candles and corrosion effects in the HEPA filter housings were observed. The reasons for the abnormalities were investigated.

Belgium

J.P. Deworm

The aim of the project was to develop related HEPA filter test methods with the source term related to normal and accident conditions. The HEPA filter testing method using heterodisperse liquid test aerosol and "Single Particle Laser Particle Size Spectrometer" (SPLPSS) was developed. Laboratory and in-situ testing of HEPA and ultra efficient particulate air filters (ULPA) were performed for quality assurance purpose. The penetration of ultra-fine particles through HEPA filters was also investigated based on the theory of resuspension due to the recoil energy of a captured particle bearing alpha-active isotopes.

German Democratic Republic

W. Ullmann

The project consisted of the following activities:

- o Testing of filter materials on the laboratory scale;
 - Modification of the existing test stand for the investigation of filter materials under high temperature and high humidity
 - Selection of a suitable test aerosol and a sensitive detection method for temperatures up to 150°C and humidities up to 60%.
 - Preliminary experimental investigations under ambient and special conditions
 - Testing of selected filter materials in accordance with the conclusions of the Second Meeting of Coordinated Research Programme, Toronto, 2-6 June 1986.

- o Testing of full-size filters in laboratory rig;
 - Modification of the existing test stand for the investigation of full-size filters under high humidity
 - Preliminary experimental investigations in connection with the testing of a special full-size filter for filtration of liquid and solid aerosols, Soviet FARTOS Z-500, type.

Federal Republic of Germany

H. Deuber

The influence of ageing of various activated carbons on the retention efficiency for methyl-iodide was investigated.

Hungary

V. Friedrich

The influence of higher temperature and relative humidity on the resistance and removal efficiency of a perchlorvinyl-based fibrous HEPA filter material was investigated. Theoretical and experimental investigations on the removal mechanism of activated carbon adsorbents were performed. The applicability of K_2CO_3 aerosol produced by nozzle-type atomizer for in-situ testing of HEPA filter systems was investigated. The particle size distribution of the K_2CO_3 aerosol was determined by cascade impactor and a centrifugal aerosol spectrometer which was developed at the Institute. The influence of temperature and relative humidity on the removal efficiency of activated carbon for methyl-iodide was also investigated using the continuous air flow apparatus developed at the Institute.

India

K. Ramarathinam

The research work was carried out on:

- Evaluation of micro glass fibre filter media under conditions of high temperature, humidity and gamma radiation;
- Performance of impregnated activated charcoal in respect of their removal and retention of radioiodine under high temperature, humidity,

gamma radiation and washout of impregnants due to bulk condensation of water vapour and

- Evaluation of prototype units of HEPA and iodine filters, to ascertain the overall performance under exposure to air streams of high temperature, humidity and gamma radiation.

Republic of Korea

Soon Heung Chang

A theoretical adsorption model was developed to predict the time dependent removal efficiency of Triethylenediamine (TEDA) impregnated charcoal for methyl-iodide under various operating conditions. The time-dependent break-through of methyl-iodide was studied in laboratory experiments. A mathematical model and the corresponding numerical solution was also developed.

United Kingdom

D. Broadbent and B. Billinge

The role of oxidative ageing and hydrocarbon poisoning was investigated in the overall weathering of both potassium iodide and triethylene diamine impregnated charcoal used in filters on air cleaning systems. The causes of the ageing of TEDA carbons and the possibility of using these at temperatures higher than ambient was also examined.

Yugoslavia

L. Vujisic

The concentration ratio of different radioiodine species (molecular iodine, organic iodides) was investigated in different ventilation and air cleaning systems of the Krsko Nuclear Power Plant. A new filter material for trapping iodine species has been developed. The performance of the new fibrous carbon material (FCM) and the impregnated version (FCM-TEDA) was studied in laboratory experiments under high temperature and high relative humidity conditions. The mechanism and the thermodynamic parameters of methyl-iodide and n-hexane adsorption on the new adsorbent were also investigated.

4. CONCLUSIONS

The following conclusions are based on direct findings of the participants of the Co-ordinated Research Programme and are valid for the range of equipment and conditions tested. Care must be taken in any extrapolation of the results.

4.1 HEPA Filtration

- The particulate removal efficiency of glass fibre filter media did not vary with exposure to high temperature up to 120°C or to exposure to humidities below about 95% RH, relative humidity.
- Static exposures of HEPA filters at up to 200°C and up to eight hours did not cause performance deterioration when tested after cooling. Further development of test methods is desirable for the direct evaluation of particulate removal performance of full size HEPA filters under high temperature and high humidity conditions.
- Comparison of the test results by the participants when carried out on filter media from a single source under ambient conditions with efficiencies less than 99.99% showed no contradictions.
- Existing test methods for HEPA filters are designed only for ambient conditions. For realistic testing under high temperature and high humidity, development work on metallic or SiO₂ aerosols showed good promise. Further development was regarded as necessary.

4.2 Activated Carbon Adsorbers

- Effect of high temperature at low RH
 - o KI/KOH-coconut carbons under dry air conditions gave constant methyl iodide removal efficiency up to 100°C
 - o KI - coal carbons are efficient up to 180°C
 - o TEDA-carbons perform well up to 100°C under dry conditions.

- The effect of high temperature at high RH
 - o All granular carbons have a high capacity for water vapour at high RH, and any of the consequent loss of methyl iodide removal efficiency may be reduced by the addition of chemical impregnants.
 - o KI-carbons show a progressive decrease in efficiency with increasing RH. Presence of the impregnant, however, maintains a sufficient efficiency even at 98% RH at ambient temperature.
 - o KI/KOH-coconut carbon showed a fall in efficiency from close to 100% down to 98% at 90°C when test conditions were changed from 20°C to 90°C at 97%RH.
 - o KI-coal carbons were found by other workers to have a slightly increased performance at higher temperature.
 - o TEDA-carbons showed constant initial efficiency independent of humidity up to 70°C and 90% RH. However, the ageing rate greatly increased above 50°C and the effect is considered below.

- Ageing

Ageing (which is defined as a deterioration of carbon performance due to moist air exposure) is slow on KI-carbons under normal conditions of <50% RH. At higher humidities ageing of these carbons can be rapid so that use of KI-carbons for continuous operation in high humidity air is not consistent with economic carbon filter life. On TEDA-carbons the ageing rate is slow at high humidities below 50°C and they are now the preferred adsorbent for ambient air environments in UK CEBG stations. Above 50°C the rate of TEDA ageing increases rapidly with relative humidity due either to vapour phase removal of the impregnant or its conversion to a less efficient compound. Continuous use at high RH above 50°C is not favoured.

- Poisoning

Poisoning is defined as the adsorption of air pollutants with subsequent loss of methyl iodide adsorption efficiency. A wide variety of organics has been found on carbon filters taken out of service after continuous operation. Using xylene as a representative

organic it was shown that adsorption of 5% by weight of xylene reduced the K values+ of both KI and TEDA carbons by five units. The effect of combined ageing and poisoning, although not additive, is still greater than either effect alone. This efficiency loss is too great even with TEDA carbons for an economic filter life and the use of guard beds of unimpregnated carbon, or deep beds is necessary for filters in continuous use.

- Effect of bulk condensation on KI carbons

Bulk condensation of moisture on the charcoal results in the rapid decrease in the CH_3I removal performance due to washout of impregnant.

- Effect of irradiation

Exposure of coconut shell carbons to gamma radiation from 2.8×10^6 to 8.4×10^7 rads had no effect on the subsequent methyl iodide removal efficiency.

- Adsorber unit behaviour

Evaluation of prototype units of impregnated charcoal, under exposure to high temperature and humidity (90°C , 90% RH) over a periods of 8 hours showed marginal decrease in the CH_3I removal efficiency. The effect was interpreted as due to the adsorption of moisture from the flow of high humidity air.

These evaluations were part of the programme to produce and confirm fixed bed models. Experimental results under dry air conditions with high CH_3I inlet concentrations are not immediately applicable to high humidity conditions since changes occur in surface area chemistry.

+ The definition of the K value: $K = (\log DF)/t$, where DF is the decontamination factor (i.e. the ratio of the inlet and outlet gas concentrations) and t is the gas residence time in the adsorption column.

5. RECOMMENDATIONS

- 5.1 Test methods for HEPA filters are appropriate only for ambient conditions and it is recommended that development work should be continued for high temperature, high humidity performance assessment. The programme should be based on SiO₂ or metallic aerosols as initiated in this CRP.
- 5.2 Further work is recommended to develop iodine adsorbing materials with extended operating life for conditions of high humidity above 50°C. The impregnated carbons currently available are limited to applications up to 50°C at high humidity impregnated with TEDA.
- 5.3 Fibrous carbon materials (FCM) have demonstrated high hydrophobicity with good iodine retention and it is recommended that further work is carried out to exploit this towards the development of more robust adsorbents.
- 5.4 Further investigations are recommended on TEDA losses from granular carbons.
- 5.5 Means for prevention of surface oxidation should be investigated for FCM and other materials to extend the operating life of KI-carbons in moist air operational conditions.

CONTRIBUTIONS OF THE PARTICIPANTS

APPLICATION OF A NEW TECHNOLOGY FOR THE QUALITY ASSURANCE TESTING OF ULTRA EFFICIENT PARTICULATE AIR FILTERS

J.P. DEWORM, W. SLEGERS

Centre d'étude de l'énergie nucléaire (SCK/CEN),
Mol, Belgium

Abstract

HEPA filter test methods were developed with source terms appropriately extended to accident conditions. A Single Particle Laser Particle Size Spectrometer (SPLPSS) method was developed using the HEPA filter testing method and heterodisperse liquid test aerosol. Laboratory and in-situ testing of HEPA and ULPA filters was performed and found very valuable for quality assurance purposes. The new SPLPSS methodology would not be limited by investment costs, requirements in qualifying operators or fragility of instrument.

1. INTRODUCTION

High efficiency particulate air (HEPA) filters are defined in the standard IES-RP-CC-001-83T as : "throw-away extended-media dry-type filters in a rigid frame having minimum particle-collection efficiency of 99.97 % for 0.3 micrometer thermally-generated dioctyl-phthalate (DOP) particles, and a maximum clean filter pressure drop of 25 daPa, when tested at rated air-flow capacity". The selection of 0.3 μm for testing HEPA-filters was based on the theoretical and experimental findings of Langmuir and Blodgett [1] forty years ago, who showed that 0.3 μm was the size of the most penetrating particle (SOMP). The dependence of filtration efficiency on particle size is now well established. An increase in particle size will cause increased filtration by the interception and inertial impaction mechanisms whereas a decrease in particle size enhance collection by Brownian diffusion. As a consequence, there is an intermediate particle size region where two or more mechanisms are simultaneously operating, this is a region where the penetration (P) through the filter is a maximum as illustrated in fig. 1 (efficiency $\eta = 1 - P$). Lee and Liu [2] have shown that the SOMP is not a constant, but varies with filtercomposition and operating variables.

It is apparent that without knowing the SOMP a priori, a filter-test procedure should be able to determine the penetration curve in function of particle size.

A review of the SOMP-values up to 1977 by Kapoor [3] indicated that 0.13 μm would be the size for the test aerosol rather than 0.3 μm . Recent evidence was obtained from research by Yamada [4], conclusions were that at a standard face velocity of 2 cm/s, the SOMP for glassfiber media and for HEPA-filter media were situated in the range 0.10 to 0.18 μm . Other evidence was given by da Roza [5] who made an interpretation of measured values of the SOMP's and calculated the ratio's penetration at SOMP over penetration at 0.3 μm . He obtained values of the order of 7 for this ratio. Similar observations were reported from research in our laboratories [6]. We obtained at nominal flow rates (2 cm/s face velocity) a SOMP of 0.12 μm and penetration ratio's (as defined above) of 10. A typical penetration particle size curve for an HEPA-filter is represented in figure 2, the SOMP-value is 0.12 μm . The present standard test procedure (DOP-Q107) uses a thermal generated monodisperse DOP-test aerosol and a light scattering photometer for the determination of the penetration in accordance to the U.S. Army 136-300-175A standard.

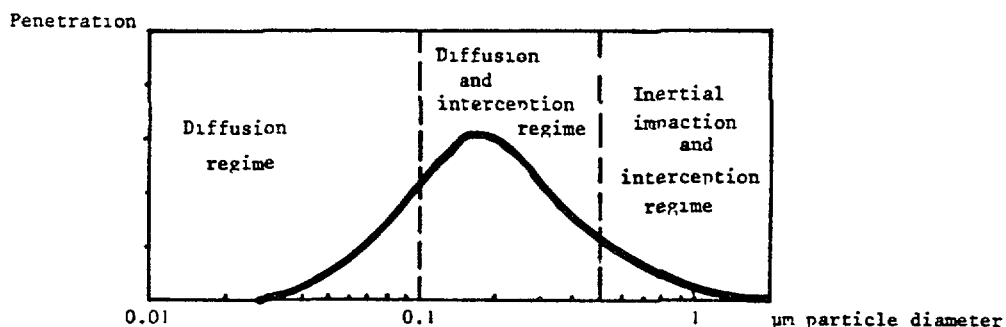


FIG 1 Schematic filter-penetration vs particle size

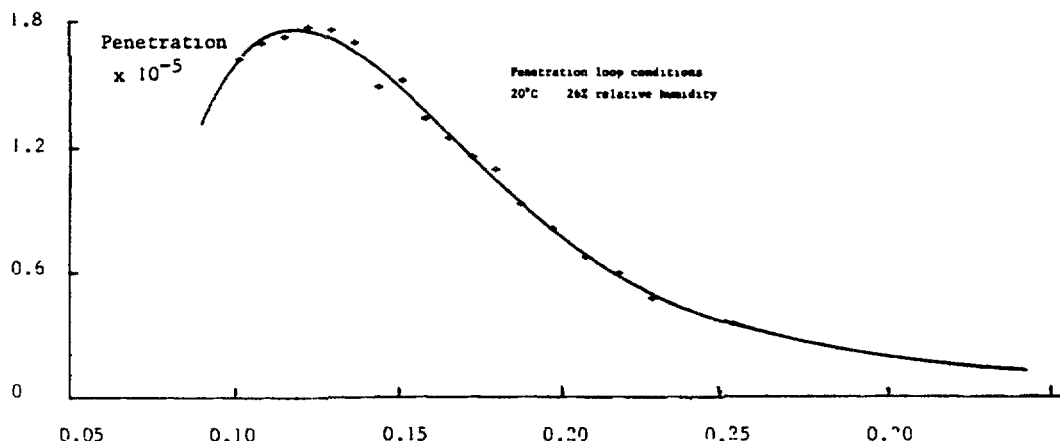


FIG 2 Penetration particle size curve

Several investigators have found recently that this DOP-testaerosol is not a 0.3 μm monodisperse aerosol as had been assumed, but rather, heterodisperse with a count median diameter of 0.18 μm and a geometric standard deviation of 1.4 [7]. The above mentioned objections for using 0.3 μm as test aerosol together with the difficulties of obtaining a 0.3 μm monodisperse DOP-aerosol, gave benefit to the development of a new technology for the quality assurance testing of HEPA-filters.

The methodology for obtaining a monodisperse aerosol for the test aerosol was a requirement forty years ago. Since reliable particle size analysers were lacking at that time, only a particle concentration system was needed as detector. At present single particle size spectrometers based on different physical properties are existing. Monodisperse aerosol generators were also developed nevertheless most of these generators give only low particle concentration, insufficient in combination with testing at high flowrates or ultra efficient filtermedia.

Therefore a methodology was developed consisting in principle of a heterodisperse liquid test aerosol together with a single particle laser particle size spectrometer (SPLPSS). The principle for testing is given in fig. 3. The reason for taking a liquid aerosol is that small pinholes cannot be plugged during the test procedure, giving a wrong indication for the penetration value. This methodology can be used with four different goals for the quality assurance testing of filters :

- * obtaining the actual filtration characteristics of the filter medium and through statistical grab sampling obtaining an index for the quality assurance of the filtermedia used for the manufacture of HEPA-filters.
- * obtaining an index for the penetration at the SOMP for a HEPA filter, this test includes the testing of the filter medium, sealing between filter medium and frame, frame and gaskets.
- * obtaining an index for the efficiency at the SOMP for the filtration system, this includes HEPA-filters and filter housing. This index is obtained at delivery of the instal-

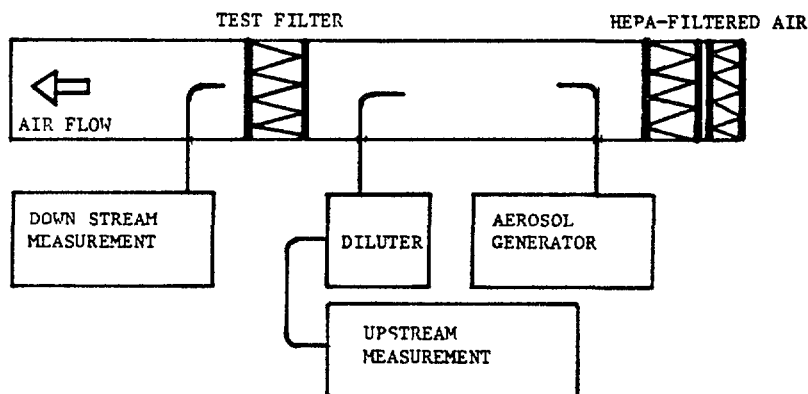


FIG 3 Schematic of SPLPSS methodology

lation and for the quality assurance programme as follow up of the installation.

2. METHODOLOGY FOR TESTING WITH THE LASER PROBE

The test method consists always in the injection of the challenge aerosol upstream of the filter (filtermedium, HEPA-filter, filtration system) and determination of up- and downstream concentrations in function of particle size (figure 3). The performance of a filter can be calculated from :

$$(DF)_{R_1} = \frac{(C_{up})_{R_1}/t_{up}}{(C_{ds})_{R_1}/t_{Cds} - (B_{ds})_{R_1}/t_{Bds}} \quad (1)$$

$(DF)_{R_1}$ = decontamination factor for the particle size range R_1 ; penetration equals $(P)_{R_1} = 1/(DF)_{R_1}$; efficiency $\eta_{R_1} = 1 - (P)_{R_1}$
 $(C_{up})_{R_1}$ = upstream total counts for the specified range R_1 (number of particles).

t_{up} = upstream sample time (s)

$(C_{ds})_{R_1}$ = downstream total counts for specified range R_1 (number of particles)

t_{Cds} = downstream sample time (s)

$(B_{ds})_{R_1}$ = background total counts (extra-neous particles) for the specified range R_1 (number of particles)

t_{Bds} = background sample time

R_1 = range of particle size under consideration for the spectrometer (in μm)

i = channel width in μm

This formula takes into account a same sample flow rate for up- and downstream sampling, otherwise a correction should be applied.

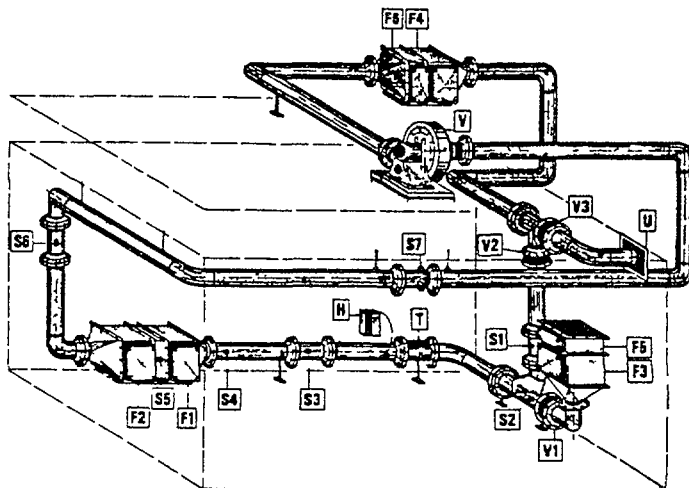
2.2. Penetrometer for HEPA-filters

2.2.1. The instrumental requirements for the application of the new test methodology.

* A laboratory test rig (fig. 4) was constructed for flow rates from 300 to 3000 m^3/h . The loop is provided with up- and downstream (S_4-S_6) sampling ports and an injection port for the challenge aerosol (S_2 or S_1). The air velocity is regulated by adjusting the fan-motor (V) speed and measured with a calibrated vane anemometer (S_3). Air is sucked from the laboratory and filtrated through HEPA-filters (F_3-F_5). The temperature (T) and humidity (H) can be adjusted in order to perform the test in standard conditions of temperature (20°C) and humidity (50 % r.h.). In this way the test is standarized and depends not on the ambient laboratory conditions.

* single particle laser particle size spectrometer

The detector for the determination of the up- and downstream particle concentration is the Knollenberg [8] aerosol counter, known as the active scattering spectrometer (ASAS-X Particle Measuring Systems Inc. Boulder). The principle of the detector consists that the particle stream (flow rate $0.5 - 1.5 \text{ cm}^3/\text{s}$) crosses the central region of a He-Ne laser beam ($2 \text{ mW}, \lambda = 632.8 \text{ nm}, \emptyset \text{ laser beam} = 200 \mu\text{m}$, operating in TEM_{00} mode). The aerosol stream and the laser beam cross in the focal point of a parabolic mirror. The scattered light is finally collected through a photodiode with the help of different optical means.



F₁, F₂ : Test section Filters
 F₃, F₄ : Prefilters HEPA-filters
 for air cleaning laboratory air.
 F₅, F₆ : HEPA-filter section for closed working conditions.
 S₁, S₂ : injection ports
 S₄ : upstream sampling port
 S₆ : downstream sampling port
 S₃ : sampling port for anemometer
 S₅ : sampling port downstream or upstream
 V : ventilator V₁, V₂, V₃ dampers for working condition in open or closed circuit.
 H : system for humidification
 T : heating coil
 U : outlet for air for open circuit

FIG 4 Schematic diagram of the test rig

The electrical pulses from the photodiode are classified by means of a pulse height analyser into 60 channels divided in four overlapping particle ranges of 15 channels (R_0 : 0.60-3 μm , R_1 : 0.24-0.84 μm , R_2 : 0.15-0.30 μm ; R_3 : 0.09-0.195 μm). The photodetector signal is a monotonic function of the diameter (or size) of the particles [9]. At present an instrument is designed to sense particles as small as 0.06 μm . The range 0.06-1 μm is an ideal range in connection with the penetration characteristics of the HEPA-filter media at the present flow rates. The whole system has the capability of providing an interface signal where data acquisition is transferred directly to a HP-85 desk computer, foreseen with a data acquisition/control unit. The same SPLPSS is used as detector for up- and downstream measurements. The methodology of a dual probe for up- and downstream measurements complicates the procedure for testing and influences the error propagation of the methodology. Another disadvantage is the cost, since the dual probe methodology requires two distinct devices at the same time. Both detectors must give identical particle number response, which is far from being the case in practice. Calibration for exact number response with an aerosol is for the moment not realistic.

* aerosol dilution system for measurement of the upstream concentration.

Indeed in the case of single particle detections, the presence of more than one particle in the scattering volume of the sensor will result in coincidence particle counting. The aerosol concentration admitted to

the laser probe is limited to about 10^4 particles/ cm^3 . This value is determined by the sensitive volume and the aerosol flow rate and admitted coincidence losses of 10^{-4} . The upstream concentration needed for a standard test is 10^6 particles/ cm^3 , necessitating dilution of the upstream concentration, of a factor 500, before admittance to the sensitive volume. A small diluter was constructed (fig. 5), consisting of two successive dilution steps. The principle of a dilution step is to split the aerosol stream into two paths, one following a pair of high efficient particulate air filters, the other passes through a capillary tube. At the exit of the capillary tube, the filtered gas stream and undiluted aerosol stream are mixed, resulting ideally in an aerosol identical in every way to the undiluted original except at reduced concentration.

The original particle concentration upstream C_{up} , is calculated from the measured concentration C_{upm} . For a dilution ratio D the expression is $C_{up} = DC_{upm}$.

The dilution ratio D is defined by the flow rate through the capillary tube Q_c and the total undiluted flow rate entering the diluter inlet Q_T : $D = Q_T/Q_c$.

The capillary serves as a laminar flow meter to measure the flow rate through the capillary.

The flow rate Q_c is determined by measuring the pressure drop ΔP over a length of the capillary tube. The experimental dilution ratios in function of the pressure drop over the capillaries, for the particle size range, under consideration, are used (table 1).

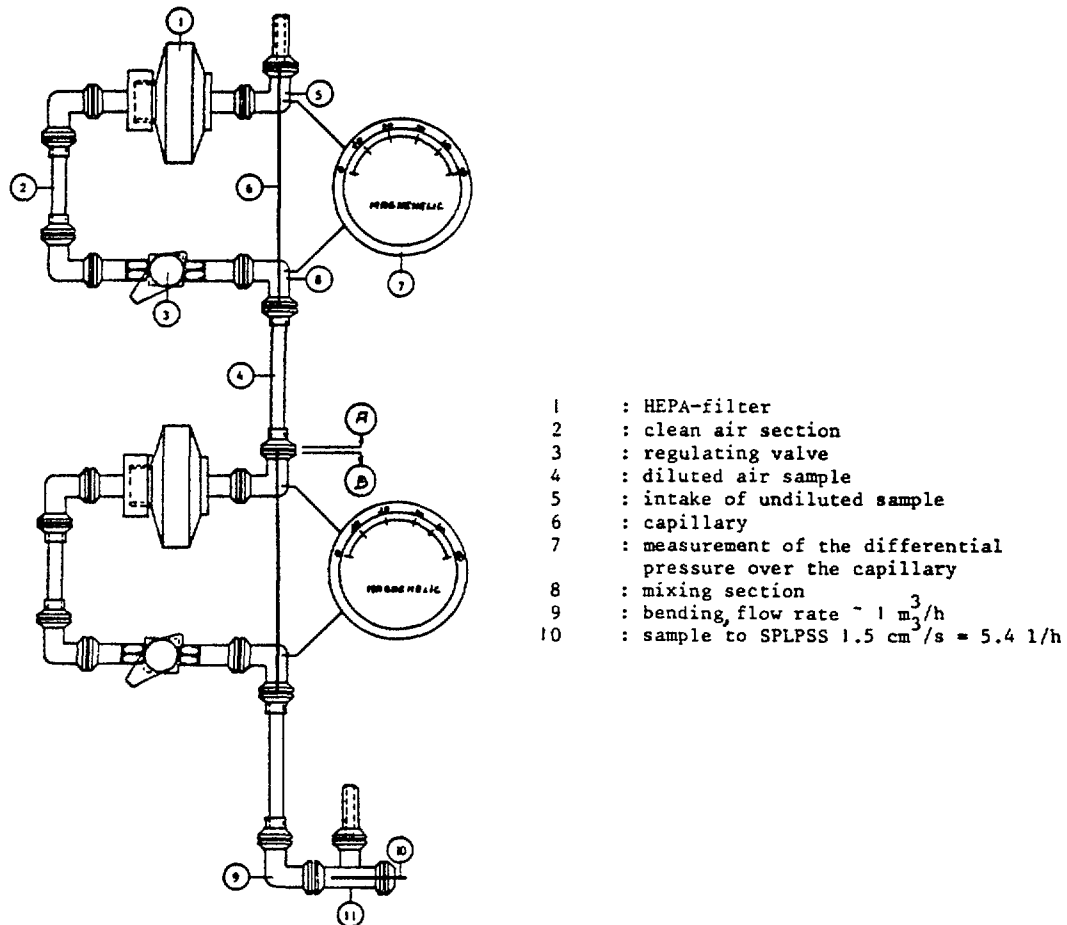


FIG.5. Schematic diagram of diluter.

Table 1 Dilution factors in function of the ΔP of the laminar flow meter
 (indicated standard deviation are standard deviations of the mean
 for $n = 10$ measurements)

Differential pressure ΔP daPa	Dilution factors				
	Particle size range (μm)				
	0.09-0.195	0.15-0.30	0.24-0.84	0.60-3	0.09-3
15	1400 \pm 17	1650 \pm 18	1770 \pm 28	1710 \pm 31	1580 \pm 21
20	960 \pm 14	1130 \pm 15	1200 \pm 16	1210 \pm 21	1080 \pm 15
25	650 \pm 5	760 \pm 5	820 \pm 6	840 \pm 13	740 \pm 6
30	490 \pm 6	580 \pm 5	620 \pm 6	630 \pm 10	560 \pm 6

The error propagation for the determination of the DF can be calculated from :

$$(DF)_{Ri} = \frac{D_{Ri} \cdot (C_{upm})_{Ri} / t_{up}}{(C_{ds})_{Ri} / t_{Cds} - (B_{ds})_{Ri} / t_{Bds}}$$

$$\left[\frac{\Delta D_{Ri}}{D_{Ri}} \right]^2 = \left[\frac{\Delta D_{Ri}}{D_{Ri}} \right]^2 + \left[\frac{\Delta (C_{upm})_{Ri}}{(C_{upm})_{Ri}} \right]^2 + \left[\frac{\Delta (C_{ds})_{Ri} + (B_{ds})_{Ri}}{(C_{ds})_{Ri} - (B_{ds})_{Ri}} \right]^2$$

$$t_{Cds} = t_{Bds}$$

Assuming that the random counting process of the spectrometer was a Poisson process, in which the standard deviation is approximated by the square root of the count number; and that all terms are random and independent, the above equation is :

$$\left[\frac{\Delta D_{Ri}}{D_{Ri}} \right]^2 = \left[\frac{\Delta D_{Ri}}{D_{Ri}} \right]^2 + \frac{1}{(C_{upm})_{Ri}} + \frac{(C_{ds})_{Ri} + (B_{ds})_{Ri}}{(C_{ds})_{Ri} - (B_{ds})_{Ri}}^2$$

since $\Delta C = \sqrt{C}$

For the calculation of the fractional standard deviation of D the measured standard deviations of the different terms are used. The term $C_{upm}R_i$ is always large, permitting to neglect him. The error at a 95 % level for the different HEPA or ULPA filters are summarized in table 2.

* an aerosol generator for the challenge aerosol. Dioctylphthalate (DOP, di-2 ethyl hexyl phthalate DEHP) is the liquid used for generating the test aerosol. The aerosol is obtained by nebulizing DOP at room temperature by compressed air, with the help of Laskin nozzles (fig. 6) [10]. This generator requires a supply of compressed air at 1.5 bar to operate a maximum of 8 nozzles. The number

median diameter of the generated particles is 0.2 μm with a geometrical standard deviation of 1.8. The output is about 0.3 g/min per nozzle. Using different nozzles permits us to obtain particle concentrations of 10^6 per cm^3 . For a flow rate of 1700 m^3/h a total counting rate in the range 0.09-3 μm of $2 \cdot 10^6$ p/s is obtained. 50 % of these particles are situated in the SOMP-range (0.09-0.195 μm). A representative particle size distribution is given in figure 7.

* The downstream sample is taken at a flow-rate of 1 m^3/h . The isokinetic conditions for aerosol sampling are without importance below 3 μm , if the air stream is well mixed.

From this small air stream only a sample stream of $1.5 \text{ cm}^3/\text{s}$ comes into the sensitive volume of the SPLPSS.

2.2.2. The procedure for the test with the penetrometer consist of :

* Calibration of the SPLPSS

Prior to the measurements, the detector is calibrated in term of particle size using polystyrene latex particles (PSL Dow Chemicals). The nominal diameters of the particles are 0.18 and 0.45 μm . The index of refraction for the PSL is 1.59 and slightly different for the DEHP with $n = 1.48$. The particle size is corrected for this difference.

* Alignment of the laser beam is performed on a regularly base.

* Determination of the instrumental background noise counting rate is determined with the SPLPSS functioning with a HEPA-filter at this sample entrance.

Table 2 Fractional error on the methodology (assumptions 10^6 p/cm^3 upstream concentration, background concentration less than 0.01 p/cm^3 , counting interval 100 s)

Efficiency at 0.12 μm	DF	Fractional error at 95 % confidence level %
99.99	10^4	10
99.999	10^5	10
99.9999	10^6	40

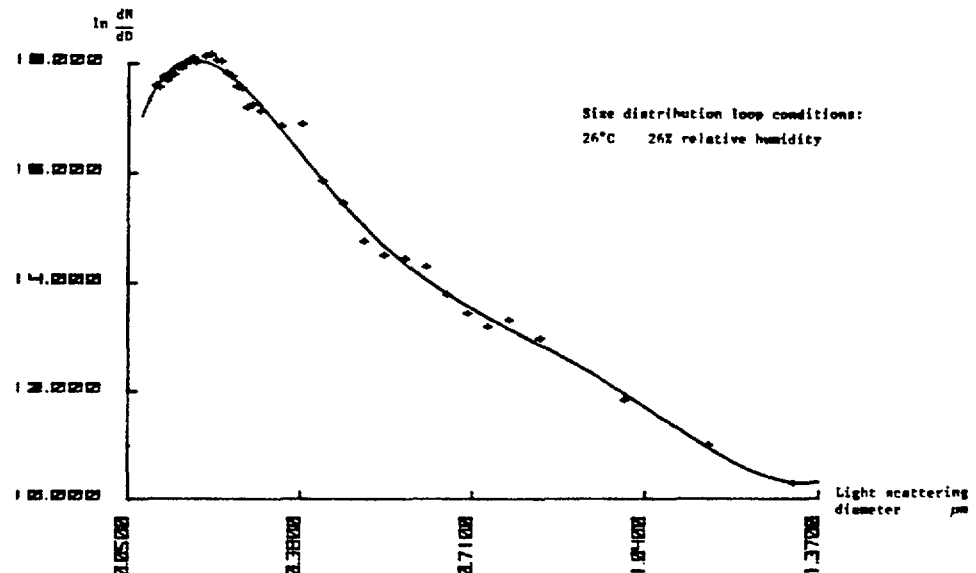


FIG.6. Particle size distribution of the challenge aerosol.

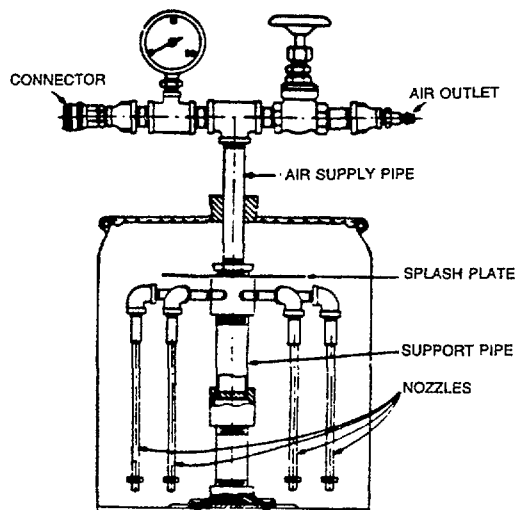


FIG.7. Aerosol generator for nebulizing DOP with Laskin nozzles.

The background particle concentration downstream the HEPA-filter is determined during a 15 minutes counting period, consisting of 5 measurement cycles.

- * The injection of the challenge aerosol is done one to five minutes prior to measurement, in order to stabilize the generator output. The injection place satisfies the condition of ensuring a uniform distribution of the test aerosol over the whole filter surface under test.
- * The downstream measurement is performed prior to the upstream determination. The condition of an homogeneous sample is fulfilled.

The sample period is 15 minutes.

- * The upstream measurement is performed with a dilutor between the upstream sample and the SPLPSS. The penetration is calculated for the size range were the SOMP is situated.

2.2.3. Sensitivity of the test methodology.
The method for defining detection limits is based on the assumptions of Currie [11]. He defines a critical level L_c which must be exceeded before a sample can be said to contain particles above the background level. This level is obtained from the standard deviation σ_B obtained from five successive measurements

of the background level of the SPLPSS

$$L_c = 2.33 \sigma_B \text{ (} \sigma_B \text{ in counts)}$$

The total count difference is defined as :

$$(C_{ds})_{Ri} - (B_{ds})_{Ri} = C' (C-B)_{ds}.Ri$$

for $t_{Cds} = t_{Bds}$

If $C' (C-B)_{ds}.Ri < 2 L_c$ than we can only report a "less than" value for the particle count rate (95 % level).

$(C_{Ri.ds})_{max} = C' (C-B)_{Ri.ds} + 2.13 \sqrt{\sigma^2_B + \sigma^2_C}$
 σ_c is the standard deviation of the real counts downstream. The $(DF)_{Ri}$ is reported as "greater than" value :

$$(DF)_{Ri} > \frac{(C_{up})_{Ri} / t_{up}}{(C_{Ri.ds})_{max} / t_{Cds}}$$

The detection limit L_D is defined as $L_D = 4.65 \sigma_B$. If $C' (C-B)_{Ri.ds} > L_D$ than we can report a particle count rate value with its two sided 95-percent confidence interval.

$$C' (C-B)_{Ri.ds} \pm 2.78 \sqrt{\sigma^2_B + \sigma^2_C}$$

In this case the $(DF)_{Ri}$ is reported as :

$$(DF)_{Ri} = \frac{(C_{up})_{Ri} / t_{up}}{C' (C-B)_{Ri} . ds}$$

together with its 95 % confidence interval.

Assuming that the random counting process of the detector follows a Poisson distribution, the detection limit at a 95 % confidence level for an upstream concentration count rate of 10^6 p/s is given in table 3.

Table 3 : Detection limit at the SOMP for different background count rates

Background p/s	DF detection limit at the SOMP	
	$t_{Cds} = t_{Bds}$	
	100 s	200 s
0.1	$7 \cdot 10^6$	10^7
0.01	$2 \cdot 10^7$	$3 \cdot 10^7$

Table 4 Determination of the penetration for commercial available HEPA and ULPA filters tested at their nominal flow rate

Particle size range μm	Penetration		
	HEPA 99.97%DOP $\Delta P = 25$ daPa at $1870 \text{ m}^3/\text{h}$	HEPA 99.995% (ULPA) at $1700 \text{ m}^3/\text{h}$	HEPA 99.999% (ULPA) at $600 \text{ m}^3/\text{h}$
	1.40×10^{-4}	1.40×10^{-5}	$5.56 \cdot 10^{-7}$
0.09-0.097	1.40×10^{-4}	1.40×10^{-5}	$5.56 \cdot 10^{-7}$
0.097-0.104	1.51	1.45	less than 4.36
0.104-0.111	1.64	1.41	less than 4.54
0.111-0.118	1.62	1.14	less than 2.78
0.118-0.125	1.65	SOMP <u>1.10</u>	less than 2.94
0.125-0.132	<u>1.70</u>	SOMP 1.14	less than 2.27
0.132-0.139	1.61	1.26	less than 1.96
0.139-0.146	1.55	0.90	less than 1.67
0.146-0.153	1.38	0.85	less than 1.52
0.153-0.160	1.34	0.81	less than 1.37
0.160-0.167	1.28	0.75	less than 1.30
0.167-0.174	1.26	0.70	less than 1.25
0.174-0.181	1.19	0.66	less than 1.20
0.181-0.188	0.99	0.56	less than 1.07
0.188-0.195	0.88	0.78	less than 0.92
0.09-0.195	1.36×10^{-4}	1.18×10^{-5}	$5.68 \cdot 10^{-7}$
ΔP daPa	22	26	30
Dimension in mm	610x610x292	610x610x292	610x610x66
Filter area m^2	16,8	23	12

For a counting time of 40 s per particle size range R_i , and for five successive measurements cycles, the total sampling time amounts to 15 minutes. This means that an efficiency less than 99.9999 % could be determined on the test rig.

Different HEPA- and ULPA-filters were tested on our test rig. Some of the obtained results are summarized in table 4.

2.3. Penetrometer for filtermedia

A special filterholder was constructed to contain a filter paper sheet of 15 x 15 cm. This filter holder was built into a duct in which the flow rate could be changed in order to obtain different face velocities through the filter paper (1 to 4 cm/s). The test aerosol was obtained by nebulizing DOP with a Collision generator (fig. 8). The upstream particle concentration was measured with the SPLPSS, depending on quality of the efficiency of the paper, dilution may be required. Such tests were performed on sheets of the

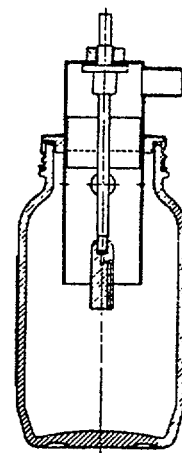


FIG.8. Collision generator, for nebulizing DOP and for small flow rates.

same lot, used for the manufacture of normal HEPA-filters. From table 5 one can conclude that filter characteristics may vary from one sheet to another, for the same paper roll. For the filtermedium tested the SOMP was situated in the particle size range 0.146 - 0.153 μm .

Table 5 Penetration of filter medium used for HEPA-filters, tested at a filtration velocity of 2 cm/s.

particle size range μm	penetration $\times 10^{-6}$			
	sheet n°1	sheet n°2	sheet n°3	mean value
				n°2 en n°3
0.09-0.097	9.9	30.3	33.1	31.7
0.097-0.104	11.2	31.0	37.3	34.1
0.104-0.111	10.6	33.3	39.0	36.1
0.111-0.118	12.5	34.6	39.8	37.2
0.118-0.125	13.4	36.0	41.8	38.9
0.125-0.132	13.9	35.7	48.1	41.9
0.132-0.139	15.8	SOMP 41.1	45.6	43.3
0.139-0.146	14.9	38.4	47.3	42.8
0.146-0.153	SOMP 15.4	39.0	SOMP 50.5	44.7
0.153-0.160	15.0	36.9	44.5	40.7
0.160-0.167	14.3	37.8	44.0	40.9
0.167-0.174	14.5	33.5	45.5	39.5
0.174-0.181	13.6	34.2	42.9	38.5
0.181-0.188	13.4	33.3	34.2	36.2
0.188-0.195	12.6	29.8	38.0	33.9
0.09-0.195	13.6	35.0	42.6	38.8
0.15-0.30	9.0	22.1	27.4	24.7
$\Delta p \text{ daPa}$	11	16	13	-

2.4. Penetrometer for testing mask canisters

The canister contains mostly a high efficiency particulate air (HEPA) filter sometimes foreseen with a quantity of activated charcoal for removal of gases and vapors.

At present the German standard DIN 3181 Teil 2 deals with differential pressure and penetration values for their standarized test. Three classes were defined in this standard (table 6).

Table 6 . Classification of mask canisters as defined by the German standard DIN3181 Teil 2

Filter-class	Differential pressure daPa		Penetration at 95 l/min		
	30 l/min max.	95 l/min max.	NaCl max.	Paraffin oil	max.
P1	6	21	$2 \cdot 10^{-1}$	-	
P2	7	24	$6 \cdot 10^{-2}$	$2 \cdot 10^{-2}$	
P3	12	42	$5 \cdot 10^{-4}$	10^{-4}	

The test is performed with a small test rig with a Collison aerosol generator (fig. 8) and a DOP-challenge aerosol. The dilution

system is not a necessity since the upstream number concentration is smaller than 10^4 p/cm³. Tests performed on two different types of HEPA filter mask canisters are summarized in table 7. These tests were performed at a constant flow rate of 120 l/min.

3. EXPERIENCE WITH IN-SITU LASER PROBE

TECHNOLOGY

3.1. Considerations

The laser probe has been applied since 1982 for in situ testing of installed HEPA-filters. The DOP test method, in accordance to the standard ANSI N510-1980 was used in Belgium since 1965 for in situ testing of HEPA-filtration systems. Nevertheless the limit of sensitivity of the sensor practically limits the "index of penetration" to values of 10^{-5} . The installation of a second HEPA-filter, after the carbon adsorption traps in the newer nuclear power plants or as a second barrier for the plutonium fuel facilities, introduced problems in the determination of the overall penetration index as determined with the above mentioned standard. Indeed, the actual overall penetrations are far below 10^{-6} . There was a trend in Belgium to use the SPLPSS as a detector for re-

Table 7 Penetrations for mask canisters

particle size range μm	penetration	
	P_2 filterclass	P_3 filterclass
0.09-0.097	$5.09 \cdot 10^{-2}$	$1.00 \cdot 10^{-4}$
0.097-0.104	6.25	1.50
<u>0.104-0.111</u>	<u>6.55</u>	<u>2.09</u>
0.111-0.118	5.14	1.04
0.118-0.125	4.96	0.95
0.125-0.132	4.72	0.82
0.132-0.139	4.50	0.76
0.139-0.145	4.43	0.64
0.145-0.153	4.25	0.57
0.153-0.160	4.10	0.48
0.160-0.167	3.83	0.37
0.167-0.174	3.60	0.30
0.174-0.181	3.26	0.28
0.181-0.188	2.42	0.20
0.188-0.195	2.60	0.13
0.09-0.195	4.07×10^{-2}	0.52×10^{-4}

solving this problem, rather than performing two successive in-situ tests with a common forward light scattering photometer. This trend was manifested by the idea to transform the leakage test into an efficiency test, which is valid for the overall system (filter medium, housing, frame, gaskets, sealants and separators).

The SPLPSS allows to obtain the penetration in function of the particle size. The maximum of the particle size penetration curve determines the minimum decontamination factor, regardless of which polydisperse challenge aerosol is used. The decontamination factor determined in this way corresponds to the safest conditions of exploitation. The advantages of this sensitive method with the laser probe are multiple :

- * existing systems can be tested without the need for auxiliary ducts and valves between the different in serie HEPA-filters, to inject the challenge aerosol, and for the actual flow rates.
- * HEPA-filter systems in series can be tested as a whole.

Testing can be performed without any interruption of the clean-up operation.

3.2. Acceptance criteria for tandem HEPA-filtration

For the nuclear power plants the second HEPA-filter is needed for retaining the carbon particles dragged along with the air flow. A decontamination factor of 10^6 is a requirement for the whole filtration system. As already explained the minimum decontamination factor corresponds to the safest conditions. This condition is fulfilled when taking the maximum penetration size of the filter as the most restrictive parameter.

The idea to establish an acceptance criterium with a particle size range of 0.09 - 0.195 μm , seems to be reasonable from the point of view for minimizing sampling time, and thus minimizing loading of the filter with DOP-aerosol as well as for the instrumental possibilities and statistical considerations. The present frequency of HEPA-filter testing is situated between 12 and 18 months, and after each replacement of filters owing to a too a high differential pressure over one stage. The flow rate for the different systems may be situated between 3.000 - 150.000 m^3/h . The results in the SOMP-range change from one year to another and is mostly increasing due to the the dustloading of the filter and thus better filtration characteristics (see table 8).

3.3. Use of a fluorescent laser spectrometer

The inleaking particles and thus the background counting rate after the second HEPA-filter in industrial installations puts mostly restrictive limits on the detection of high DF-factors.

This problem can be resolved with a fluorescent laser spectrometer [12].

Testing with the fluorescent laser spectrometer is performed with a dye labelled DOP-aerosol (dye = Potomac yellow n° 838 Dayglo Color Corp. Cleveland) with an excitation wave length of 440 nm, well within the bandwidth of the He-Cd laser and an emission wave length of 490 nm.

The fluorescent SPLPSS works in two modes : all particles or only fluorescent particles. In this way a distinction can be made between in-leaking particles and those coming from the challenge aerosol.

Table 8 Determination of the decontamination facts in function of time for a filtration system with a nominal flow rate of $13\ 600 \text{ m}^3/\text{h}$, consisting of two HEPA-filters in serie

Date of in situ testing	Tandem system DF 0.09-0.195 μm
March/82	$> 1,3 \cdot 10^6$
December/83	$> 3,5 \cdot 10^6$
March/85	$> 3,8 \cdot 10^6$

At present with the He-Ne laser only a upper limit can be determined for the decontamination factor for tandem filtration systems. Nevertheless with the fluorescent SPLPSS, decontamination factors as high as 10^{+8} could be investigated.

* the filtration system for quality assurance and follow up by in situ testing. The investment costs, requirements on the qualification of operators and fragility of the instrument are not a limitation for this new methodology.

4. SUMMARY

The SPLPSS is a very valuable instrument for testing of :

- * very high efficient filtermedia
- * HEPA-filters of different sizes (penetrometers)

ACKNOWLEDGEMENTS

The authors are indebted for the technical assistance of R. BOLLEN, C. CAERS, J.B. PAUWELS, F. VAN MIERLO and L. VANDERVEER.

REFERENCES

- [1] I. Langmuir and K. Blodgett (1944)
Supplement section I and section II
U.S. Office of Scientific Research and Development n° 3460
- [2] K.W. Lee B.Y.H. Liu (1980)
J. of the Air Poll. Cont. Ass. Vol. 30 p. 377-381
- [3] J.C. Kapoor K.G. Subramanian A.A. Khan (1977)
Filtration and Separation March/April 1978 p. 133-134
- [4] Y. Yamada K. Migamoto T. Mori A. Koizumi (1984)
Health Physics Vol. 46 p. 543-547
- [5] R.A. daRoza (1982)
UCRL - 53311 Lawrence Livermore Laboratory
- [6] J.P. Deworm (1984)
Laser detector methodology for laboratory and in situ testing of very efficient filters.
Proc. 7th international Symp. Cont. Control - Paris Sept. 1984
- [7] W. Bergman A. Bierman (1984)
18th DOE Nuclear Airborne Waste - Conf. 840806 Vol. 1 and 2
Management and Air Cleaning Conference Baltimore Maryland USA - Aug. 1984
- [8] R.G. Knollenberg B. Luehr in Fine Particles ed. Liu p. 669
Academic Press Inc. (1976) ISBN 0-12-452950-X
- [9] G.C. Salzman H.J.E. Ettinger M.I. Tillery L.S. Wheat W.K. Grace - 1982
17th DOE Nuclear Air Cleaning Conference Conf. 820833
- [10] W.H. Echols J.A. Young - report NRL-5929 1963 - Departement of Commerce
- [11] L.A. Curie (1968) Anal. Chem. Vol. 40 p. 583-593
- [12] J.C. Elders T.G. Kyle M.I. Tillery H.J. Ettinger (1982)
17th DOE Nuclear Air Cleaning Conference July 1982 Conf. 820833

FILTER TESTING UNDER SPECIAL CONDITIONS

W. ULLMANN, P. HAMEL, W. SCHULZ
Staatliches Amt für Atomsicherheit
und Strahlenschutz,
Berlin, German Democratic Republic

Abstract

It is reported on the results of preparative work to construct or reconstruct testing equipment for testing of filter materials under normal conditions and at increased temperature and humidity and for testing of full-size filters under normal conditions and at increased humidity and on experimental investigations. For aerosol measurement a scintillation particle counter and a laser aerosol spectrometer Partoscope R-LA were used. The generation and the properties of the test aerosols are described in detail.

The investigations of filter materials were concentrated on testing selected filter materials on lab-scale, using a NaCl test aerosol ($CMD = 0.18 \mu m$; $\sigma_g = 1.8$). In addition, extensive investigations on a full-size filter FARTOS-Z-500 have been made. This filter is intended for separating liquid or solid polydisperse aerosols from air or gases and can be regenerated by spraying or washing.

1. WORKING PLAN

The research project No. 3700/RB on "Filter testing under special conditions" is part of the IAEA coordinated programme on "Retention of iodine and other airborne radionuclides in nuclear facilities during abnormal and accident conditions".

The work to be done in the GDR in accordance with contract No. 3700/RB will be concentrated on aerosol filtration. Investigations are necessary concerning especially the influence of increased temperature and humidity on the filtration process because there are no or only insufficient experiences in this field for new filters under accident conditions and for aged filters, both under normal and accident conditions. For the situation in the GDR maximum values of $150^{\circ}C$ and 100 % relative humidity are assumed to be valid.

In accordance with the "Recommendations for coordinating research on retention of particles" elaborated during the Research Coordination Programme Meeting in MOL/Belgium (September 24 to 28, 1984), the GDR has to perform the following investigations:

- Testing of filter materials
 - . Quantities to be determined: penetration, pressure drop
 - . Parameters: temperature, humidity
- Testing of HEPA-filters on laboratory rig
 - . Quantities to be determined: penetration, pressure drop
 - . Parameter (new and aged filters): humidity

In the SAAS at first extensive work was done to construct or reconstruct testing equipment for these investigations. Since the required laser aerosol spectrometer Partoscope R-LA was delivered only in September, 1985, and was then out for repair for a longer period, a postponement of deadlines by one year for the research project was applied for and confirmed by the Agency.

Out of the seven contracts concluded within the framework of the Coordinated Research Programme five will expire in 1987. Therefore, as a result of the Second Meeting of the Coordinated Research Programme in TORONTO/Canada (June 2 to 6, 1986) it was recommended to finish the research programme in 1987 and, in consideration of the latest findings from the accidents in TMI and CHERNOBYL, to prepare a new coordinated research programme. The discussions in TORONTO also led to a modification of the working programme for the contracts at present being implemented. The following provisions were made:

- (1) Testing selected filter materials made available to all workers interested on lab-scale under provided normal conditions (see 2.1.),
- (2) After submitting the results of (1) a decision is to be made for the establishment of test standards for investigation under abnormal conditions,
- (3) Full-size HEPA-filter tests will be performed in the years to come.

Below, it is reported on the results of preparative work and on experimental investigations. As scheduled, the investigation of filter materials on lab-scale was concentrated on testing selected filter materials under normal conditions (see 2.1.). In addition, extensive investigations have already been made on a full-size

filter (see 5.1.) to gain experience for future investigations in accordance with the data to be elaborated by the workers of the research programme and confirmed by the IAEA.

2. AEROSOL MEASUREMENT

For aerosol measurement a scintillation particle counter and a laser aerosol spectrometer were used.

Fig. 1 shows the principal set-up of the scintillation particle counter. The aerosol measurement is based on the light emission of atomic Na vapour excited in an air-hydrogen flame. In contrast to flame-photometric determination of the concentration of NaCl aerosols /1/, here the particle size distributions of NaCl aerosols were measured /2/. For this purpose it was presupposed that there is only one particle each in the excitation part of the flame. In this case there is an unambiguous relationship between light intensity and particle mass. Since the particles have to be individually and successively introduced into the flame, the measurable particle concentration is limited. The measurement of single particles requires high sensitivity. Therefore, a special burner was used which produces a very small, extremely stable flame. After amplitude analysis, the pulses were registered in ten counters, all particles above a size adjusted in calibration being indicated.

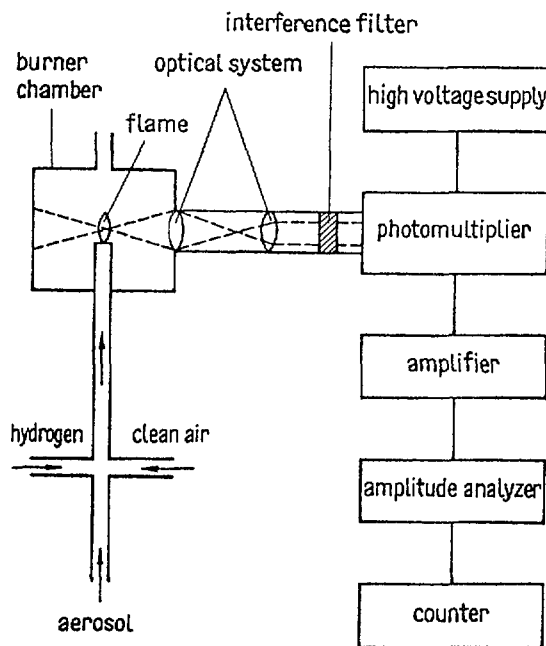


Fig. 1 Design of scintillation particle counter (schema)

The laser aerosol spectrometer used is the Partoscope R-LA type from KRATEL Instrumente GmbH. This laser light-scattered spectrometer represented as block diagram in Fig. 2 was supplied with the Agency's support. The measuring device is characterized by the following data /3/ :

- Principle: right angle light scattering
- Laser: helium-neon laser (632.8 nm) with open cav.
- Measuring range: 0.1 to 2.0 μm
- Maximum concentration: 2300 particles per cm^3
- Flow rate: 300 cm^3/min
- Display: 8-digit decimal display

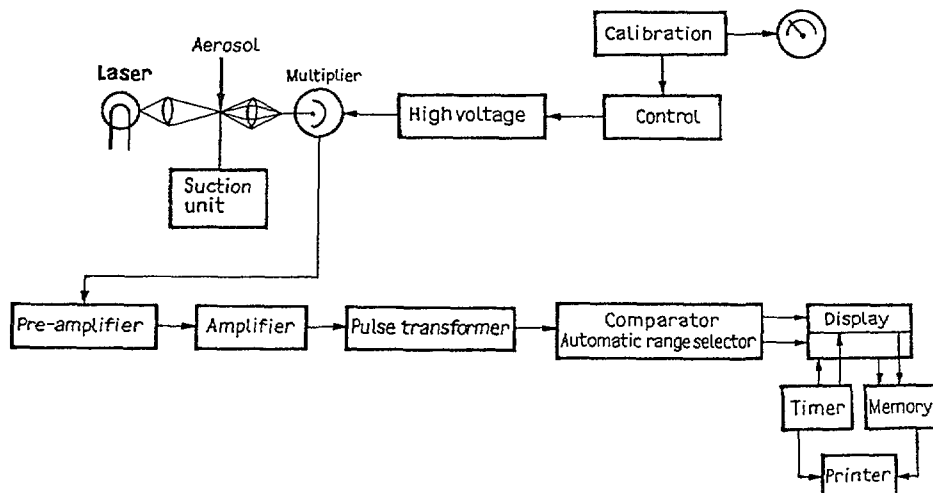


Fig. 2 Laser scattered-light spectrometer Partoscope R-LA (block diagram)

3. GENERATION OF TEST AEROSOLS

For filter testing three routine methods are available in the SAAS (see 4.1.3.) using the following test aerosols:

- Polydisperse NaCl aerosol,
- Polydisperse paraffin aerosol,
- Polydisperse NaCl aerosol with attached short-lived radon daughter products.

For the investigations described in 4. and 5.1. mainly the polydisperse NaCl test aerosol was used, the particle size distribution of which is shown in Fig. 3. If the particle size distribution is approximated by a logarithmic normal distribution the following values for the median value CMD (50 %-value; Count Medi-

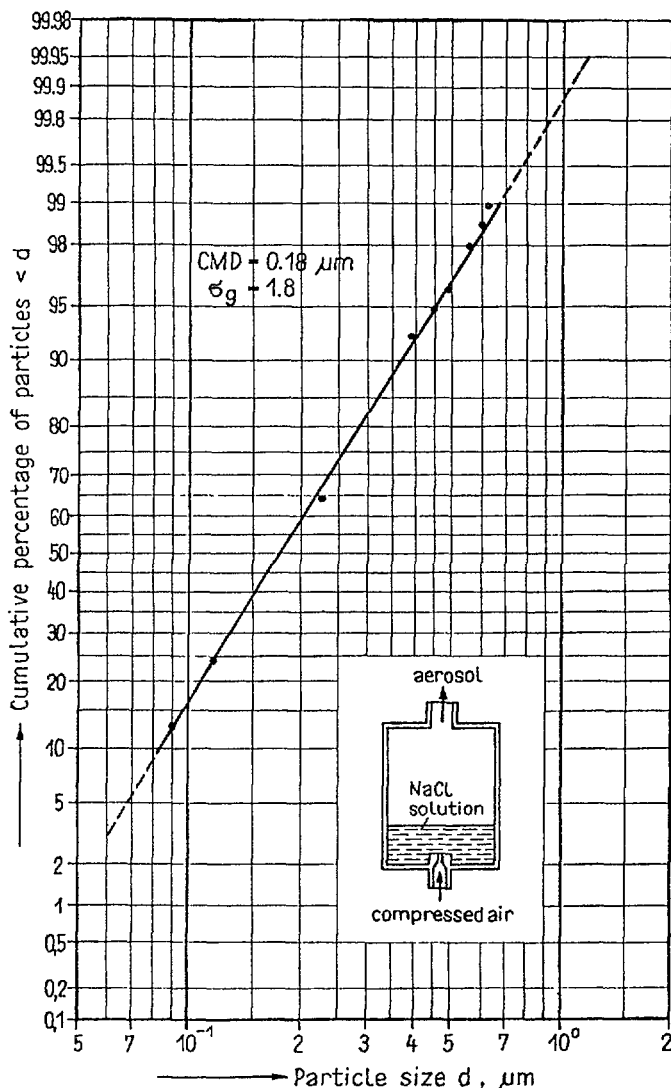


Fig. 3 Measured cumulative distribution of the used NaCl test aerosol, relative to the number of particles

an Diameter) related to particle number and for the geometric standard deviation σ_g are obtained:

$$CMD = 0.18 \text{ } \mu\text{m} ; \sigma_g = 1.8$$

The NaCl test aerosol can be used for investigations at high temperature ($\leq 150^\circ\text{C}$) and normal humidity. Electron-microscopic investigations of heated NaCl particles in the SAAS showed that, up to 150°C scheduled for investigations, no destruction of crystal form occurred. At increased humidity the use of NaCl aerosol is possible only to limited extent because, from a certain level of humidity, the known growth in size of NaCl crystals and their transformation to liquid droplets will occur.

Besides, Fig. 3 schematically shows the aerosol generator used for aerosol generation. In its development particular emphasis was laid on simple design and simple operation. The generator consists of a cylindrical vessel partly filled with an aqueous

NaCl solution. The compressed air fed in at the bottom bubbles through the NaCl solution and thus produced liquid drops. These are partly precipitated at the wall and the lid of the vessel and partly carried along on the air flow out of the generator. After mixing with the testing air flow which is by far greater the water evaporates. Therefore, the filters are tested with dry NaCl crystals. The concentration and size distribution of the particles supplied by the aerosol generator mainly depend on the geometric dimensions of the vessel, the diameter of the compressed air inlet, the working pressure, the liquid level in the vessel and the concentration of the aqueous NaCl solution (e.g. 2.5 % aqueous NaCl solution). Thus it is possible to adjust optimal conditions for the given testing task. Both with respect to concentration and particle size distribution, the aerosol generator has a very good long-term constancy.

For special investigations (see 5.1.4.), monodisperse latex test aerosols of different particle size are available.

To investigate aerosol filters at increased temperature and humidity, SiO_2 test aerosols are very well suited as standard test aerosols. Fig. 4 shows the particle size distributions and geometric standard deviations of seven monodisperse SiO_2 aerosols generated in the SAAS by Römmler and Blume. After respective radioactive labelling, such aerosols were used in the SAAS for investigating the penetration depth of aerosols into filters.

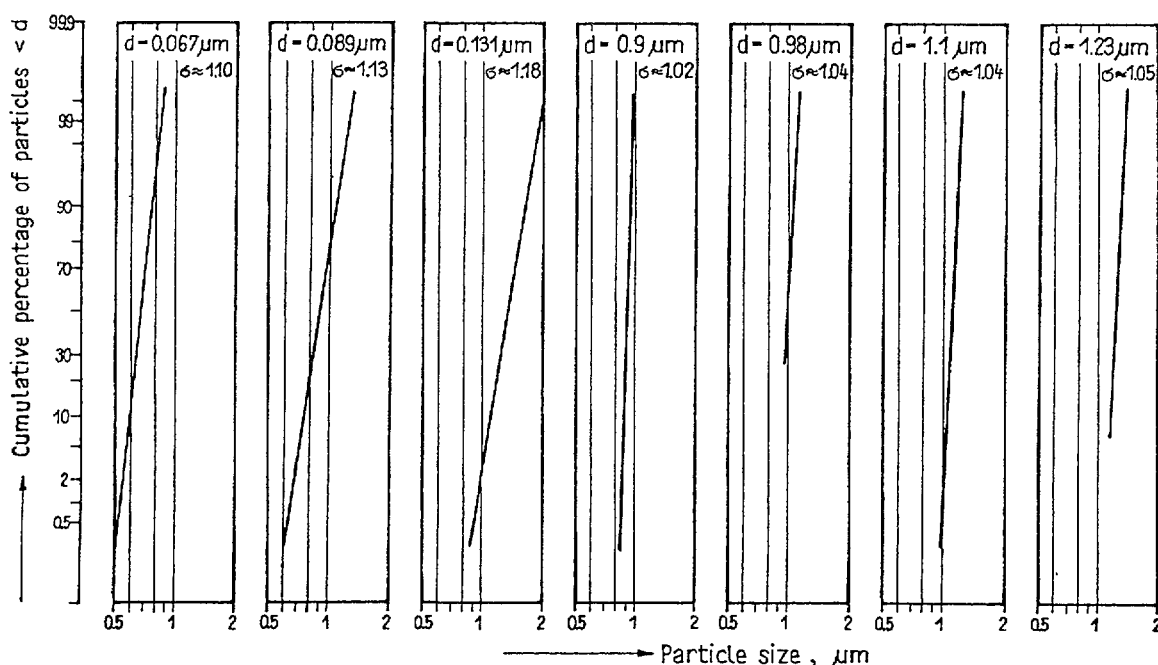


Fig. 4 Measured cumulative distribution of seven SiO_2 aerosols generated in the SAAS, relative to the number of particles

4. TESTING OF FILTER MATERIALS ON LAB-SCALE

4.1. Testing of selected filter materials under normal conditions

4.1.1. Test programme

The filter materials made available to all interested workers are four different types of microtex FH from J. C. Binzer Paper manufacture. They are intended to be used in HEPA-filters and consist of micro-glass fibres. The producers specify the following properties /4/ :

Quality	FH 863/2	FH 863/1 W	FH 929	FH 1047
Basis weight, g/m ²	70 ± 3	80 ± 5	82 ± 5	77 ± 3
Thickness, mm	0.42 ± 0.03	0.58 ± 0.08	0.46 ± 0.05	0.37 ± 0.39
Pressure drop, Pa (at 5.3 cm/s)	350 ± 30	370 ± 30	530 ± 50	580 ± 30
Penetration (at 5 cm/s; BS 4400)	3.10 ⁻⁴	1.10 ⁻⁴	2.10 ⁻⁵	1.10 ⁻⁶

These materials are to be investigated with respect to their penetration and their pressure drop under the following test conditions:

Humidity: 50 % relative humidity

Temperature: 25 to 30 °C

Linear velocity: 2 cm/s

Test aerosol: Selection is up to the respective worker (see 4.1.2.)

4.1.2. Test rig and test aerosol

Fig. 5 schematically represents the set-up of available test rigs in the SAAS for investigating filter material under normal conditions. Three different test methods are used /5/ :

- Test method I

- Test aerosol: polydisperse NaCl aerosol
- Aerosol measuring device: scintillation particle counter for measurement of particle size distribution, total number and total mass of NaCl particles
- Measurement of total penetration and of penetration as a function of particle size

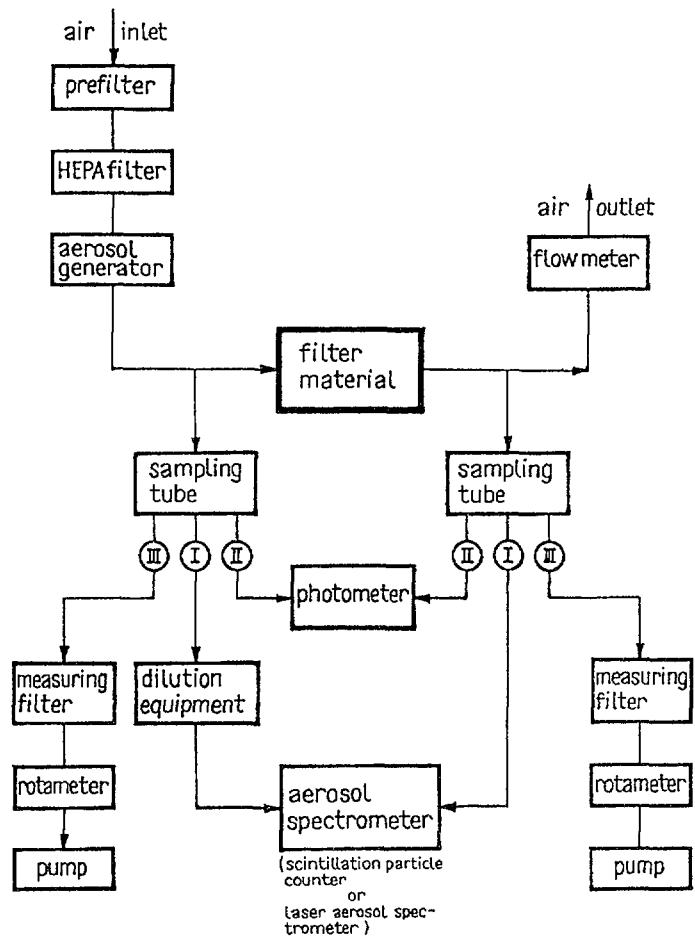


Fig.5 Existing test stand for the investigation of filter materials under normal conditions (block diagram)

- Test method II

- . Test aerosol: polydisperse paraffin oil aerosol
- . Aerosol measuring device: aerosol photometer for determination of total scattered light
- . Measurement of total penetration

- Test method III

- . Test aerosol: short-lived radon daughter products attached to polydisperse NaCl aerosol
- . Aerosol measuring device: alpha counter (after separation of aerosol by using measuring filters)
- . Measurement of total penetration

For investigations of the selected filter materials test method I was used. Test method III was used only for a number of additional measurements. The NaCl test aerosol used is characterized by the values $CMD = 0.18 \mu\text{m}$ and $\sigma_g = 1.8$ (see 3. and Fig. 3).

4.1.3. Measuring results and conclusions

The values measured for the pressure drop of the selected filter materials agree with the producers' data. The values measured are represented in Fig. 6 for linear velocities of up to 10 cm/s.

Devices used for penetration measurement were both the laser aerosol spectrometer Partoscope R-LA and the scintillation particle counter. Fig. 7 shows for the four selected filter materials the dependence of penetration from the particle size of the NaCl test aerosol measured with the Partoscope R-LA. The measuring results confirm the sequence stated under 4.1.1. of the penetration of the selected filter materials. The penetrations obtained for small particles are higher than the values stated by the filter material producers. It is assumed that this is due to the different test methods.

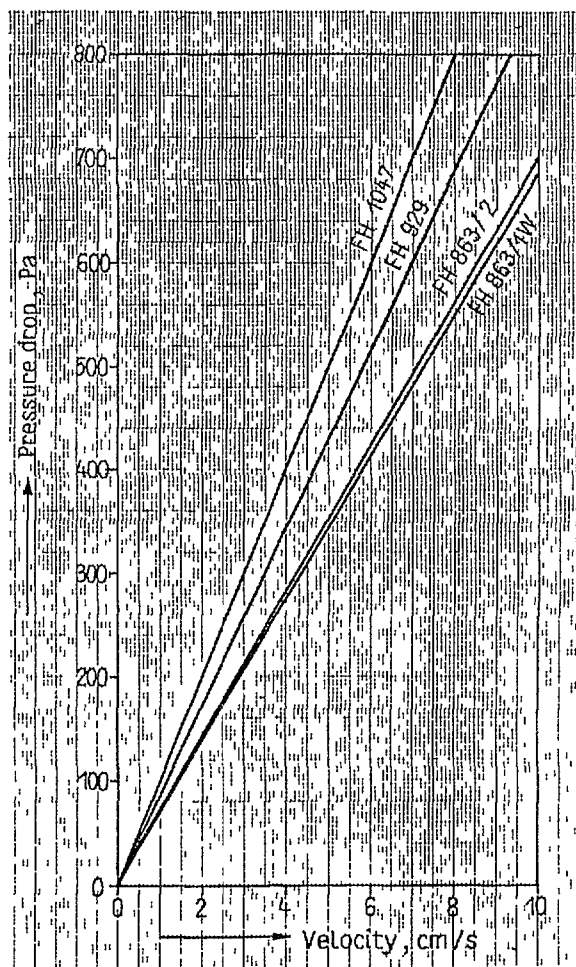


Fig.6 Pressure drop of the selected Mikrotex filter materials as a function of the linear velocity

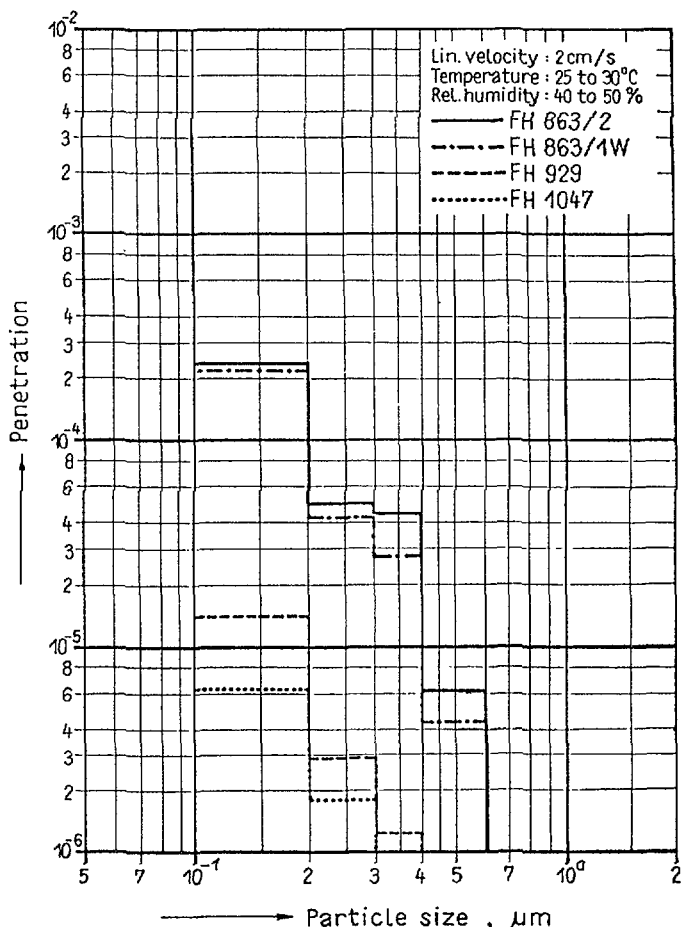


Fig. 7 Penetration of the selected Microtex filter material for NaCl test aerosol (laser aerosol spectrometer Partoscope R-LA)

Fig. 8 and Fig. 9 show the dependence of penetration from the particle size of the NaCl test aerosol for the Microtex filter materials FH 863/2 and 863/1 W measured by using the Partoscope R-LA and the scintillation particle counter. The results obtained with the two devices agree relatively well. Existent deviations are due to different measuring principles.

For high-quality filter materials the available equipment for the defined dilution of the aerosol withdrawn before the filter material to be tested has to be improved. For the time being, they allow only the adjustment of dilution factors of up to 1 : 1,000, so that great uncertainties follow particularly for very low penetrations of the filter materials.

4.2. Testing at increased temperature and humidity

For the investigation of samples of filter material at increased temperature and humidity various components of the test rigs used for investigations under normal conditions were modified.

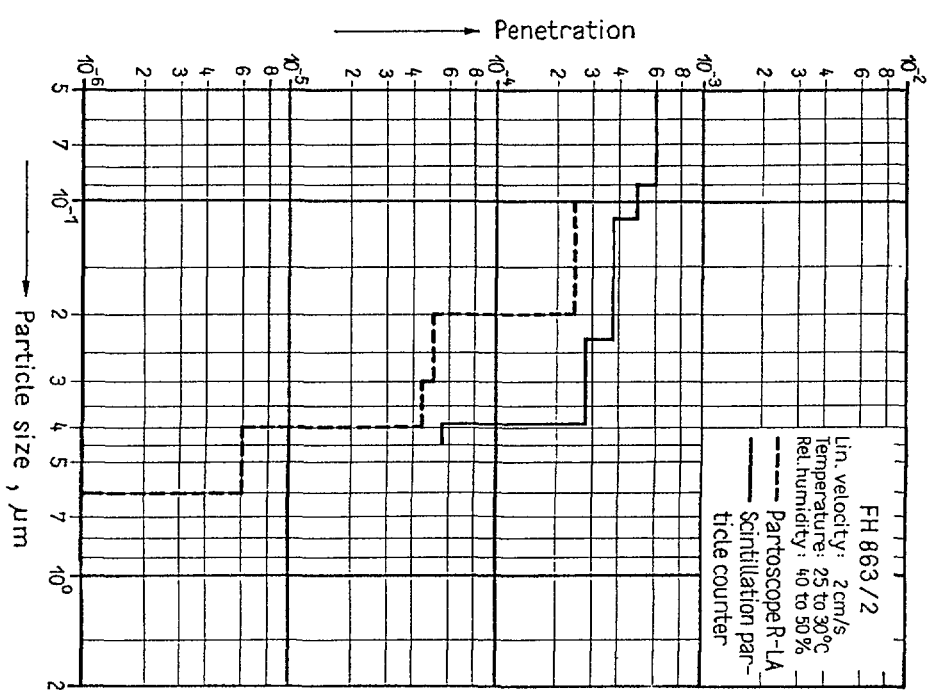


Fig. 8 Penetration of the filter material Microtex FH 863/2 for NaCl test aerosol (laser aerosol spectrometer Partoscope R-LA and scintillation particle counter)

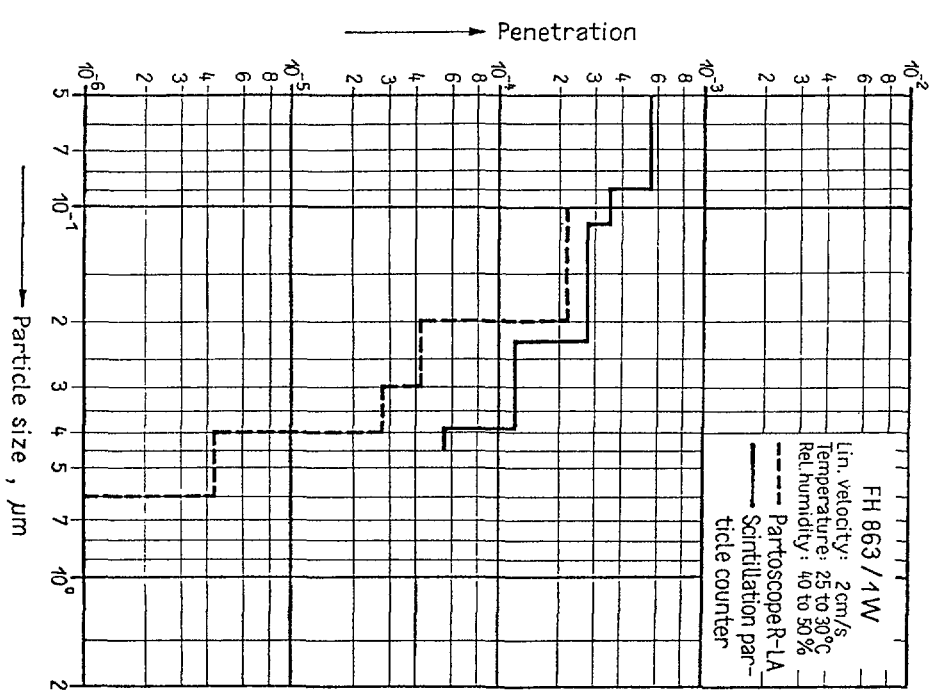


Fig. 9 Penetration of the filter material Microtex FH 863/1W for NaCl test aerosol (laser aerosol spectrometer Partoscope R-LA and scintillation particle counter)

Fig. 10 shows the block diagram of the modified test rig. To moisten the air, an electrically heated steam generator is used. The test aerosol is heated up by an electric air heater. The test rig is equipped with sensors for temperature and relative humidity as well as respective indicating and writing devices. The section for testing samples of filter material has been completely reconstructed. Fig. 11 shows details. The sample of filter material to be tested is fixed in special clamping rings. In the central part of the testing section several clamping rings can be also arranged successively, if necessary.

Two testing sections (A and B) have been set up as shown in Fig. 10. Both are installed in an electric furnace in parallel connection, as shown in Fig. 12. When running testing section A with and testing section B without a sample of filter material the penetration of the material sample tested can be determined by mutual connection of both sections to a suitable aerosol measuring device, using heated connection pipes. Thus the difficulties are avoided which are associated with sampling at high temperature and humidity.

To check the testing equipment, various preliminary investigations have been made at increased temperature. At first, the thermal decomposition process of glass fibre paper NK 13-100 (made in the GDR) was investigated. For this purpose the filter material was heated for 120 min and then the pressure drop characteristic was measured at room temperature. Fig. 13 shows the results. Above 300 °C the pressure drop decreases, probably as a result of thermal decomposition of filter paper.

Then the filter paper was measured after preparation with water vapour for 3 min. The pressure drop of filter paper decreased again above 300 °C (see Fig. 14).

Using test method I (see 4.1.2.) and the modified test stand (see Fig. 5), the penetration of glass fibre paper NK 14-120 was measured at normal and higher temperature (50, 100 and 150 °C) as a function of particle size. Fig. 15 shows the results of this paper made in the GDR and used for pre-filtration (linear velocity 10 cm/s). The change of penetration at higher temperature of up to 150 °C seems negligible for this type of filter material.

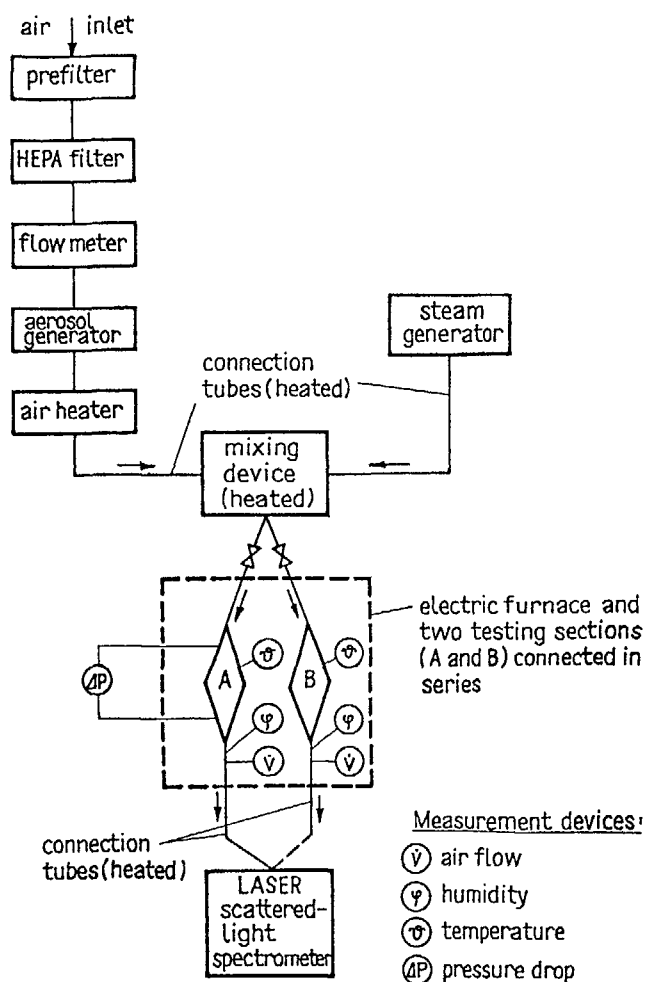


Fig.10 Modified test stand for the investigation of filter materials under high temperature and high humidity (block diagram)

64

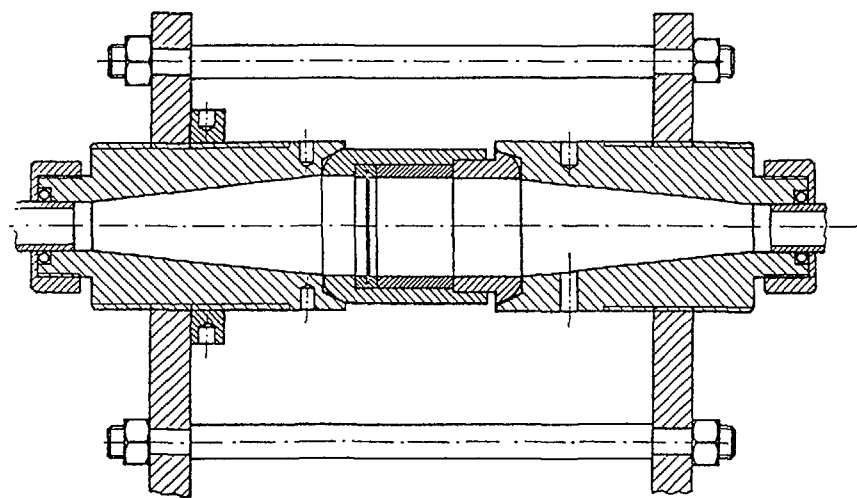


Fig.11 Testing section for filter material

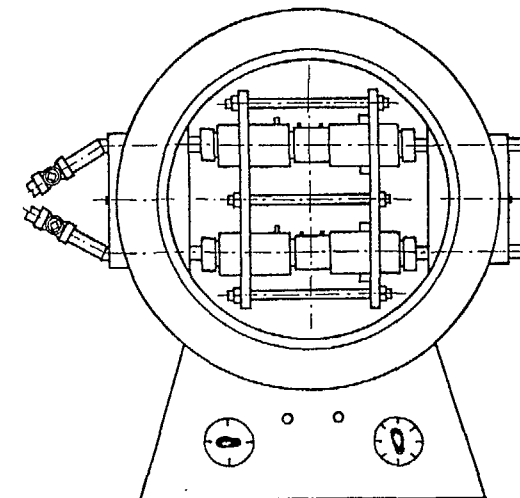


Fig.12 Two testing sections for filter material installed in an electric furnace in parallel connection

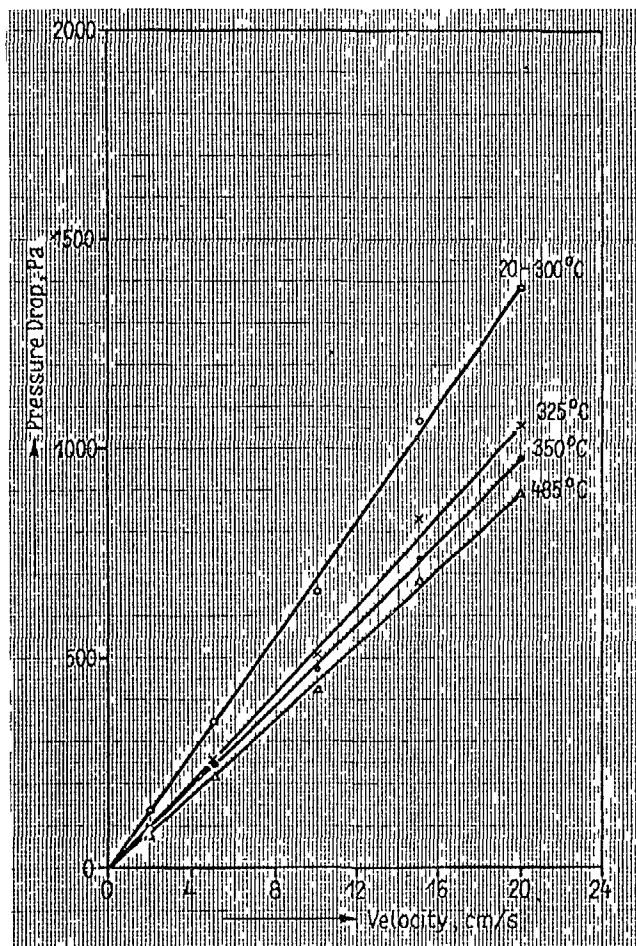


Fig.13 Pressure drop of unheated and heated (120 min) glass fibre paper NK13-100

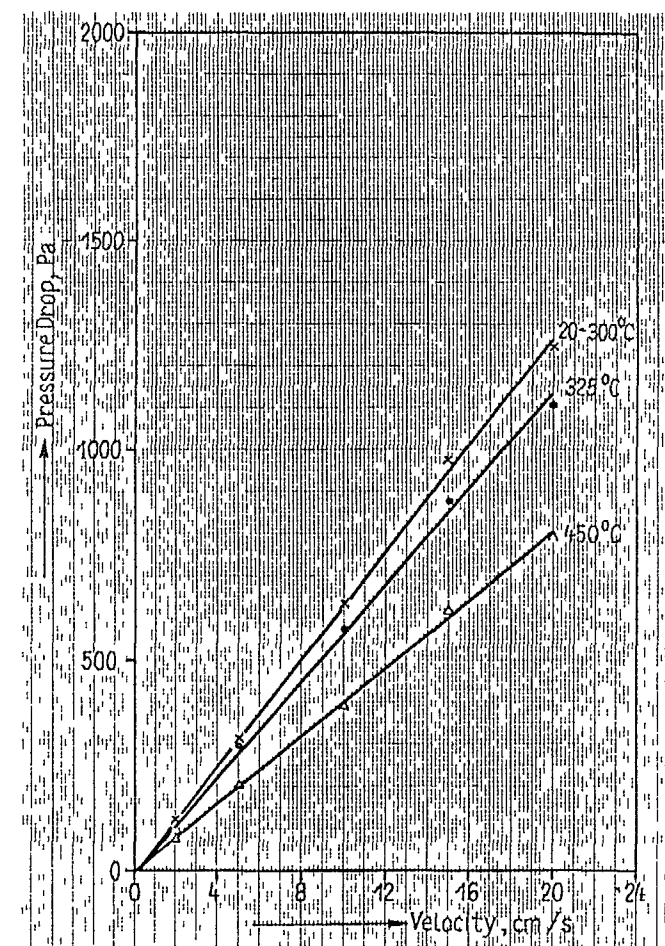


Fig.14 Pressure drop of unheated and heated (120 min) glass fibre paper NK13-100 measured after preparation with water vapour (3 min)

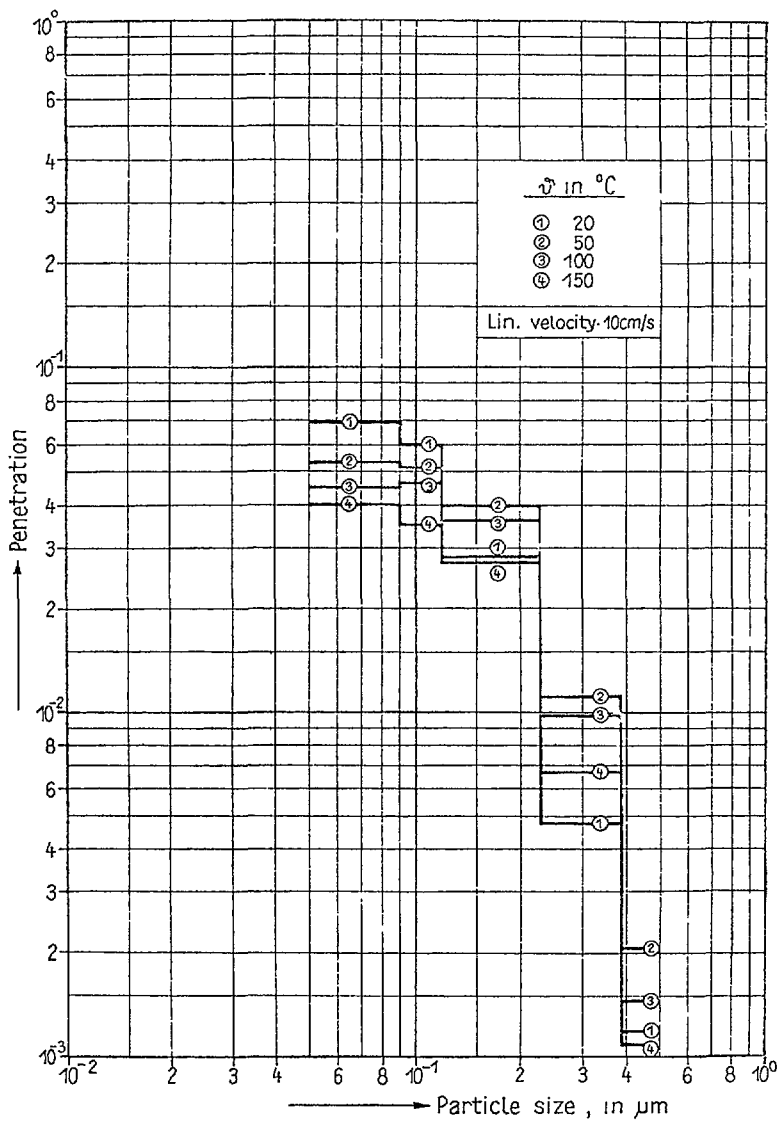


Fig.15 Penetration at normal and higher temperature for NaCl test aerosol
(glass fibre paper NK 14-120; scintillation particle counter)

5. TESTING OF FULL-SIZE FILTERS ON LABORATORY RIG

5.1. Testing of filter FARTOS-Z-500 under normal conditions and after regeneration with water

5.1.1. Description of filter FARTOS-Z-500

FARTOS-type aerosol filters from Soviet production are intended for separating liquid or solid polydisperse aerosols from air and other gases. The filters can be regenerated by spraying or washing. When using the filters for retention of liquid aerosols or fogs a continuous "self-cleaning regime" can be attained. For this purpose the liquid separated in the filter layer and drained by gravitation is continuously let out of the filter casing.

Fig. 16 shows the design of a FARTOS-Z-500 filter. The filter layer is about 5 mm thick and between covering layers of glass fibres tissue. It consists of glass fibres of about 1 μm diameter and is undulatorily arranged around a perforated cylinder, using separators of stainless steel sheet. The filter casing is designed as a pressure vessel. It consists of stainless steel. The connecting branches are arranged axially (gas inlet) and radially (gas outlet). The producers specify the following technical data for the FARTOS-Z-500 filter:

- Nominal volume flow: $\dot{V} = 500 \text{ m}^3/\text{h} (0.139 \text{ m}^3/\text{s})$
- Pressure drop of dry filter: $\Delta p \leq 500 \text{ Pa}$
- Pressure drop of wet filter: $\Delta p \leq 3,000 \text{ Pa}$
- Penetration of dry filter: $P \leq 10^{-4}$
- Penetration of filter at self-cleaning regime: $P \leq 10^{-3}$
- Permissible operating pressure for filter casing: 20 kPa (pressure below atmospheric pressure) up to 150 kPa (excessive pressure)
- Operating temperature: $\leq 100^\circ\text{C}$
- Permissible mass concentration: 50 mg/m³ for dry aerosols
500 mg/m³ for mists
- Separable substances: Dispersions of salts, acids or organic compounds, water and oil mists as well as soluble aerosols

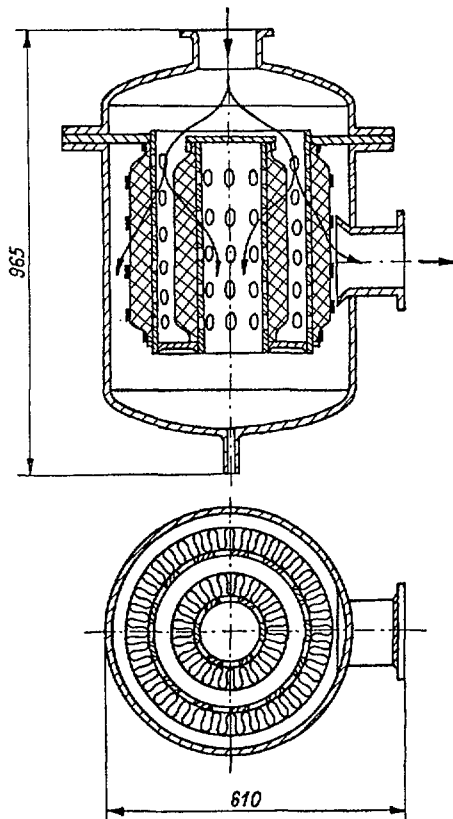


Fig. 16 Aerosol filter FARTOS-Z-500

5.1.2. Test programme

The use of FARTOS-Z-500 filters as safety-relevant components requires detailed knowledge of filter properties, particularly under conditions of long-term operation, as a basis for planning and designing as well as for assessing the reliability and safety properties of filter equipment.

The test programme implemented so far covers the investigation of the following parameters:

- Pressure drop of filter in dependence of volume flow, on drying time after regeneration and on number of regeneration cycles
- Penetration of filter in dependence on volume flow and number of regeneration cycles
- Penetration of filter in dependence on volume flow, on particle size of test aerosol and on number of regeneration cycles.

5.1.3. Set-up of filter test rig

The investigations were made on the filter test rig of the SAAS. The test rig is dimensioned for a steplessly adjustable test air volume in the range from 300 to 5,000 m³/h (dependent on the pressure drop of the filter to be tested). Fig. 17 shows the details of the test rig important for performing the test programme according to 5.1.2.

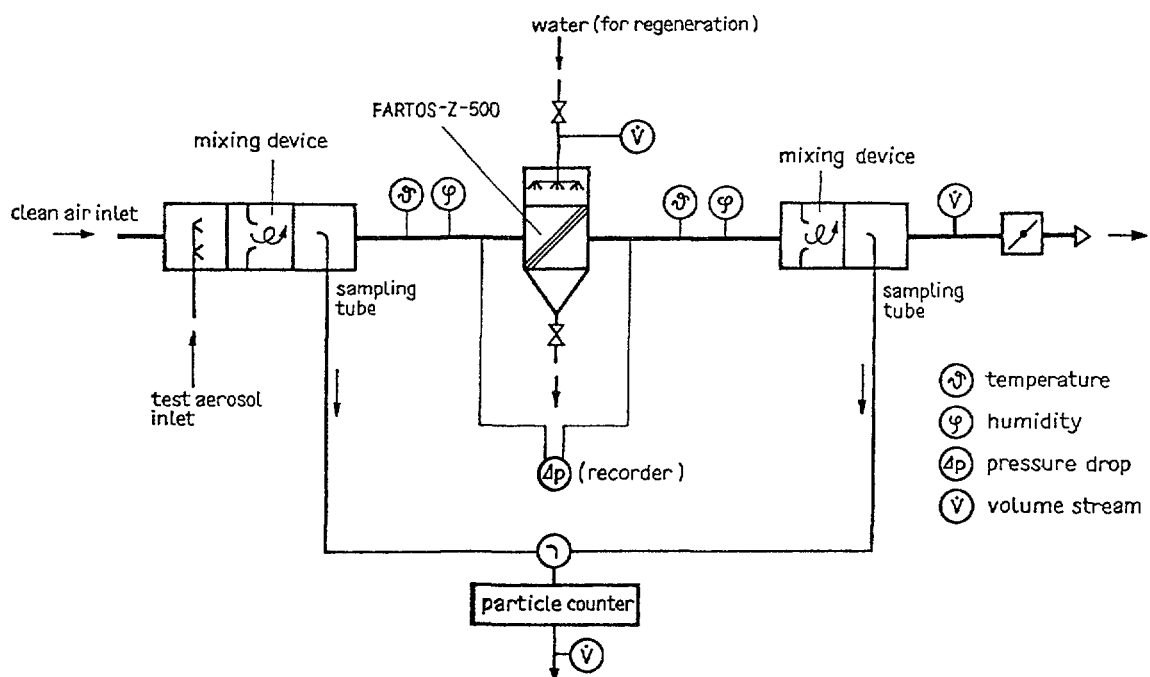


Fig. 17 Testing of the filter FARTOS-Z-500 on laboratory rig (see Fig 25)

The test aerosol is admixed via probe to the test air cleaned in several steps. The air-aerosol mixture is homogenized and fed into the filter to be tested. Filter penetration is determined by taking samples and comparing aerosol concentrations and particle size distributions before and behind the filter.

The duct network of the test stand is subjected to excessive pressure. Therefore, possible leaks in the channel network cannot affect particle concentration. The temperature and relative humidity of air can be controlled within certain limits. They are measured before and behind the filter to be tested. For the determination of humidity, a capacitative humidity sensor (QUARZ AG, Zuerich) has proved a success.

A spraying system installed in the filter casing serves to regenerate the FARTOS-Z-500 filter.

5.1.4. Measuring results and conclusions

- Pressure drop of the FARTOS-Z-500 filter

To check the producers' data, the pressure drop of the unused filter was determined in dependence on the volume flow through the filter. The measuring values represented in Fig. 18 agree with the producers' data. As expected, the course of pressure drop within the range of nominal passage is approximately linear.

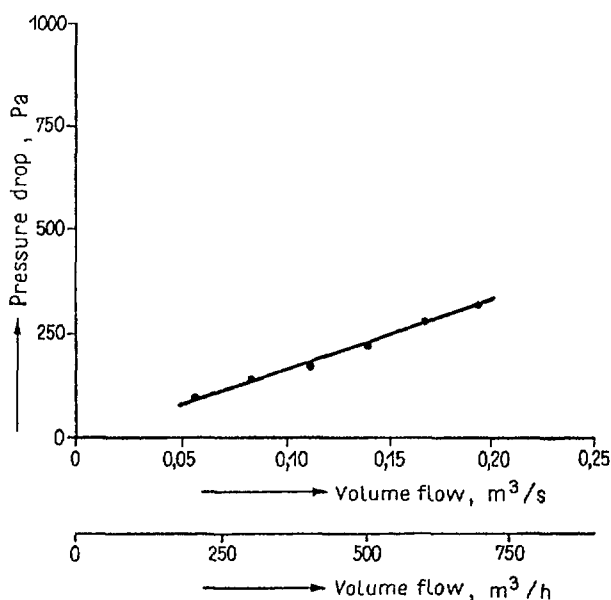


Fig.18 Pressure drop of the new filter unit FARTOS-Z-500

The pressure drop of the filter intensively sprayed with regeneration liquid or immersed into it was determined for the nominal volume flow ($500 \text{ m}^3/\text{h}$) in dependence of the temporal course of regeneration cycles (Fig. 19). To dry filter material, $500 \text{ m}^3/\text{h}$ were passed through the filter. On an average, air temperature was about 24°C , relative humidity of ^{air} fed into the filter about 40 %.

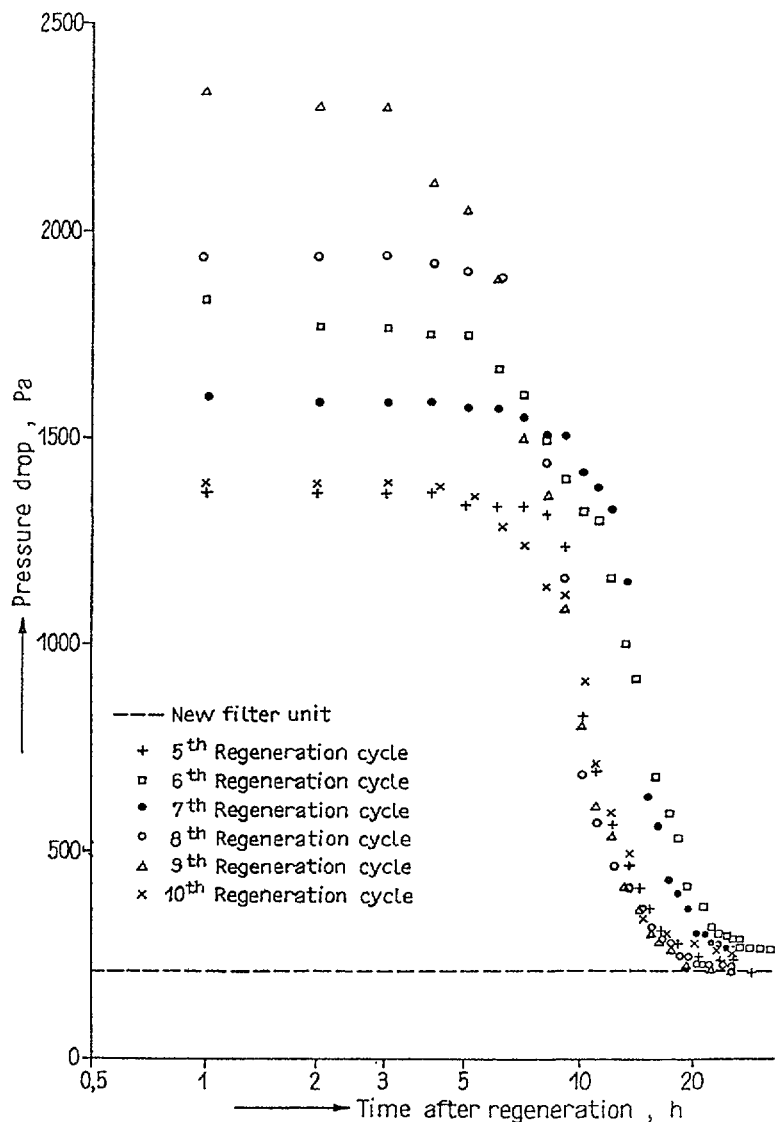


Fig.19 Pressure drop of a filter FARTOS-Z-500 corresponding to the drying process

- Penetration of the FARTOS-Z-500 filter

To measure filter penetration, the aerosol measuring devices described in 2. were used. The results of investigations are shown in Fig.s 20 to 24:

- Fig. 20 shows the penetration of the filter for monodisperse latex aerosol having a particle size of $0.52 \mu\text{m}$ as a function

of volume flow and number of regeneration cycles. The measurements were made by Partoscope R-LA.

- Fig. 21 shows the penetration of the unused filter when using NaCl test aerosol (see 3.) for the volume flows of 300, 500 and 750 m³/h in dependence of particle size. The measurements were also made by Partoscope R-LA.
- Fig.s 22 (volume flow 300 m³/h), 23 (500 m³/h) and 24 (750 m³/h), respectively, show the penetrations for the unused filter and for that used after individual regeneration cycles in dependence on the particle size of the NaCl test aerosol (see 3.). For aerosol measurement, the scintillation particle counter could be used since the investigations of the regenerated filter were made only after drying the fibre layer (see 5.1.3.) at a relative air humidity of about 40 % (maximally 50 %).

The values measured at volume flows within the range from 300 to 750 m³/h for the penetration of the dry filter are greater than the values stated by the filter producers. This holds both for the unused filter and for that used after individual regeneration cycles. It is assumed that this is due to the measuring method underlying the producers' data (testing by oil mist). In comparison, the test method used in the SAAS also allows an assessment of the protective effect of the filter at particle sizes in the maximum range of filter penetration.

The maximum values of penetration were found out in dependence on volume flow and, thus, on flow velocity at particle diameters in the range from 0.25 to 0.4 µm. With increasing volume flow, the penetration maximum shifts towards smaller particle sizes.

The measurements made so far show a relatively good agreement between the results obtained with laser aerosol spectrometer and with scintillation particle counter. Existent deviations are due to different measuring principles. Independent of the water content of particles, the scintillation particle counter allows an indication proportional to the NaCl-mass of particles. Independent of the salt content of particles, the measuring result of the laser aerosol spectrometer is approximately proportional to the surface of particles. Consequently,

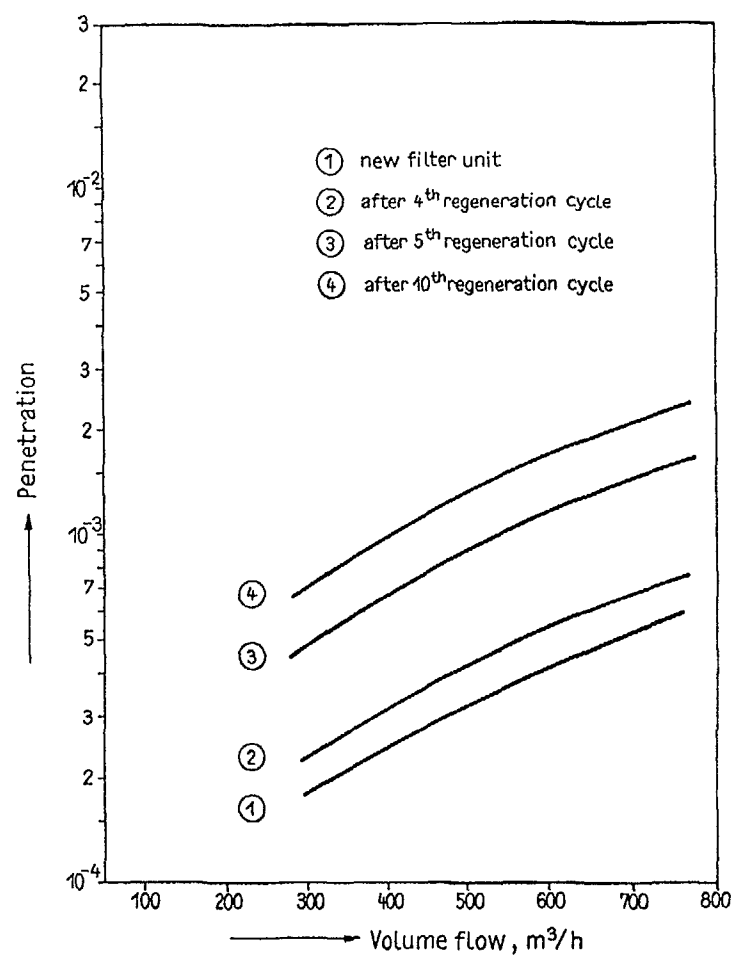


Fig.20 Penetration of the filter FARTOS-Z-500 for monodisperse Latex test aerosol ($0.52\text{ }\mu\text{m}$)

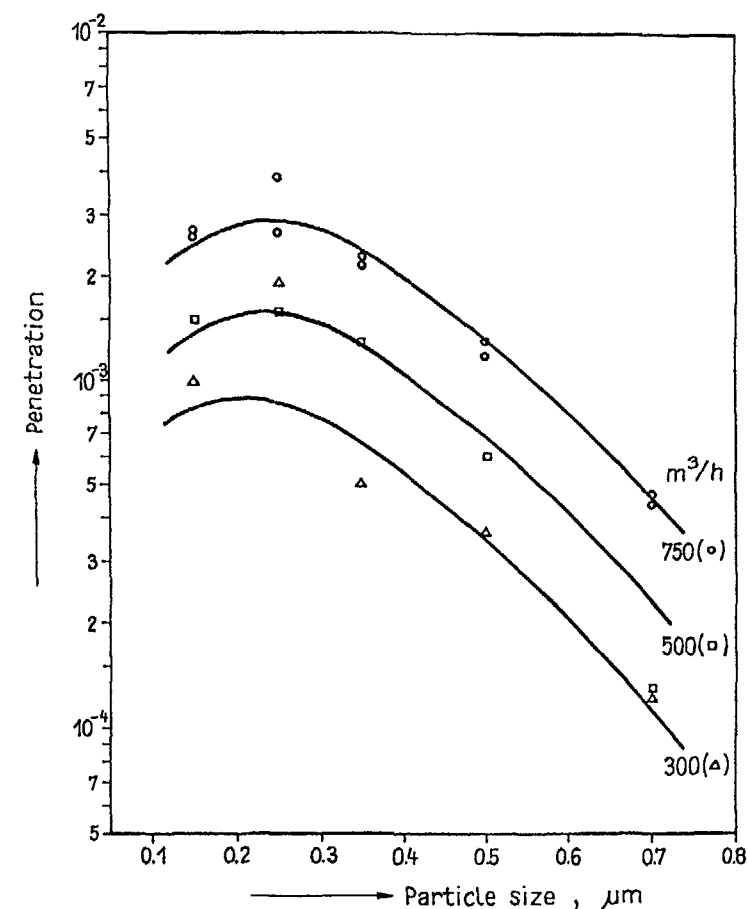


Fig.21 Penetration of the unused filter FARTOS-Z-500 for NaCl test aerosol

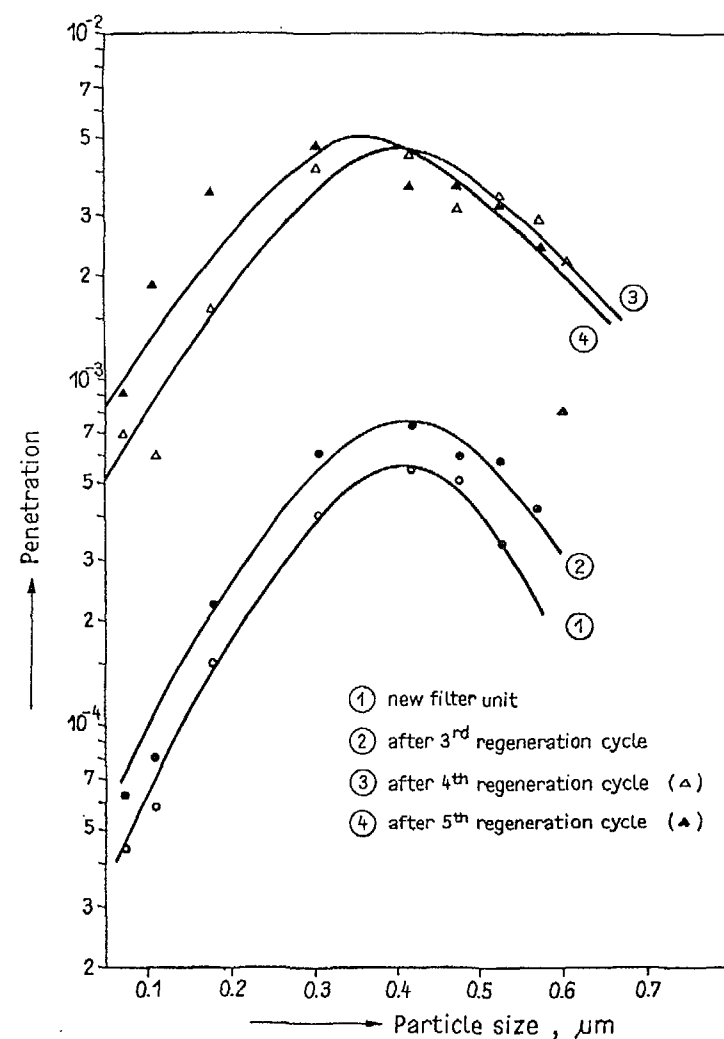


Fig.22 Penetration of the filter FARTOS-Z-500 for NaCl test aerosol (volume flow $300 \text{ m}^3/\text{h}$)

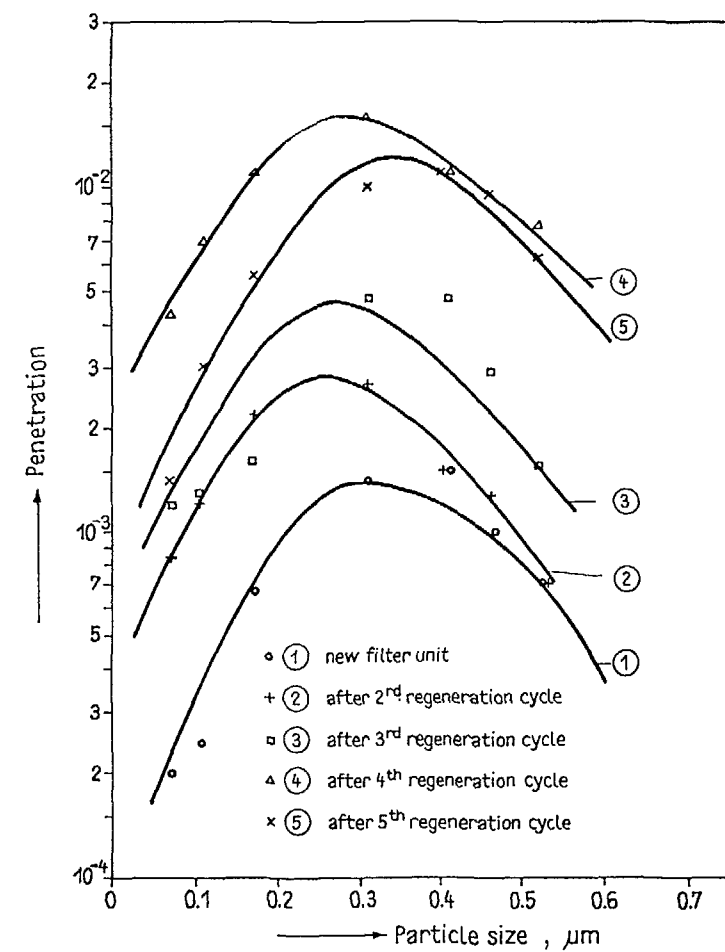


Fig.23 Penetration of the filter FARTOS-Z-500 for NaCl test aerosol (volume flow $500 \text{ m}^3/\text{h}$)

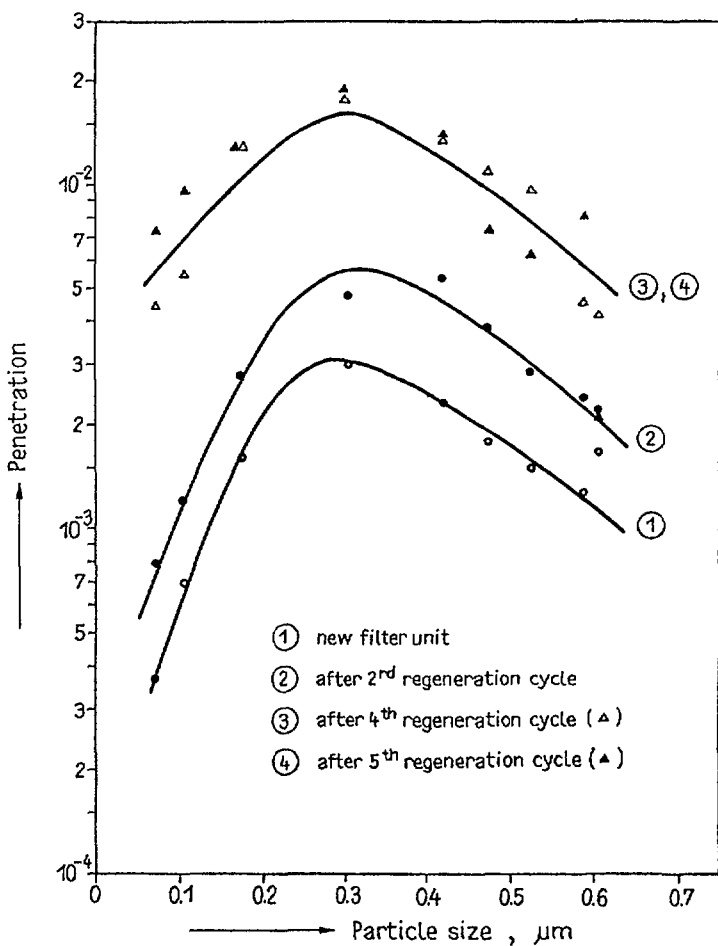


Fig. 24 Penetration of the filter FARTOS-Z-500 for NaCl test aerosol (volume flow $750 \text{ m}^3/\text{h}$)

water drops without or with small salt content carried along by the air stream, which can occur e.g. at incomplete drying after filter regeneration, cause different results of measurement by the mentioned devices.

With increasing number of regeneration cycles, the penetration of the filter increases much more for the NaCl test aerosol than for the latex test aerosol (compare Fig. 20 and 22 to 24). This likely is due to the complete soaking of the fibre layer due to the effect of the spraying agent since, in this way, the NaCl separated on the inflow side of the fibre layer is distributed in the entire filter material. Consequently, after subsequent drying of filter material, NaCl-particles can be split off by mechanical stress. This effect has to be allowed for when assessing the filter since this can also occur when the filter is used in practice.

To fully clear up the states-of-affairs, supplementary investigation have been scheduled. These include the investigation of the effect of the drying state of the filter after regeneration on filter penetration and the determination of filter properties at operation under largely steam-saturated air.

5.2. Testing at increased humidity

Fig. 25 shows the filter test rig dimensioned for experimental investigations at increased relative humidity of air. It meets the following requirements:

- Effective humidification to attain relative humidities of up to 100 % at constant values for several hours
- Possibility of separating drops and mist
- High-grade cleaning of air from atmospheric aerosol particles or those introduced by humidification before adding test aerosol
- Dynamic humidity measurement before and behind the test filter
- Possibility of circuit operation to improve constancy of temperature and humidity of the test flow.

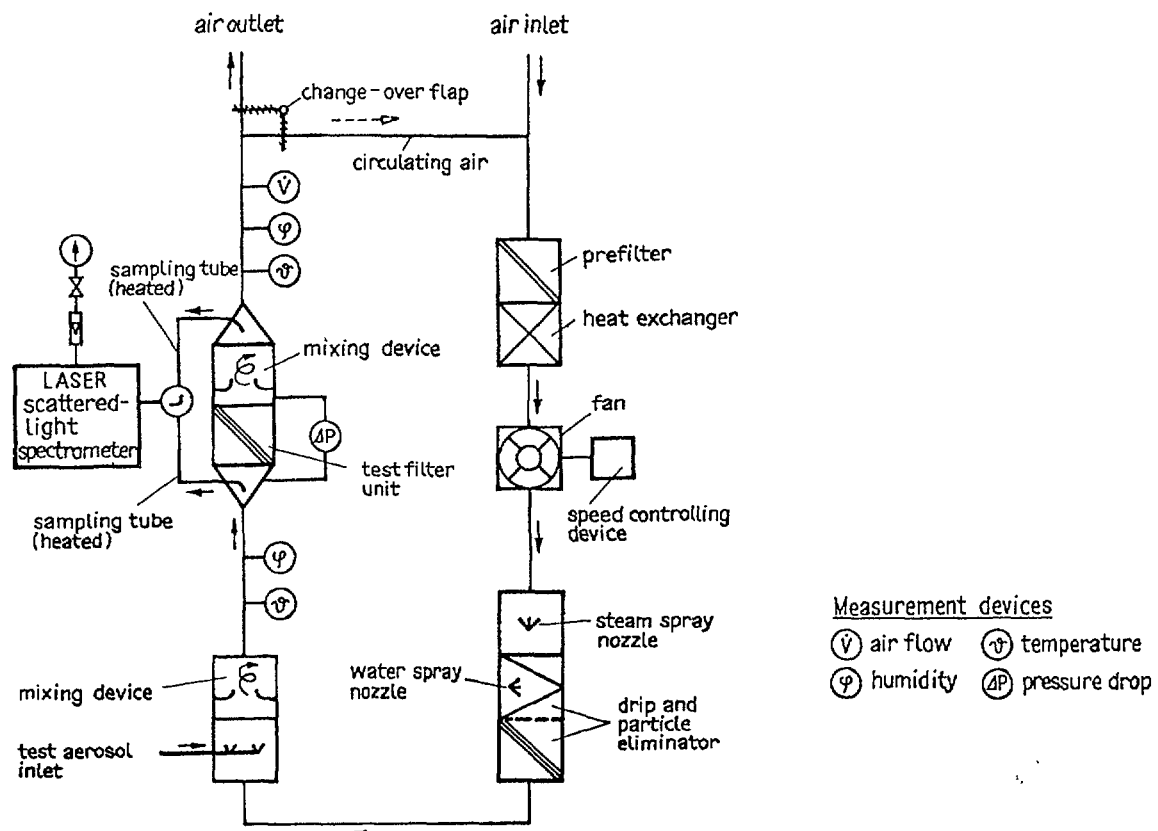


Fig.25 Testing of HEPA filters on laboratory rig under high humidity (schema)

To moisten the air, steam is introduced since, at this type of humidification, considerable changes of air temperature are avoided and high efficiency of humidification can be attained. To keep the saturation state constant, steam introduction is overdosed and subsequently the excessive steam is retained and simultaneously the undesired solid aerosol developed during humidification separated in a special fibre-mat separator. To monitor air parameters, the measuring equipment is supplemented by corresponding measuring devices for relative humidity (see 5.1.3.). The possibility of testing filters over periods of several hours at stable parameters is realized by switching to circuit operation. The sampling pipes are equipped with a heater to avoid condensation of humidity and thus an impairment of representative sampling.

For aerosol measurement scattered-light spectrometers are suitable.

In accordance with the recommendations elaborated at the Second Meeting of the Coordinated Research Programme in TORONTO (see 1.), investigations of full-size filters under abnormal conditions are to be made only at a later time. To this effect, respective data are to be supplied by the Agency.

REFERENCES

- / 1 / BRITISH STANDARD INSTITUTION
British Standard BS-2831 (1965)
- / 2 / BINEK, B., DOHNALOVA, B., PRZYBOROWSKI, S., ULLMANN, W.
Die Anwendung des Szintillationsspektralanalysators für
Aerosole in Forschung und Technik
Staub, Reinhalt. Luft 27 (1967) 379
- / 3 / INSTRUCTION BOOK
Laser light-scattered aerosol spectrometer Partoscope
R-LA
KRATEL Instrumente GmbH
- / 4 / SPECIFICATION
Mikrotex FH 863/2, 863/1 W, 929 and 1047
J.C. BINZER Paper Manufacture

- / 5 / ULLMANN, W., PRZYBOROWSKI, S.
Comparison of testing methods for particulate filters
IAEA-TECDOC-355 (1985) 31
- / 6 / SCHIRJAJEW, F. S., KARPOW, W. M., KRUPTSCHATNIKOW, E.L.,
MAKAJEW, JU. N. et al.
Environmental protection in nuclear facilities
Moscow, Energoisdat, 1982, 79-82 (in Russian)

INVESTIGATIONS ON THE AGEING OF ACTIVATED CARBONS IN THE EXHAUST AIR OF A PRESSURIZED WATER REACTOR (PWR 4)

H. DEUBER, K. GERLACH, R. KAEMPFER
Laboratorium für Aerosolphysik und Filtertechnik,
Kernforschungszentrum Karlsruhe GmbH,
Karlsruhe, Federal Republic of Germany

Abstract

Investigations were performed on the aging of five activated carbons in the containment exhaust air of a German pressurized water reactor to find out whether longer stay times can be obtained with activated carbons other than that usually employed (207B (KI)) in the Federal Republic of Germany.

The aging with respect to the retention of methyl iodide ($\text{CH}_3^{131}\text{I}$) was smaller with activated carbons impregnated with KI_x only than with those impregnated additionally or exclusively with a tertiary amine (e.g. TEDA). It is concluded that, for the exhaust air examined, presently no longer stay times can be obtained with activated carbons other than 207B (KI).

INTRODUCTION

In German nuclear power plants the exhaust air filters must exhibit a minimum retention of 90 to 99 % for organic radioiodine (methyl iodide) under the most unfavorable conditions /1, 2, 3/. With iodine filters that are continuously operated (e.g. the containment exhaust air filters of pressurized water reactors) the stay times are frequently less than one year because of the relatively rapid aging of the activated carbon contained in the filters /4, 5/.

The aging of activated carbons in iodine filters is essentially due to the adsorption of organic compounds (e.g. solvents) and of inorganic compounds (e.g. O_x , SO_2 , NO_x). In the first case the effective surface of the activated carbon is lowered. In the second case reactions with the carbon (and the impurities such as sulphur) as well as with the impregnant may occur. Moreover, the alcalinity of the activated carbon may be reduced /6, 7/. The physical and

chemical processes during the aging of activated carbons are being investigated both experimentally /8/ and theoretically /9/.

In the iodine filters of German nuclear power stations the activated carbon 207B(KI) (Table I) is usually employed. Investigations are being conducted on the retention of methyl iodide ($\text{CH}_3^{131}\text{I}$) and other iodine species by different impregnated activated carbons as a function of the aging time under simulated normal operational conditions to find out whether longer stay times can be achieved with other activated carbons, in particular with those developed in recent years /10, 11/.

Table I: Data of the activated carbons investigated

Name	Impregnant	Base material	Size ^a (mesh)	Supplier
207B (KI)	KI	coal	8 - 12	Sutcliffe Speakman (UK)
727	KI_3	coconut shell	8 - 16	Barnaby and Cheney (USA)
207B (KI, TEDA)	KI, TEDA	coal	8 - 12	Sutcliffe Speakman (UK)
Kiteg II	KI, amine	coconut shell	8 - 16	Nucon (USA)
207B (TEDA)	TEDA	coal	8 - 12	Sutcliffe Speakman (UK)

^a 8 - 12 mesh: BS 410 /29/; 8 - 16 mesh: ASTM D2862 /30/

In the present paper investigations are covered on the aging of five different impregnated activated carbons in the containment exhaust air of a pressurized water reactor (PWR4) over a period of three months. Apart from the retention of $\text{CH}_3^{131}\text{I}$, the retention of ^{131}I contained in the exhaust air was examined. Moreover, the reasons for aging were determined.

A report has already been published on measurements in the containment exhaust air of PWR4, which partly had the same objectives /12/.

FORMER INVESTIGATIONS

Numerous investigations have been performed on the aging of activated carbons in the exhaust air of nuclear power stations /6, 7, 13/. However, it is difficult to judge from these investigations the aging of different activated carbons in the exhaust air of other nuclear power stations. This is in

particular due to the complexity of the aging process and to the differences in type and concentration of the pollutants in the exhaust air.

The investigations in the Federal Republic of Germany were so far nearly exclusively conducted with KI impregnated activated carbons, essentially in order to identify the pollutants and optimize the layout of iodine filters /14, 15/. Solely in the exhaust air of a research reactor was a TEDA impregnated activated carbon tested, with a positive result /16/.

In other studies a good aging behavior was found with activated carbons impregnated additionally or exclusively with TEDA or other tertiary amines /17, 18/. Also during the storage of activated carbons (in closed containers), in which the aging is relatively small, the best aging behavior was observed with a TEDA impregnated activated carbon /19, 20/.

EXPERIMENTAL

Data of the investigated commercial activated carbons are contained in Table I. Three groups of impregnants can be distinguished:

- a) KI_x;
- b) KI + tertiary amine;
- c) tertiary amine (TEDA).

The activated carbons 207B (KI), 727 and 207B (TEDA) have been on the market since many years, whereas 207B (KI, TEDA) and Kiteg II have been developed in recent years.

In the investigations covered in this paper the activated carbons were challenged with the containment exhaust air of PWR4 over a period of three months during power operation of the reactor. (During refueling outage both weaker and stronger /15/ aging has been observed.) The operating conditions of the beds of activated carbons corresponded essentially to the operating conditions of the iodine filters of German nuclear power stations in normal situations and were largely identical with those in the subsequent laboratory tests with methyl iodide. The parameters of the laboratory tests are given in Table II.

Table II: Parameters of the tests with $\text{CH}_3^{131}\text{I}$

Parameter	Unit	Value
Temperature	°C	30 ^a
Relative humidity	%	40 ^a
Throughput	m^3/h	0.88 ^a
Face velocity	cm/s	50 ^a
Preconditioning time	h	1 ^b
Injection time	h	1
Purging time	h	2
Bed depth	cm	50 ^{a, c}
Residence time	s	1 ^a
^{131}I injected	mCi	0.01 - 0.1
^{127}I injected	mg	1

^a Value (largely) identical with that during the aging in the nuclear power plant

^b ≥ 16 h with fresh carbon

^c 20 beds of a depth of 2.5 cm (diameter: 2.5 cm); sequence identical with that during the aging in the nuclear power plant

As for methyl iodide ($\text{CH}_3^{131}\text{I}$), this compound is usually used as a model substance for organic iodine compounds in retention tests. Generally, it is to be found in large proportions in the exhaust air of nuclear power plants /12, 21, 22/.

The tests with $\text{CH}_3^{131}\text{I}$ were run both with fresh and aged activated carbon. In the second case, the original arrangement of the activated carbon was maintained. Thus, the geometrical course of the aging within the sectioned beds could be ascertained. As indicated in Table II, the aged carbon was preconditioned over a period of one hour only to minimize the desorption of pollutants.

Details on the performance of the tests with $\text{CH}_3^{131}\text{I}$ are to be found in the literature /7, 12/. The reproducibility in these tests is excellent /23/. The minimum detectable penetration, determined with NaI detectors, was 10^{-5} to 10^{-4} %. Prior to the test with $\text{CH}_3^{131}\text{I}$, the ^{131}I retained by the activated carbon from the exhaust air was measured with Ge(Li) detectors.

Because of the low ^{131}I concentration in the exhaust air, the detection limit, related to the total ^{131}I retained, was about 1 % per bed in this case. (The ^{131}I from the plant was allowed to decay to a negligible quantity prior to the test with $\text{CH}_3^{131}\text{I}$.)

In order to ascertain the reasons for aging, an additional sectioned bed of the activated carbon 207B (KI) was simultaneously challenged with the exhaust air. After three months, the loading of this bed with organic compounds and - by the alkalinity - with inorganic compounds was determined. In the first case the CCl_4 extracts of the activated carbon were analyzed gas chromatographically (14,24/. In the second case the $P_{\text{H}_2\text{O}}$ values of the H_2O extracts were measured /25/.

RESULTS

The results obtained with $\text{CH}_3^{131}\text{I}$ are generally presented in terms of penetration here. Fig.1 displays the penetration of 207B (KI) by $\text{CH}_3^{131}\text{I}$ as a function of the bed depth at different aging times. With the fresh carbon, using a semilogarithmic plot, the usual linear decrease of penetra-

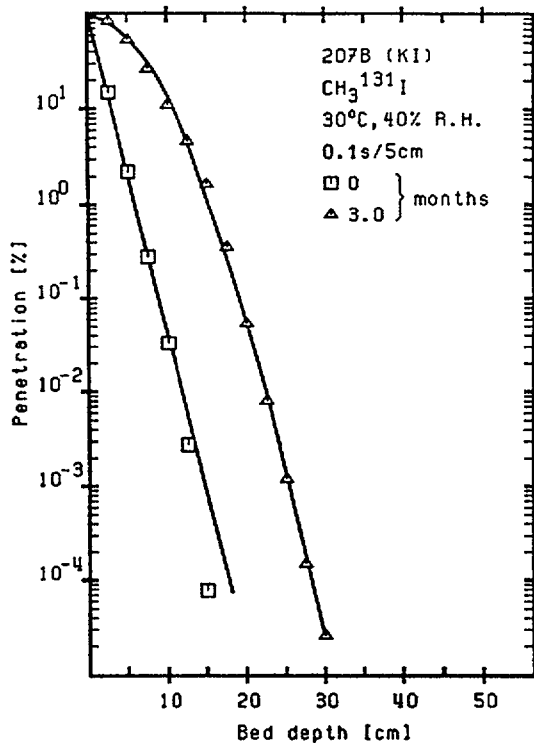


FIG. 1.
Penetration as function of bed depth
at different aging times

tion with increasing bed depth was found /23, 26/. With the aged carbon a nonlinear course (flat at a low bed depth) of the penetration curve was obtained. This form of the penetration curve corresponds to a decrease in aging with increase of the bed depth. With the other carbons qualitatively similar penetrations were observed.

Important results for the activated carbons investigated are given in Table III and in Fig. 2. The main results are as follows:

- a) Prior to aging the carbons impregnated with KI_x only exhibited a much higher penetration than those impregnated additionally or exclusively with an amine. At a bed depth of 12.5 cm (residence time of 0.25 s) the difference in penetration was up to three orders of magnitude. The highest penetration was found with 207B (KI), the lowest with 207B (TEDA).
- b) After aging the penetration of the carbons was relatively similar. At a bed depth of 12.5 cm the difference was maximally only somewhat greater than one order of magnitude. The highest penetration was found with the carbon 727, the lowest again with 207B (TEDA).

Table III: Penetration of various impregnated activated carbons by $\text{CH}_3^{131}\text{I}$ at different aging times
(Data of activated carbons: Table I; test data: Table II)

Activated carbon	Bed depth (cm)	Residence time (s)	Penetration (%) ^a	
			0 months	3 months
207B (KI)	12.5	0.25	2.77 (-3)	4.65 (0)
	25.0	0.50	-	1.21 (-3)
727	12.5	0.25	1.52 (-3)	3.67 (+1)
	25.0	0.50	-	5.35 (-1)
207B (KI,TEDA)	12.5	0.25	2.60 (-6) ^b	5.20 (0)
	25.0	0.50	-	1.77 (-3)
Kiteg II	12.5	0.25	3.61 (-5)	1.21 (+1)
	25.0	0.50	-	2.23 (-2)
207B (TEDA)	12.5	0.25	1.10 (-6) ^b	1.12 (0)
	25.0	0.50	-	5.80 (-5)

^a $2.77 \text{ (-3)} = 2.77 \cdot 10^{-3}$ etc.;

- : penetration lower than minimum detectable penetration ($10^{-5} - 10^{-4}$ %)

^b extrapolated

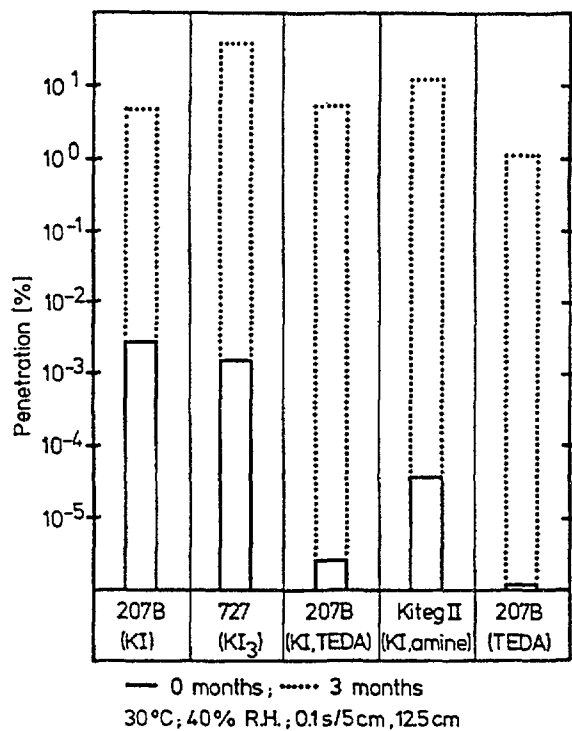


FIG. 2.

Penetration of various impregnated activated carbons by $\text{CH}_3^{131}\text{I}$ at different aging times

The low penetration of fresh amine impregnated activated carbons by $\text{CH}_3^{131}\text{I}$ is in keeping with results in the literature /27/, also the same finding after aging /17, 18/. However, as found here, the aging of amine impregnated carbons can be stronger than that of KI impregnated carbons. The low penetration of amine impregnated carbons after aging is consequently due to the better performance prior to aging. (Mention is made here of the fact that some experts do not recommend TEDA impregnated activated carbons for use in iodine filters of nuclear power plants because of the low inflammation temperature and high volatility of TEDA /31/.)

The aging behavior of the activated carbon 207B (KI) corresponds essentially to that observed earlier in the same exhaust air /12/.

As for the $\text{CH}_3^{131}\text{I}$ from the exhaust air, Fig. 3 displays the distribution of $\text{CH}_3^{131}\text{I}$ on the beds of 207B (KI). The corresponding distribution obtained in the subsequent test with $\text{CH}_3^{131}\text{I}$ is also indicated. At high bed depths the penetration by $\text{CH}_3^{131}\text{I}$ from the plant was higher than that by $\text{CH}_3^{131}\text{I}$. This may be attributed to more penetrating iodine species occurring in small proportions in the exhaust air of pressurized water reactors /12, 28/. With the other carbons, essentially the same distributions were observed.

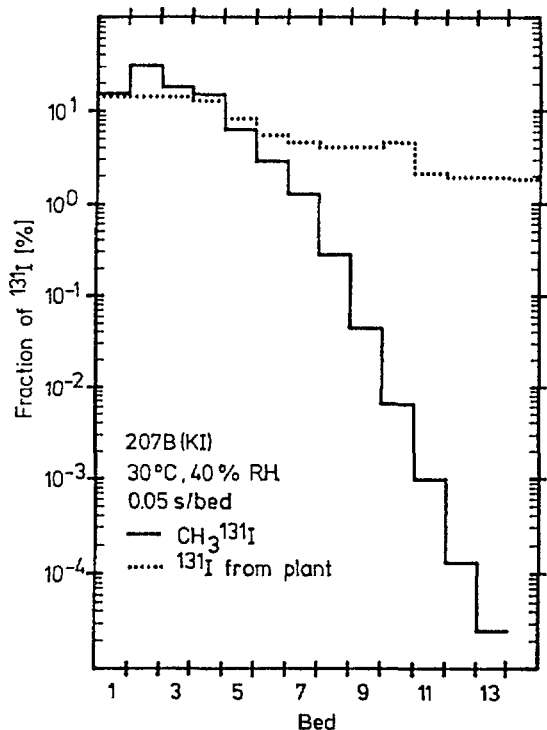


FIG. 3.

Distribution of ^{131}I on activated carbon beds
at an aging time of 3 months

The loading of 207B (KI) with organic compounds is shown in Fig.4. Compounds of high and low volatility are distinguished. The former consisted in particular of toluene, xylene and nonane, the latter of decane and dodecane. The high-volatile compounds were found on all the beds, in particular on the beds 3 to 12. The low-volatile compounds, however, were practically only observed on the beds 1 to 4. These are the beds with a

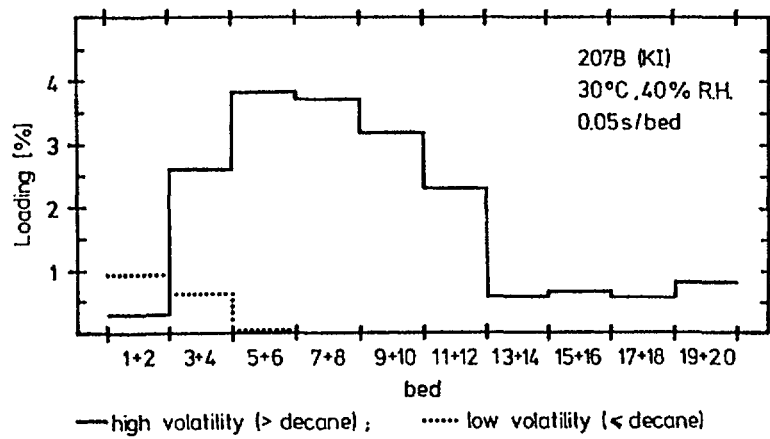


FIG. 4.

Loading of activated carbon beds with organic compounds of different volatility
at an aging time of 3 months

particularly low removal of $\text{CH}_3^{131}\text{I}$. As the alcalinity of the aged 207B (KI) was found to be unchanged, it is obvious that, in agreement with former measurements, the aging was largely due to the adsorption of low-volatile organic compounds.

CONCLUSION

From the investigations performed on the aging of five activated carbons in the containment exhaust air of a German pressurized water reactor it is concluded that, for the exhaust air examined, presently no significantly longer stay times can be obtained with activated carbons other than that usually employed (207B (KI)) in the Federal Republic of Germany.

ACKNOWLEDGEMENT

The investigations were sponsored by the Federal Minister of the Interior of the Federal Republic of Germany.

REFERENCES

- /1/ Reaktorsicherheitskommission,
RSK-Leitlinien für Druckwasserreaktoren,
Gesellschaft für Reaktorsicherheit (1981)
- /2/ Normenausschuß Kerntechnik im DIN,
Lüftungstechnische Anlagen in Kernkraftwerken, DIN 25 414 (1983)
- /3/ Der Bundesminister der Justiz,
Bekanntmachung von Empfehlungen der Reaktor-Sicherheitskommission
und der Strahlenschutzkommission (Störfallberechnungsgrundlagen für
die Leitlinien des BMI zur Beurteilung der Auslegung von Kernkraft-
werken mit DWR gemäß § 28 Abs. 3 StrlSchV),
Beilage zum Bundesanzeiger 245 (1983) 10
- /4/ Wilhelm, J.G. et al.,
Behavior of gasketless deep bed charcoal filters for radioiodine removal
in LWR power plants,
16th DOE Nuclear Air Cleaning Conference, San Diego, 20 - 23 Oct. 1980,
CONF - 801 038, p. 465
- /5/ Wilhelm, J.G. et al.,
Operational experience with iodine filters at German LWRs,
CEC Seminar on Iodine Removal form Gaseous Effluents in the
Nuclear Industry, Mol, 21 - 24 Sept. 1981,
V/5283/82, p. 625

- /6/ Kovach, J.L.,
The evalution and current state of radio-iodine control,
16th DOE Nuclear Air Cleaning Conference, San Diego, 20 - 23 Oct. 1980,
CONF - 801 038, p. 417
- /7/ Wilhelm, J.G.,
Iodine filters in nuclear installations,
Commission of the European Communities,
V/2110/83 (1982)
- /8/ Billings, B.H.M. et al.,
The desorption of chemisorbed oxygen from activated carbons and its
relationship to ageing and methyl iodide retention efficiency,
Carbon 22 (1984) 83
- /9/ Ben-Haim, Y.,
Design against weathering of iodine filters,
Nucl. Techn. 47 (1980) 110
- /10/ Underhill, D., Laskie, J.,
Modified TEDA impregnants for methyl iodide removal,
16th DOE Nuclear Air Cleaning Conference,
San Diego, 20 - 23 Oct. 1980,
CONF - 801 038, p. 531
- /11/ Kovach, J.L. et al.,
TEDA vs. quinuclidine: evaluation and comparision of two tertiary
amine impregnants for methyl iodide removal from flow air stream,
17th DOE Nuclear Air Cleaning Conference, Denver, 2 - 5 Aug. 1982,
CONF - 820 833, p. 652
- /12/ Deuber, H.,
Untersuchungen zur Abscheidung von ^{131}I durch ein Iodfilter eines
Druckwassereaktors,
KfK 3594 (1983)
- /13/ Holladay, D.W.,
A literature survey: methods for the removal of iodine species from
off-gases and liquid waste streams of nuclear power and nuclear fuel
reprocessing plants, with emphasis on solid sorbents,
ORNL/TM - 6350 (1979)
- /14/ Furrer, J. et al.,
Alterung und Vergiftung von Iod-Sorptionsmaterialien in Kernkraftwerken/
Ageing und poisoning of iodine filters in nuclear power plants,
Kerntechnik 18 (1976) 313
- /15/ Wilhelm, J.G. et al.,
Untersuchung zur Ertüchtigung von Iodsorptionsfiltern zur Reinigung
der Abluft von Kernkraftwerken,
KfK 3194 B (1981)

- /16/ Wilhelm, J.G. et al.,
Alterung von Spaltiod-Sorptionsmaterialien,
KfK 2050 (1974) 84
- /17/ Deitz, V.R.,
Effects of weathering on impregnated charcoal performance,
NUREG / CR - 2112 (1981)
- /18/ Kovach, J.L., Rankovic, L.,
Evaluation and control of poisoning of impregnated carbons used for
organic iodide removal,
15th DOE Nuclear Air Cleaning Conference, Boston, 7 - 10 Aug. 1978,
CONF - 780 819, p. 368
- /19/ Collins, R.D. et al.,
The ageing of charcoals used to trap radioiodine,
IAEA/NEA (OECD) Symposium on Management of Gaseous Wastes from
Nuclear Facilities,
Vienna, 18 - 22 Feb. 1980, STI/PUB/561, p. 571
- /20/ Hillary, J.J. et al.,
The ageing of European charcoals used to trap radio-iodine,
CEC Seminar on Iodine Removal from Gaseous Effluents in the
Nuclear Industry, Mol, 21 - 24 Sept. 1981, V/5283/82, p. 167
- /21/ Deuber, H.,
Die physikalisch-chemischen Radioiodkomponenten in der Abluft eines
Druckwasserreaktors (DWR 3),
KfK 3207 (1981)
- /22/ Deuber, H.,
Die physikalisch-chemischen ^{131}I -Komponenten in der Abluft eines
Siedewasserreaktors (SWR 5),
KfK 3666 (1984)
- /23/ Deuber, H., Gerlach, K.,
Laboratory tests of activated carbon for methyl iodide retention:
influence of various parameters,
IAEA Seminar on the Testing and Operating of Off-Gas Cleaning Systems
at Nuclear Facilities,
Karlsruhe, 3 - 7 May 1982, IAEA - SR - 72/34
- /24/ Furrer, J. et al.,
Alterung und Vergiftung von Iodsorptionsmaterialien,
KfK 2600 (1978) 126
- /25/ American Society for Testing and Materials,
Standard test method for pH of activated carbon,
ASTM D 3838 (1980)

- /26/ Shiomi, H. et al.,
A parametric study on removal efficiency of impregnated activated charcoal and silver zeolite for radioactive methyl iodide,
17th DOE Nuclear Air Cleaning Conference, Denver, 2 - 5 Aug. 1982 ,
CONF - 820 833, p.199
- /27/ Hillary, J.J., Taylor, L.R.,
The performance of commercially prepared impregnated charcoals for the trapping of methyl iodide,
TRG 2906 (W) (1977)
- /28/ Deuber, H., Wilhelm, J.G.,
Occurrence of penetrating iodine species in the exhaust air of PWR power plants,
16th DOE Nuclear Air Cleaning Conference, San Diego, 20 - 23 Oct. 1980 ,
CONF - 801 038, p. 1354
- /29/ British Standard Institution,
Specification for test sieves,
BS 410 (1976)
- /30/ American Society for Testing and Materials,
Standard test method for particle size distribution of granular activated carbon,
ASTM D 2862 (1970)
- /31/ Wilhelm, J. G.,
Kernforschungszentrum Karlsruhe,
private communication (1984)

INVESTIGATION OF THE INFLUENCE OF ACCIDENT CONDITIONS ON THE PERFORMANCE OF HEPA FILTER AND IODINE TRAPPING SYSTEMS

V. FRIEDRICH

Institute of Isotopes,
Hungarian Academy of Sciences,
Budapest, Hungary

Abstract

The removal efficiency obtained in operation of a perchlorvinyl-based fibrous HEPA filter was investigated at higher temperatures and relative humidities. A reduced performance relationship was determined due primarily to high relative humidity at low air flowrates and to high temperature at high flowrates. The applicability of potassium carbonate aerosol produced by nozzle type atomisation was investigated for in-situ HEPA filter testing. Particle sizing by cascade impactor and centrifugal aerosol spectrometer was developed.

Theoretical and experimental investigations were made into mechanisms for radioiodine removal on carbon-based adsorbents at higher temperatures and humidities and included the use of specially developed continuous airflow apparatus.

1. Introduction

The performance of off-gas cleaning systems under abnormal and accident conditions at nuclear facilities is an important question from the point of view of safe operation. The aim of the investigations being performed within the scope of the IAEA coordinated research programme on "Retention of Iodine and Other Airborne Radionuclides in Nuclear Facilities During Abnormal and Accident Conditions" is to investigate the influence of accident conditions /elevated temperature, relative air humidity, flow rate, etc./ on the performance of aerosol /HEPA/ filters and charcoal adsorbers, and to develop testing methods

applicable for laboratory tests under simulated accident conditions as well as in situ testing of operating filter systems.

During the first and second year of the present research programme the influence of higher temperature and relative humidity on the resistance and removal efficiency of a perchlor-vinyl-based fibrous HEPA filter material was investigated and theoretical and experimental investigations on the removal mechanism of activated carbon adsorbents were performed /1/.

In the course of the third year the applicability of K_2CO_3 aerosol /produced by nozzle-type atomizer/ for in situ testing of HEPA filter systems was investigated. The particle size distribution of the K_2CO_3 aerosol was determined by cascade impactor and centrifugal aerosol spectrometer developed at the Institute earlier. The influence of temperature and relative humidity on the removal efficiency of activated carbon for methyl-iodide was also investigated using the continuous air flow apparatus developed at the Institute earlier.

2. Determination of the particle size distribution of K_2CO_3 test aerosol

Potassium carbonate aerosol has been selected for in situ testing of HEPA filters in the NPP air cleaning systems. The test aerosol is produced by nozzle-type atomizer. Upstream and downstream aerosol concentrations are determined by flame-photometric method using the specific light emission of potassium ions. The method is a modification of the well known sodium-chloride test standardized in the UK. The reasons why using potassium carbonate

instead of sodium chloride are the following:

- there are different sodium compounds in the air causing a higher background for the flame-photometric determination. Potassium background is much lower.
- the use of chloride in NPPs is to be avoided because of its corrosion effect.

According to recent investigations reported by many authors the removal efficiency of HEPA filters depends on the particle size distribution of the aerosol to be removed. Therefore it was necessary to determine the particle size distribution of the K_2CO_3 aerosol. These investigations were carried out using a centrifugal aerosol spectrometer developed at the Institute earlier /2/.

2.1. Determination of the particle size distribution of K_2CO_3 aerosol by centrifugal aerosol spectrometer

The principle of the measurement: two concentrical cylinders rotate together. The aerosol is introduced into the slit between the two cylinders by adjusted air flow. While following the air flow between the two cylinders the particles will sediment on the outer cylinder due to centrifugal force caused by the high speed rotation of the cylinders. The sedimentation process, ie. relationship between particle size and place of precipitation can be described by the following formula based on Stokes law:

$$d = K \cdot \left[\frac{Q}{g \cdot n^2} \right]^{\frac{1}{2}} \cdot \left[\frac{1}{L} \right]^{\frac{1}{2}}$$

where Q: volumetric flow rate of the aerosol
 d: aerodynamic diameter of the particle
 ρ : density of the particle
 L: distance of the precipitation place from the entering
 n: speed of rotation of the centrifuge
 K: apparatus constant

The centrifuge can be operated at four speeds /800/min, 1500/min, 3000/min and 6000/min./, and with two different inner cylinders /ie. two different slit sizes/. For cylinders "A" and "B" the K values were 6,084 and 5,904, respectively.

The measurement was carried out by using K_2CO_3 aerosol labelled with ^{42}K radioisotope. The radioactive aerosol was fed into the rotating centrifuge until measurable quantity was collected on the wall of the outer cylinder. The count-rate - proportional with the radioactivity - was then measured along the cylinder axis by scintillation counter. Mass and number distribution of the particles can be calculated by the help of the above equation.

Only one section of the aerosol spectrum can be determined at a fixed speed of rotation with suitable resolution. The measuring ranges are the following:

<u>n, 1/min</u>	<u>d, μm</u>
800	2,65 - 0,70
1500	0,71 - 0,36
3000	0,37 - 0,18
6000	0,18 - 0,08

Measurements were carried out in every ranges. The data of the four measurements resulted in the spectrum of the K_2CO_3 aerosol in the range of 0,091 - 2,653 μm by cylinder "A" and 0,088 - 2,575 μm by cylinder "B".

Mass distribution of the aerosol is shown in Figs.1 and 2. The maximum of mass distribution was found at 0,7 - 0,8 μm . The mass ratio of the 0,4 - 0,5 μm particles is significant too.

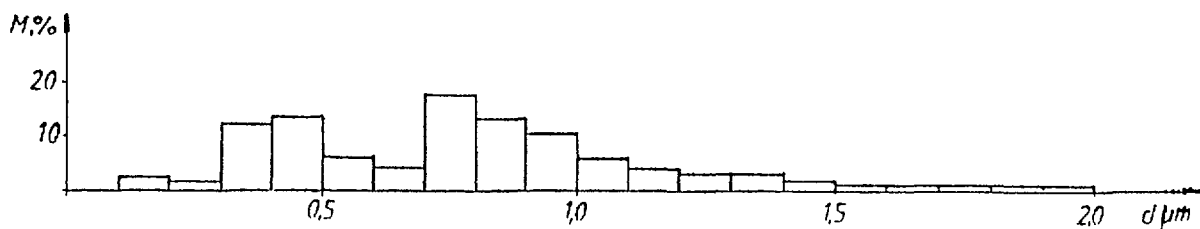


Figure 1. Mass distribution of K_2CO_3 aerosol as a function of particle size, measured by cylinder "A". Resolution 0,1 μm .



Figure 2. Mass distribution of K_2CO_3 aerosol as a function of particle size, measured by cylinder "B". Resolution 0,1 μm .

Figs. 3 and 4 show the mass distribution at a higher resolution. Number distribution of the aerosol is shown in Figs. 5 and 6 with a resolution of 0,1 μm and in Figs. 7 and 8 with a resolution of 0,01 μm . The maximum of the number distribution was found at about 0,1 μm , as it can be seen in Figs. 7 and 8.

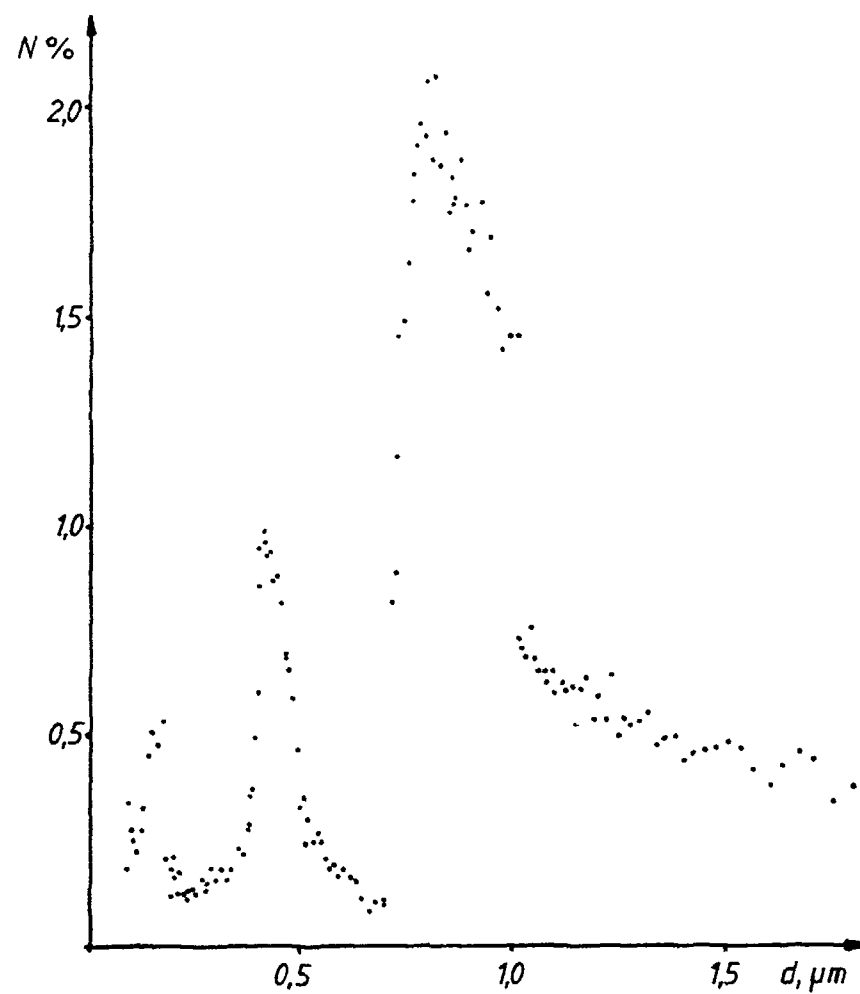


Figure 3. Mass distribution of K_2CO_3 aerosol as a function of particle size, measured by cylinder "A". Resolution $0,01 \mu\text{m}$.

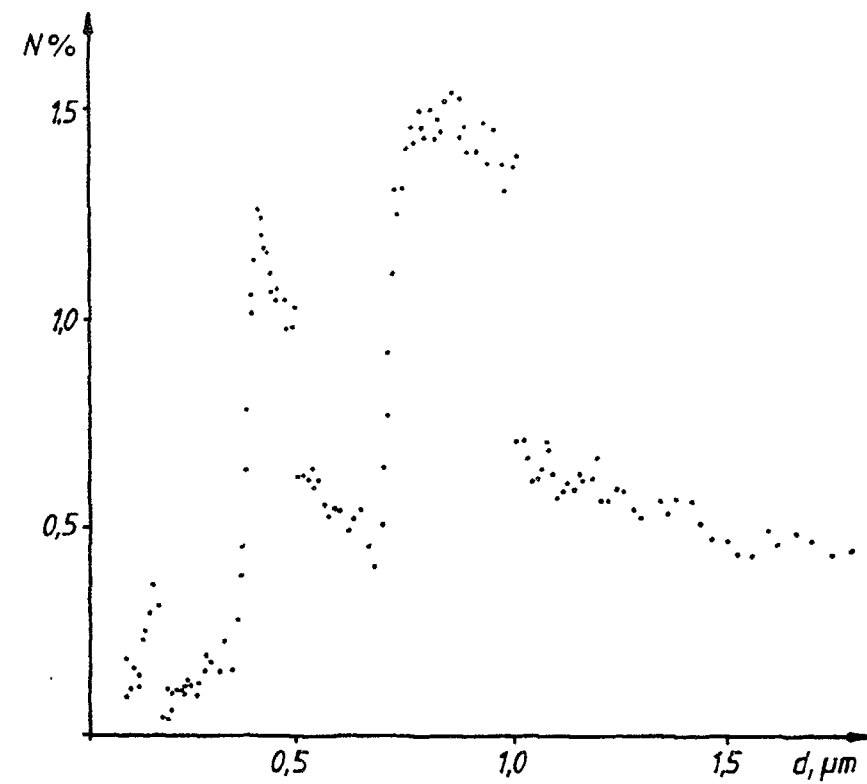


Figure 4. Mass distribution of K_2CO_3 aerosol as a function of particle size, measured by cylinder "B". Resolution $0,01 \mu\text{m}$.

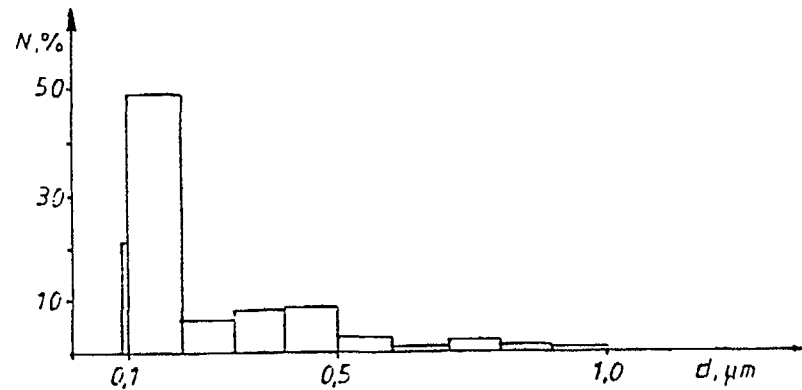


Figure 5. Number distribution of K_2CO_3 aerosol as a function of particle size, measured by cylinder "A". Resolution $0,1 \mu m$.

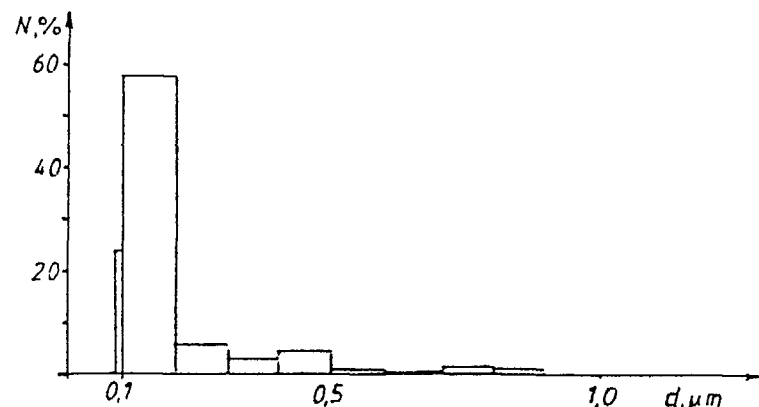


Figure 6. Number distribution of K_2CO_3 aerosol as a function of particle size, measured by cylinder "B". Resolution $0,1 \mu m$.

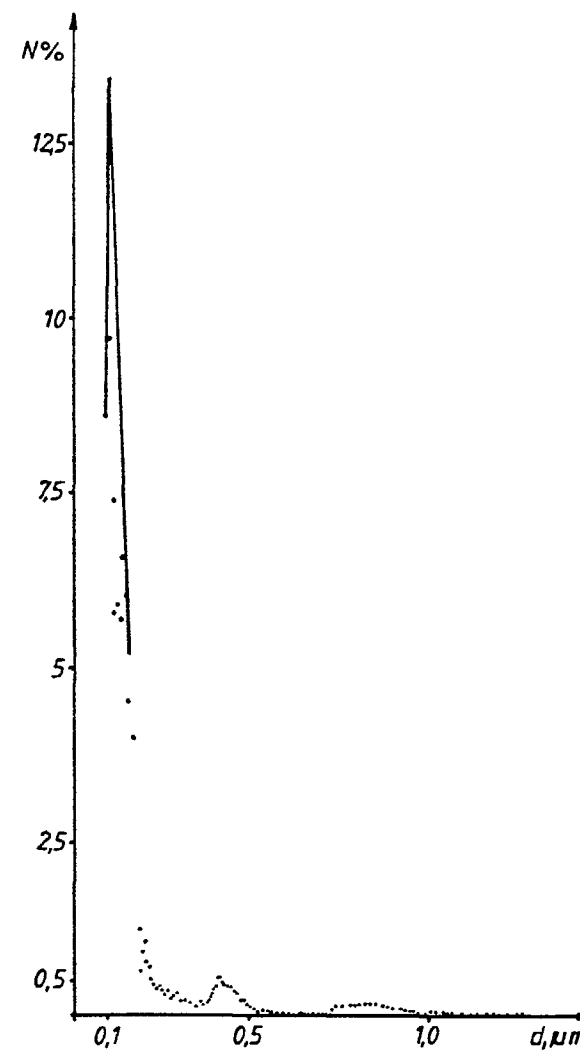
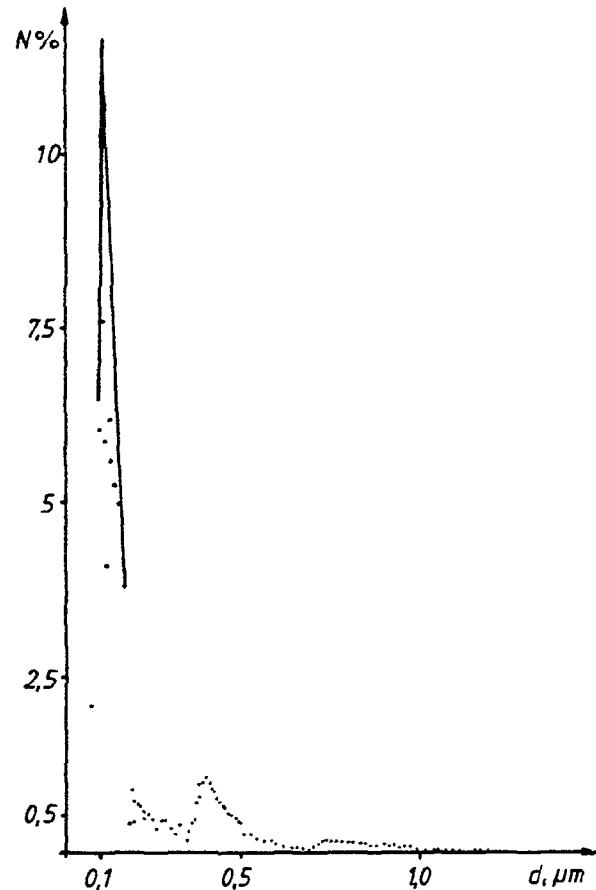
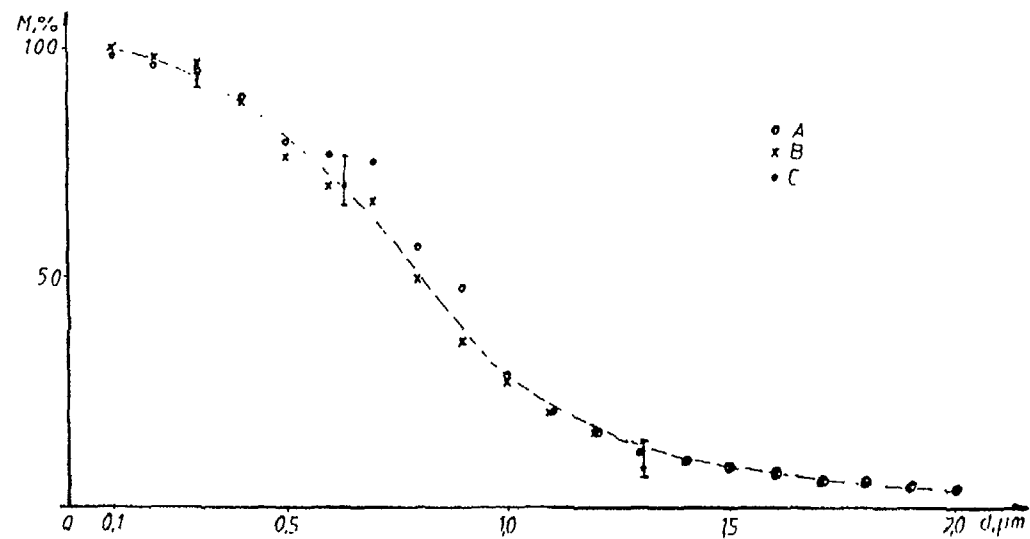


Figure 7. Number distribution of K_2CO_3 aerosol as a function of particle size, measured by cylinder "A". Resolution $0,01 \mu m$.

Figure 8.

Number distribution of K_2CO_3 aerosol as a function of particle size, measured by cylinder "B". Resolution 0,01 μm .

Figure 9.

Cumulative mass distribution of K_2CO_3 aerosol as a function of particle size, measured by centrifugal spectrometer /A - cylinder "A", B - cylinder "B"/ and cascade impactor / C /

2.2. Determination of the particle size distribution by cascade impactor

To verify the particle size ranges of the centrifugal aerosol spectrometer a precision cascade impactor /Type PI 1 by firm Retsch GmbH/ was used. Although the resolution of this equipment is much lower the results were in good agreement with those obtained by the centrifugal spectrometer. The cumulative mass distribution of the K_2CO_3 aerosol determined by centrifugal spectrometer and cascade impactor is shown in Fig. 9.

3. Experimental investigation of fiber-glass filter material under simulated accident conditions

In the course of a previous IAEA programme on particulate filter testing methods two traditional methods /DOP and flame-photometric/ and the radioisotopic tracing method were investigated regarding their applicability, accuracy, advantages and disadvantages. In our final report /3/ it was pointed out that the radioisotopic tracing method /developed in our Institute/ was specially useful for exact determination of HEPA filter efficiencies due to its high sensitivity. The used test aerosol /finely dispersed, submicron size aerosol of iridium/ was not inclined to coagulate, it was insoluble in water and insensitive to high temperature. Because of these properties of the test aerosol and the method itself it seemed to be the most suitable experimental technique for investigating HEPA filter performance under simulated accident conditions.

For preparation of radioactive test-aerosol a spark-excited generator was used /3/. The equipment prepares finely dispersed, submicron size aerosol from the neutron activated metal electrode of high specific activity. The spark-excited aerosol-generator prepares vapour-condensated aerosols by the help of low intensity and high voltage Tesla-current. The average of the particle diameters was 0.3 m.

The scheme of the laboratory apparatus used for filter tests under simulated accident conditions is shown at Figure 10.

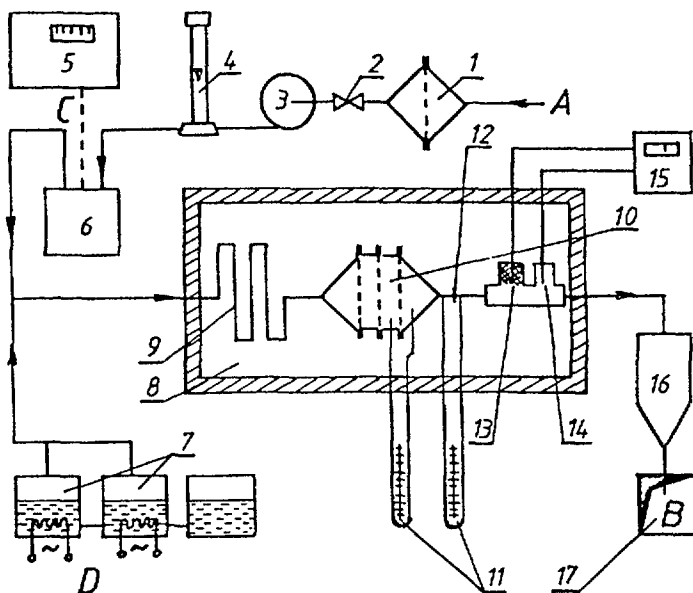


Figure 10. The scheme of the laboratory apparatus for filter tests under simulated accident conditions.

1-prefilter, 2-valve, 3-air pump, 4-rotameter, 5-Tesla-current source, 6-spark-excited aerosol generator, 7-steem generator, 8-electric oven, 9-spiral tube, 10-filter housing with filters to be tested, 11-U-tube manometers, 12-orifice, 13-dry thermometer, 14-wet thermometer, 15-temperature-recorder, 16-cooler, 17-condenser, A-air inlet, B-air outlet, C-Tesla-current, D-heating

The inlet air is filtered by an absolute filter FPP-15-3. The air flow is adjusted by valve 2 and air pump 3, measured by rotameter 4. The air flow enters the spark-excited aerosol generator 6, where iridium aerosol is produced by the help of Tesla current excited by Tesla-generator 5. For the experiments at high air humidity steam can be generated by the steem generator 7 and can be mixed to the main flow. The filter housing /10/ is put into the electric oven 8 where the temperature is regulated. In the spiral tube 9 the air-aerosol mixture is conditioned before reaching the filter housing. The filter resistance is measured by manometer 11. The flow rate of the humid air is determined by the help of measuring orifice 12 and manometer 11. The relative humidity of the air is calculated from the data of dry

and wet thermometers 13 and 14. Oven temperature is recorded by temperature recorder 15. Water is condensed from outlet air by cooler 16 and collected in 17.

The radioactivity of the filter samples were measured by scintillation detector and impulse scaler. The count-rate was proportional to the amount of aerosol removed on the filters. Since the same quantity of air passed through all the three filter samples with the same mass rate, the sampling was isokinetic. In that case the filter efficiency /retention/ of filter 1 could be calculated in the following way:

$$R = 1 - \frac{I_2}{I_1}$$

where I_1 and I_2 were the measured count-rates on filter 1 and 2. Similarly the retention of filter 2 could be calculated from I_2 and I_3 as well.

The first aim of the laboratory experiment was to investigate the influence of elevated temperature on the resistance and removal efficiency of a fiber glass HEPA filter material used in Hungarian nuclear power station. The temperature range was 24-420°C. Since the air flow rate adjusted at ambient temperature increases with increasing temperature, for comparison purposes the flow rate dependence of the pressure drop on the filter was determined at ambient temperature /24 °C/. The results can be seen in Table 1.

Table 1. The flow rate dependence of the filter resistance

linear flow rate		pressure drop /Pa/
/m/h/	/cm/s/	
249,5	6,93	166,6
519,8	14,40	352,8
675,7	18,80	480,2
883,6	24,50	862,4
1039,5	28,90	1117,2
1247,4	34,70	1225,0

The temperature /and flow rate/ dependence of the filter resistance is shown in Table 2.

Table 2. The temperature dependence of the filter resistance

/t/ °C/	linear flow rate		pressure drop /Pa/
	/m/h/	/cm/s/	
24	249,5	6,93	166,6
56	276,4	7,68	215,6
101	318,3	8,84	303,8
198	401,2	11,14	421,4
307	494,0	13,72	617,4
418	580,5	16,12	1019,2

The flow rate dependence of the removal efficiency at ambient temperature was also measured as it is shown in Table 3.

Table 3. The flow rate dependence of the removal efficiency /R/

linear flow rate		R /%
/m/ h/	/cm/s/	
249,5	6,93	99,927
519,8	14,40	99,882
675,7	18,80	98,882
883,6	24,50	98,220
1039,5	28,90	97,606
1247,4	34,70	96,826

Finally, the temperature dependence of the removal efficiency was measured. The results can be seen in Table 4.

Table 4. The temperature dependence of the removal efficiency /R/

/t /°C/	linear flow rate		R /%
	/m/h/	/cm/s/	
24	249,5	6,93	99,927
56	276,4	7,68	99,930
101	318,3	8,84	99,943
198	401,2	11,14	99,959
307	494,0	13,72	99,981
418	580,5	16,12	98,696

Comparing the measured data collected in Tables 1-4. the following conclusions can be summarized:

- The resistance of the filter increased with increasing flow rate of ambient temperature and this effect was significantly stronger at higher temperatures.
- Although the removal efficiency decreased with increasing flow rate at ambient temperature, when increasing temperature, the removal efficiency did not change or slightly increased up to about 300°C.
- Over 300°C the removal efficiency rapidly decreased indicating that the filter material was damaged. A yellow-brown colour could be observed on the filter surface. It is remarkable that even at 418°C the removal efficiency is still higher than that of ambient temperature at the same flow rate.

4. Experimental investigation of synthetic fibrous HEPA filter material under simulated accident conditions

The aim of these experiments was to investigate the influence of elevated temperature, relative air humidity and flow rate on the resistance and removal efficiency of the FPP-15-30 type HEPA filter material used in the off-gas cleaning and ventilation systems of Hungarian nuclear facilities. The

radioisotopic tracing method developed in the Institute and described earlier /3, 4/ was used for the measurements. The method is based on radioactive ^{64}Cu metal test-aerosol produced by spark-excited generator, and experimental apparatus consisting of filter sample housing, units for adjusting and measuring flow rate, temperature and humidity. The test-apparatus used in the first year of the contract was modified according to the discussion and suggestions obtained on the first research coordination meeting. As a result of these modifications the most important experimental parameters (e.g. flow rate, temperature) became independently adjustable.

4.1. The experimental apparatus

The scheme of the laboratory apparatus used for filter test under simulated accident conditions is shown in Figure 11. The pressure of compressed air entering the

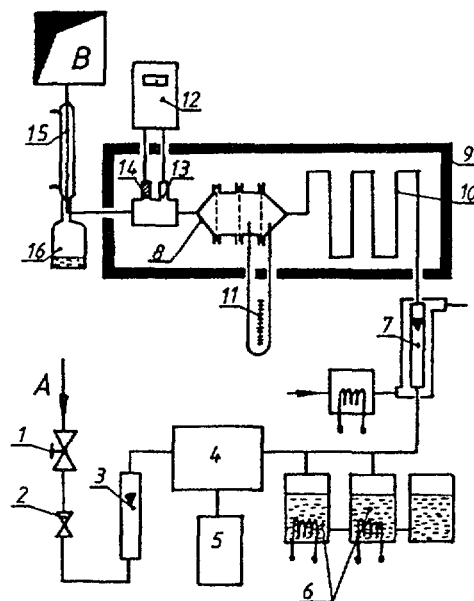


Figure 11. The scheme of the laboratory apparatus for filter tests under simulated accident conditions

1-control valve, 2-valve for adjusting the flow rate, 3-rotameter, 4-spark-excited aerosol generator, 5-Tesla current generator, 6-steam generator, 7-heated rotameter, 8-filter housing, 9-electric oven, 10-spiral tube for conditioning, 11-manometer, 12-temperature recorder, 13-dry thermometer, 14-wet thermometer, 15-cooler, 16-collecting vessel, A-air inlet, B-air outlet

aerosol generator is reduced to 3 bar by control valve 1. The flow rate is adjusted by valve 2, and measured by rotameter 3. The air flow enters the spark-excited aerosol generator 4, where vapour-condensated radioactive copper aerosol is produced by the help of neutron-activated copper electrodes and low intensity-high voltage Tesla current excited by Tesla generator 5. For the experiments at high humidity steam can be generated by steam generator 6, and mixed to the main flow. The flow rate is measured by heated rotameter 7 at the temperature of the filter test. Filter housing 8 is put into the electric oven 9 where the temperature is regulated. In spiral tube 10 the air-steam-aerosol mixture is conditioned before reaching the filter housing. The filter resistance is measured by manometer 11. Temperature data are recorded by temperature recorder 12. The relative humidity (RH, %) of the air is calculated from the data of dry and wet thermometers 13 and 14. Water is condensed from the outlet air by cooler 15 and collected in vessel 16.

The resistance of the filter samples can be measured continuously during the experiment. For the determination of the removal efficiency the filter samples are removed from the housing after appropriate loading time. The radioactivity of the samples are measured by NaI scintillation detector and impulse scaler. The count-rate is proportional to the amount of aerosol collected on the filter. Calculation of filter efficiency from the measured count-rate is described in 4.4.

4.2. The flow-rate-dependence of filter resistance at ambient temperature

The variation of the filter resistance of different flow rates is shown in Figure 12. The temperature of the air was about 24 °C. The relative humidity of the air was 60 %.

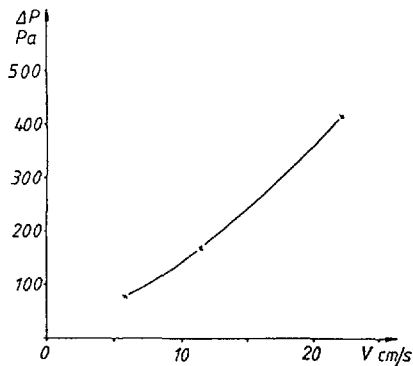


Figure 12. Filter resistance vs. flow rate at 24 °C and 60 % relative humidity.

4.3. The effect of higher temperature and relative humidity on filter resistance

The investigated filter material made of synthetic perchlorvinil fibres suffers a significant loss above 100 °C. As a result of shrivelling and roasting the filter resistance increases, the removal efficiency rapidly decreases. The investigations were carried out between 60-100 °C and at RH=80 and 93 % relative humidities. The values of the linear air flow rate varied between 5-25 cm/s.

The measured pressure drops are shown in Tables 5 and 6.

Table 5. The influence of flow rate and temperature on the filter resistance (ΔP , Pa) at 80 % relative humidity.

v [cm/s] \ t [°C]	60	80	90
5,78	245	396	484
11,55	498	897	996
23,11	1505	1794	2002

Table 6. The influence of flow rate and temperature on the filter resistance (ΔP , Pa) at 93 % relative humidity

$t/{}^{\circ}\text{C}$	60	80	90
$V/\text{cm/s}$	398	451	505
11,55	900	1001	1097
23,11	1790	1903	2197

4.4. Investigation of the removal efficiency at higher temperature and relative humidity

The removal efficiency of the filter sample can be calculated from the measured count-rates that are proportional to the amount of aerosol collected on the filter:

$$\eta = \left(1 - \frac{I_2}{I_1} \right) \cdot 100$$

where I_1 and I_2 are the measured count-rates on filter 1 and 2 and η is the removal efficiency in %.

The removal efficiency values determined under various conditions are shown in Tables 7 and 8.

Table 7. The influence of flow rate and temperature on the removal efficiency at 80 % relative humidity

$t/{}^{\circ}\text{C}$	65	80	95
$V/\text{cm/s}$	99,920	99,821	99,560
11,55	99,836	99,703	95,923
23,11	99,576	98,164	95,610

Table 8: The influence of flow rate and temperature on the removal efficiency at 93 % relative humidity

$t/{}^{\circ}\text{C}/$ $V/\text{cm/s}/$	65	80	95
5,78	98,333	97,650	97,486
11,55	97,697	96,386	96,011
23,11	97,262	96,277	95,435

4.5. Discussion

The results of the experiments are shown in Tables 5-8. The individual and combined effects of the experimental parameters will be discussed here.

The influence of temperature on filter resistance

Pressure drop values as the function of temperature and air flow rate are shown in Figure 13 (RH = 80 %) and Figure 14 (RH = 93 %). It can be established that both increasing temperature and flow rate result in increasing of the filter resistance.

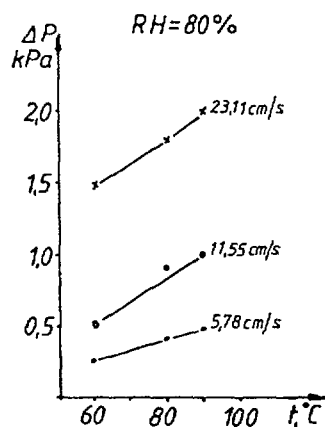


Figure 13. Filter resistance vs. temperature at 80 % relative humidity

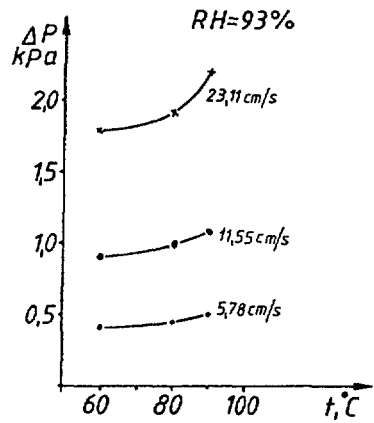


Figure 14. Filter resistance vs. temperature at 93 % relative humidity

The influence of relative humidity on filter resistance

Figure 15 shows that filter resistance significantly increases with increasing relative humidity (see also Figure 12).

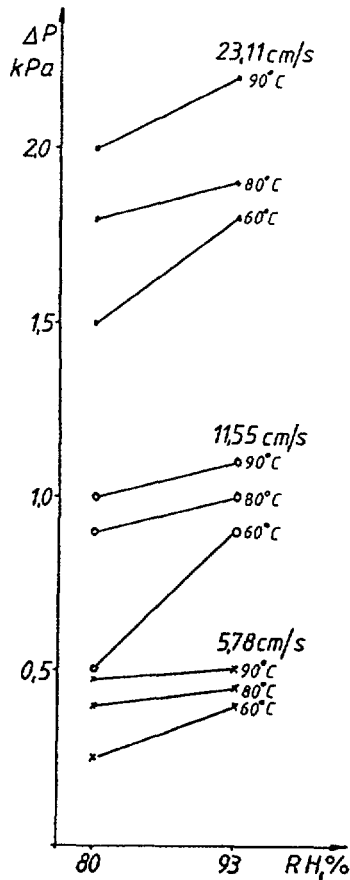


Figure 15. The influence of relative humidity on the filter resistance at different flow rates and temperatures.

The influence of temperature on the removal efficiency

Figure 16 (RH = 80 %) and Figure 17 (RH = 93 %) show the removal efficiency as the function of temperature at different flow rates. It can be established that both increasing temperature and flow rate result in decreasing of the removal efficiency.

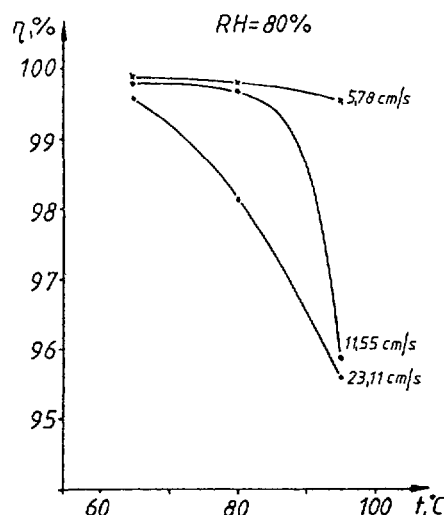


Figure 16. Removal efficiency vs temperature at 80 % relative humidity

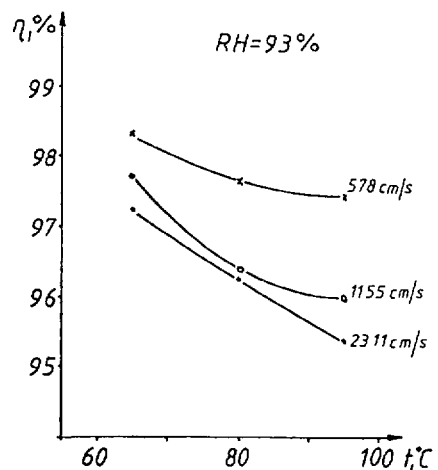


Figure 17. Removal efficiency vs temperature at 93 % relative humidity

The influence of relative humidity on the removal efficiency

The removal efficiency as the function of relative humidity at different air flow and temperature values is shown in Figure 18. Conclusions of these results are the followings:

- at 5,78 cm/s air flow rate the influence of increasing relative humidity is near the same at every tested temperature
- at 11,55 and 23,11 cm/s flow rates the effect of temperature decreasing the removal efficiency is stronger than the effect of relative humidity.

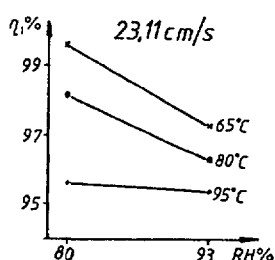
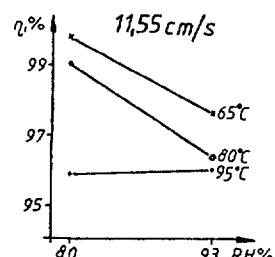
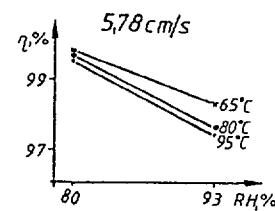


Figure 18. Removal efficiency as the function of relative humidity at different flow rates and temperatures

Combined effect of temperature and relative humidity on the removal efficiency.

The combined effect of temperature and relative humidity is shown in Figures 19 ($V = 5,78 \text{ cm/s}$), 20 ($V = 11,55 \text{ cm/s}$) and 21 ($V = 23,11 \text{ cm/s}$).

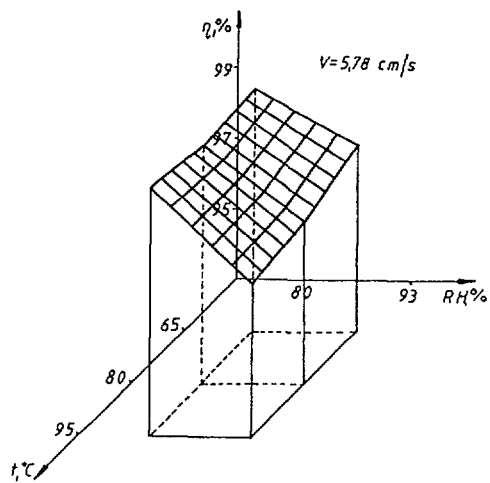


Figure 19. Removal efficiency as the function of temperature and relative humidity at a flow rate of 5,78 cm/s

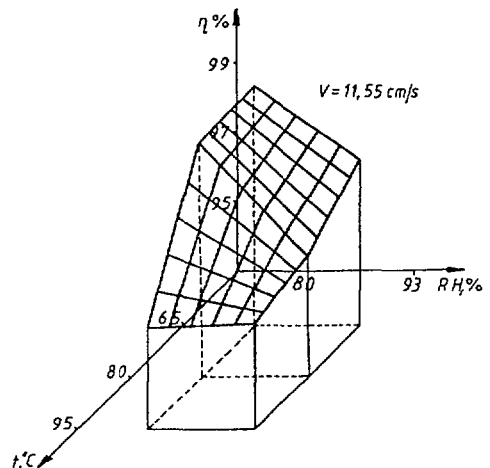


Figure 20. Removal efficiency as the function of temperature and relative humidity at a flow rate of 11,55 cm/s

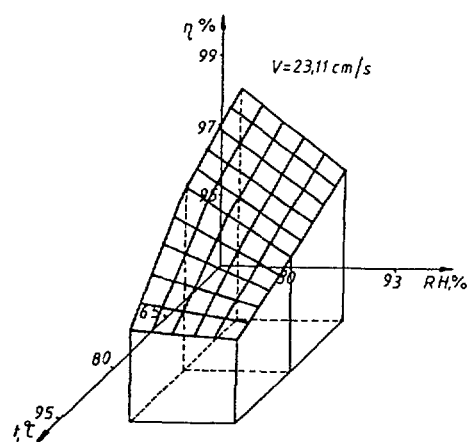


Figure 21. Removal efficiency as the function of temperature and relative humidity at a flow rate of 23,11 cm/s

Figure 19 shows that the effect of relative humidity is much stronger than the effect of temperature at that flow rate. The effect of temperature increases, the effect of relative humidity decreases between 80-95 °C at 11,55 cm/s and 23,11 cm/s flow rates (see Figures 20 and 21).

Summarizing the conclusions it can be established that the influence of relative humidity on the removal efficiency is stronger than the influence of temperature at low air flow rates. At higher flow rates the removal efficiency will be decreased by increasing temperature rather than by increasing relative humidity.

One of the conclusions of the second research coordination meeting was that most of the test-aerosols used by different HEPA filter testing methods are not suitable under high temperature and high humidity conditions. For investigating and comparing appropriate test methods for such conditions, it is desirable to use similar types of filter materials being investigated in other laboratories. Filter papers of four different efficiencies supplied by M/s J.C. Binzer have therefore been taken up for evaluation.

According to the recommendations of the second research coordination meeting the investigations were carried out under the following test conditions:

- temperature 25 °C
- relative humidity 50%
- linear air velocity 3 m/min.

The measured filter papers were made by J.C. Binzer Paper manufacture /FRG/. The efficiency and permeability values specified by the manufacturer compared with the results measured by the radioactive metallic aerosol method are shown in Table 9.

Table 9. Comparison of the measured efficiency and permeability values with those given by the manufacturer

Filter paper /manufacturer's mark/	Efficiency %			Permeability /mbar/	
	Given by the manufacturer	Exp. No.	Measured	Given by the manufacturer	Measured
FH 863/2	99.97	1.	99.9775		
		2.	99.9743		
		3.	99.9658	3.5 [±] 0.3	3.48 [±] 0.04
		4.	99.9666		
		Average: 99.9711 [±] 0.006			
FH 863/1	99.99	1.	99.9878		
		2.	99.9862		
		3.	99.9899	3.7 [±] 0.3	3.69 [±] 0.002
		4.	99.9900		
		Average: 99.9885 [±] 0.002			
FH 929	99.998	1.	99.9926		
		2.	99.9915		
		3.	99.9946	5.3 [±] 0.5	4.82 [±] 0.25
		4.	99.9947		
		Average: 99.9934 [±] 0.002			
FH 1047	99.9999	1.	99.9993		
		2.	99.9992		
		3.	99.9992	5.8 [±] 0.3	5.37 [±] 0.15
		4.	99.9992		
		5.	99.9993		
		Average: 99.99924 [±] 0.0001			

It can be established that the efficiency values measured by the radioactive metallic aerosol method sufficiently agree with those specified by the manufacturer, except in the case of the most efficient filter sample /FH 1047/. In this case the count-rate measured on the second filter sheet was too close to the background due to the high efficiency of the preceding sheet and this could result in systematic error. These measurements will be repeated using low background arrangement or higher loading of the filters.

The good agreement of the measured and specified efficiency values shows that under well-defined, identical conditions, on carefully selected filter samples the radioactive tracer method can provide sufficiently correct results for filter materials of very high efficiency. Since a significant effect of temperature and relative humidity on the behaviour of metallic particles is not expected, the method can be considered as one possible way to investigate HEPA filters under abnormal and accident conditions.

5. Theoretical model for the investigation of the performance of iodine adsorbers

The performance of iodine adsorbers are usually characterized by the removal efficiency /similarly to HEPA filters/ or by index of performance /K factor in ref. 5.

However, industrial practice and laboratory experiments show that the performance of adsorbers has a dynamic character, i.e. the removal efficiency changes /decreases/ in time, and this process is effected by many parameters such as geometry of the column, temperature, gas composition, relative humidity, face velocity, e.t.c. Investigations were performed to evaluate the dependence of the removal efficiency on some of these parameters /5/, /6/, /7/, but most of these relations are of empirical character. Therefore the comparison of the results of different laboratory tests and the extrapolation for long term operation and for accident conditions is difficult.

The aim of this work is to describe the kinetics of adsorption in continuous flow columns by the help of suitable model containing the physico-chemical parameters of the process /adsorption and desorption rate constants, concentrations, specific surface of the adsorbent/.

Assuming that the adsorption mechanism can be represented by the reversible processes of adsorption and desorption Jonas and Svirbely /8/ investigated the kinetics of adsorption of carbon tetrachlorid and chloroform from air mixtures by activated carbon.

A similar model served as the starting point of our investigations:



where g is a gas molecule, a is a free active site on the adsorbent, e is an occupied active site, k_F is the adsorption rate constant and k_B is the desorption rate constant. The rate of the process can be described by the following equation:

$$\frac{dE/x, t}{dt} = k_F \cdot G/x, t \cdot A/x, t - k_B \cdot E/x, t \quad /2/$$

where G , A and E are the concentrations of the gas, free active sites and occupied active sites, respectively, that depend on time t and distance x measured from the inlet site. Because of the conservation of /free+occupied/ active sites we have

$$A = A_0 - E \quad /3/$$

where A_0 is the concentration of the active sites /that is proportional to the specific surface of the sorbent/.

If the inlet gas concentration is constant in time, i.e. if

$$G = G_0 \quad /4/$$

then equation /2/ can be rewritten as follows:

$$\frac{dE}{dt} = k_F \cdot A_0 \cdot G_0 - /k_F \cdot G_0 + k_B/.E \quad /5/$$

Dividing the adsorption column into elementary layers such that the difference between inlet and outlet concentrations for one layer is negligible, and assuming that one active site can be occupied by one gas molecule only, the solution of equation /5/ at the outlet face of

the first layer reads

$$E_{1,t} = \frac{\frac{k}{k_B} \frac{F}{A_0} G_0}{\frac{k}{k_B} G_0 + 1} \left[\frac{-/k_F \cdot G_0 + k_B / \cdot t}{1 - e} \right] /6/$$

It can be seen that the first factor on the right side of equation /6/ is the Langmuir-isotherm /according to the initial conditions/ and the second one is the kinetic factor describing the time dependence of the gas accumulation in the elementary layer. On the basis of this model a step-by-step cascade method can be built up to compute concentration break-through curves and gas accumulation for an adsorption column of finite length X divided into N layers.

Figure 22 shows typical accumulation and break-through curves calculated by the cascade method. The purpose of these calculations was to test the mathematical equations and the numerical method, therefore the values of k_p , k_B , A_0 were fictive. Both accumulation and break-through curves show inlet concentration dependence /input parameters are the same with the exception of G_0 /.

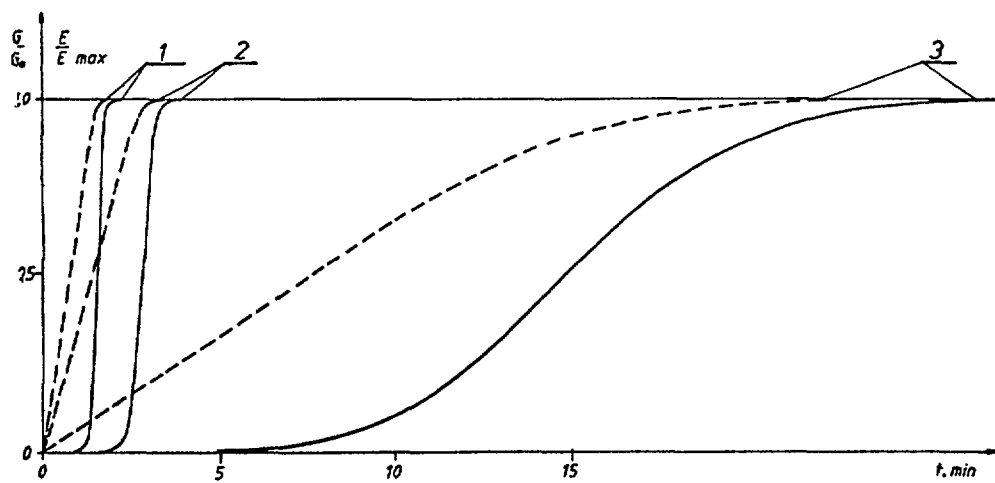


Figure 22.

Accumulation /----/ and break-through /—/ curves calculated by the cascade method in the case of $N=100$, $DT=0.01s$, $\alpha=0.4$, $\beta=20.$, and $D_0=10.$, 5. and 0,1 for the curves No.1, 2 and 3, respectively. $\alpha=k_p \cdot k_B \cdot A_0$; $\beta=k_p \cdot A_0$; $D_0=k_F \cdot G(x,t)/k_B$

When searching an analytical solution for the problem of the column of finite length, the following system of partial differential equations is to be solved. Again equation /2/ describes the rate of the process.

$$\frac{E/x, t/}{t} = k_F \cdot G/x, t/ \cdot A/x, t/ - k_B \cdot E/x, t/ \quad /7/$$

Equation /3/ gives the active site conservation

$$A/x, t/ = A_0 - E/x, t/$$

while gas conservation calls forth the relation

$$\int_0^x [E/y, t/ + G/y, t/] dy = V \cdot G_0 \cdot t - V \cdot \int_0^t G/x, t'/ dt' \quad /8/$$

where V is the linear face velocity, x and t are variables for distance and time. Equation /7/ describes the reaction rate, equation /8/ represents the mass balance for the continuous flow column of finite length. This system of partial differential equations can be solved.

In the analytical solution we assume that $A/x, t/$ in equation /7/ can be replaced by its maximum value A_0 . It can be seen that this assumption is equivalent to the approximation

$$D \cdot \mathcal{N}, \tilde{\tau}/ = k_F \cdot G / \mathcal{V}, \tilde{\tau}/ / k_B \ll 1 \quad /9/$$

By the help of Laplace-transformation the following solutions were found:

$$\bar{E} / \mathcal{V}, \tilde{\tau}/ = \beta \cdot G_0 \cdot e^{-\beta \mathcal{V}} \cdot \int_0^{\tilde{\tau}} e^{-k_B \cdot t} \cdot I_0 / 2 \sqrt{\alpha t \mathcal{V}} / dt \quad /10/$$

$$\bar{G} / \mathcal{V}, \tilde{\tau}/ = G_0 \cdot e^{-\beta \mathcal{V}} \left[e^{-k_B \cdot \tilde{\tau}} I_0 / 2 \sqrt{\alpha \tilde{\tau} \mathcal{V}} / + k_B \cdot \int_0^{\tilde{\tau}} e^{-k_B \cdot t} I_0 / 2 \sqrt{\alpha t \mathcal{V}} / dt \right] \quad /11/$$

where $\bar{E}/\mathcal{V}, \bar{\tau}/$ is the concentration of the accumulated gas at any and values

$\bar{G}/\mathcal{V}, \bar{\tau}/$ is the outlet gas concentration at any and values

$$\mathcal{V} = \frac{x}{v}; \bar{\tau} = t - \frac{x}{v}$$

I_0 is the zero order Bessel-function

$$\alpha = k_F \cdot k_B A_0 \quad /12/$$

$$\beta = k_F \cdot A_0 \quad /13/$$

In evaluating the calculational models above it is remarkable that the analytical solution is proportional to the inlet concentration G_0 but no other concentration dependence appears in equations /10/ and /11/. On the other hand equation /6/ shows an explicit concentration dependence of E/G_0 . This contradiction is due to the approximation, equation /9/, in the analytical method. In fact if $D_0 = k_F \cdot G_0 / k_B \ll 1$ then the G_0 - dependence of the cascade method also vanishes.

Dependence of the break-through curves on inlet concentration as calculated by the cascade method is given in Figure 23.

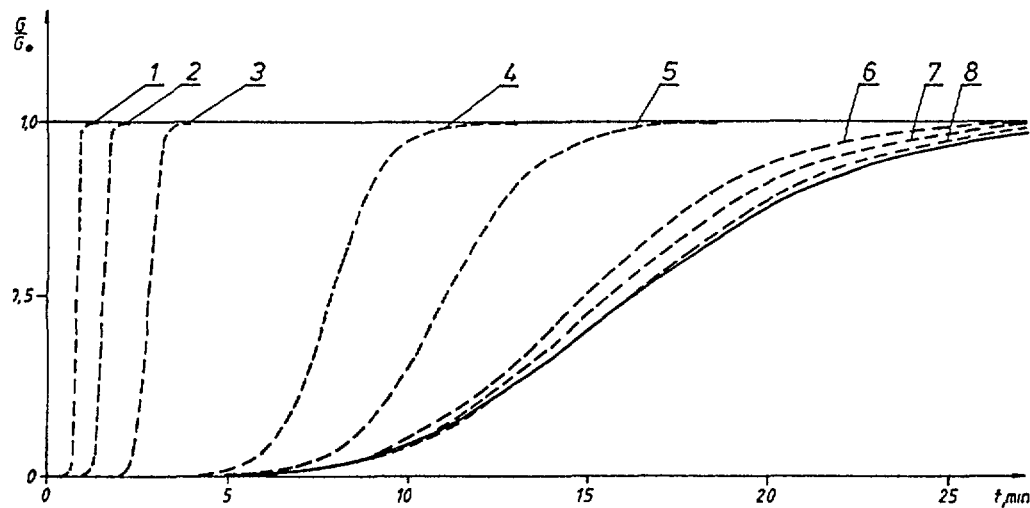


Figure 23

Break-through curves calculated by the cascade method /----/ and the analytical solution /—/ Equation/11/. In the cascade method $N = 100$, $DT = 0.01$ s, and $D = 20., 10., 5., 1., 0.5, 0.1, 0.05$ and 0.01 for the curves No. 1, 2, 3, 4, 5, 6, 7, and 8, respectively. For both cascade and analytical calculations $\alpha = 0.4$ and $\beta = 20.$

It is seen that with decreasing inlet concentration the curves asymptotically tend to the analytical curve and at $D_0=0,01$ the two curves practically coincide.

6. Experimental investigation of the removal of methyl iodide by activated carbon

A simplified scheme of the laboratory apparatus is shown in Figure 24. The vapour of CH_3I labelled with ^{125}I was produced from liquid CH_3I . The concentration of gaseous CH_3I was adjusted by the temperature of the thermostat and the air flow. The CH_3I concentrations were in the order of 0,01 - 0,5 mg/l. The length /bed depth/ of the adsorbent /activated carbon granules/ was 3-6 cm, diameter 1 cm. Accumulation curves were observed when measuring the ^{125}I activity on the column by scintillation detector and impulse-scaler, break-through curves were registered by gas-chromatograph /using flame-ionisation detector/. The first experiments were carried out at ambient temperature and 25-30 % relative humidity.

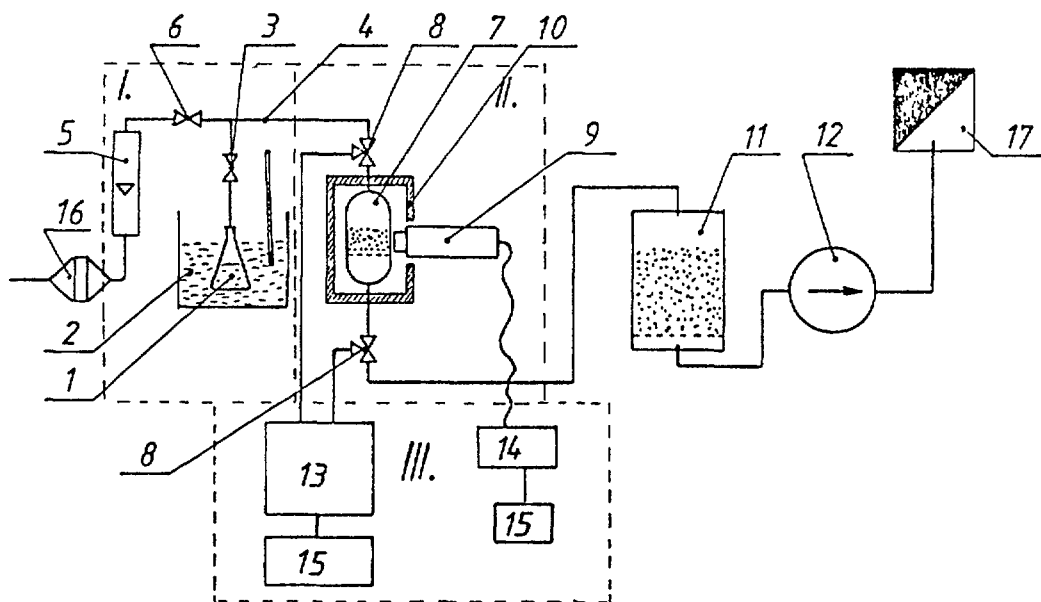


Figure 24. The laboratory apparatus

1-liquid methyl-iodide, 2-ultra-thermostat, 3-valve for adjusting CH_3I vapour flow, 4-mixing tube, 5-rotameter, 6-valve for adjusting air flow, 7-adsorption column, 8-gas samplers, 9-scintillation detector, 10-lead shielding, 11-safety adsorber, 12-air pump, 13-gas-chromatograph, 14-impulse-scaler, 15-recorders, 16-air filter, 17-central ventilation system

Figure 25 shows the inlet concentration dependence of experimentally measured accumulation curves, in Figure 26. a pair of simultaneously measured accumulation and breakthrough curves are plotted.

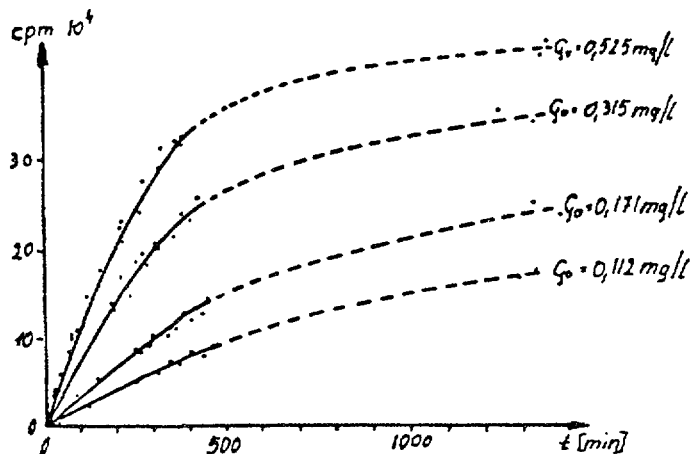


Figure 25. Measured accumulation curves at various inlet concentrations G_0 .

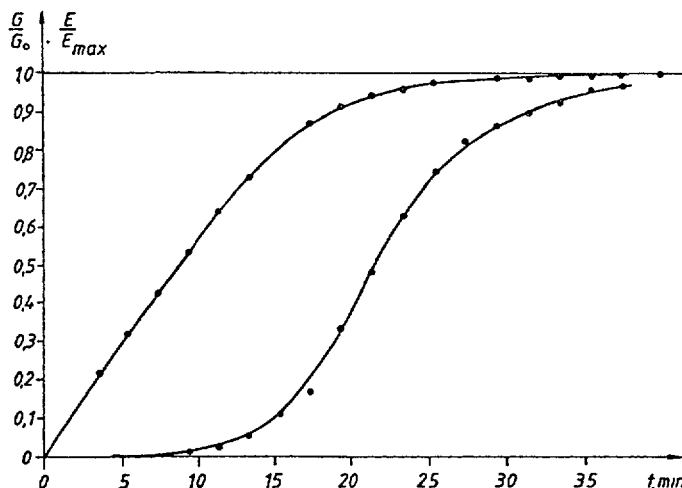


Figure 26. Simultaneously measured accumulation and break-through curves.

It is interesting that again a controversy is observed between the results obtained in our experiments and those resulting from reported industrial and laboratory experiments. The resolution of this apparent contradiction is again obvious, our laboratory experiments were carried out with relatively high inlet concentrations for the reasons discussed below. At such high concentrations approximation

/9/ is not justified, i.e. the analytical model does not apply. Nuclear applications, on the other hand, usually assume very low concentrations where the analytical treatment is justified. The link provided by the cascade method between the two extreme concentration cases gives us a viable strategy of experimental investigations of industrial processes. Namely by numerical /cascade-type/ reproduction of the experimental results the material constants α , β and D in equations /12/, /13/ and /9/ are determined and with this constants analytical calculations prognosticate industrial functioning.

This strategy makes high-concentration laboratory experiments possible that have the advantage that the process of reaching dynamical saturation is significantly faster. From the obtained break-trough and/or accumulation curves the physico-chemical parameters k_F , k_B , A_0 can be calculated. The sorbent material can be better characterized by these parameters since they are independent of the experimental conditions.

In the course of the experiments the inlet-concentration-dependence of the break-through curves were measured. The same laboratory apparatus was used as described in the first progress report /4/ and in Ref. /9/. The inlet methyl-iodide concentrations varied from $1,5 \cdot 10^{-4}$ mol/l to $6 \cdot 10^{-4}$ mol/l. The used adsorbent was granulated activated carbon with a specific surface of $1125 \text{ m}^2/\text{g}$ determined by BET method. Bed depth was 4 cm, bed diameter 2 cm, linear flow rate on the bed 3 cm/s, and the experiments were carried out at 25°C and 30 % relative humidity. The results of these experiments are shown in Figure 27. From the results can be seen that the break-trough curves show a strong inlet concentration dependence as it was prognosticated by the theoretical model.

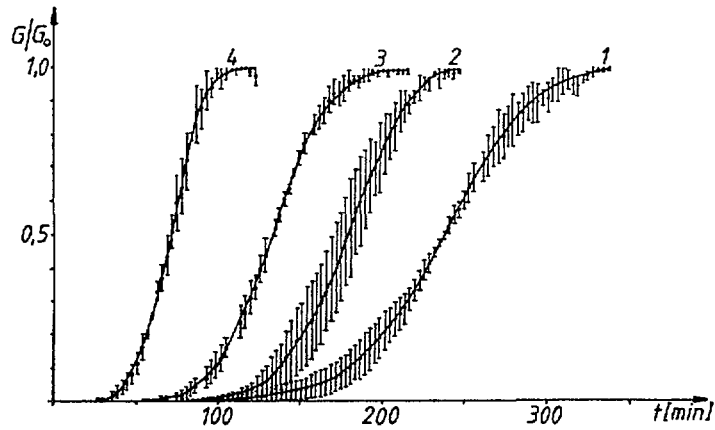


Figure 27.

Experimentally measured break-through curves at 25 °C and 30 % relative humidity. Bed depth-4 cm, bed diameter 2 cm, linear flow rate- 9 cm/s. Methyl iodide concentration /upstream/: $1,62 \cdot 10^{-4}$ mol/l (curve 1) $2,12 \cdot 10^{-4}$ mol/l (curve 2), $3,06 \cdot 10^{-4}$ mol/l (curve 3) and $5,8 \cdot 10^{-4}$ mol/l (curve 4).

6.1. The influence of temperature and air humidity on the performance of activated carbon adsorbent

According to our previous investigations /1, 9/ the performance of charcoal adsorbers can be better characterized when observing the dynamic operation of the adsorber than measuring the removal efficiency after a definite loading time. The time-dependent accumulation or break-through of the gas to be retained by the adsorbent /in our case methyl-iodide/ is very sensitive to the various conditions as gas concentration, flow rate, temperature, humidity, etc. The influence of temperature and humidity was therefore investigated measuring the break-through curves of methyl-iodide at different temperature and relative humidity values.

Experimental conditions

The laboratory apparatus described in /1/ has been modified so that adjusting of temperature and relative humidity became possible. The scheme of the new apparatus is shown in Fig. 28.

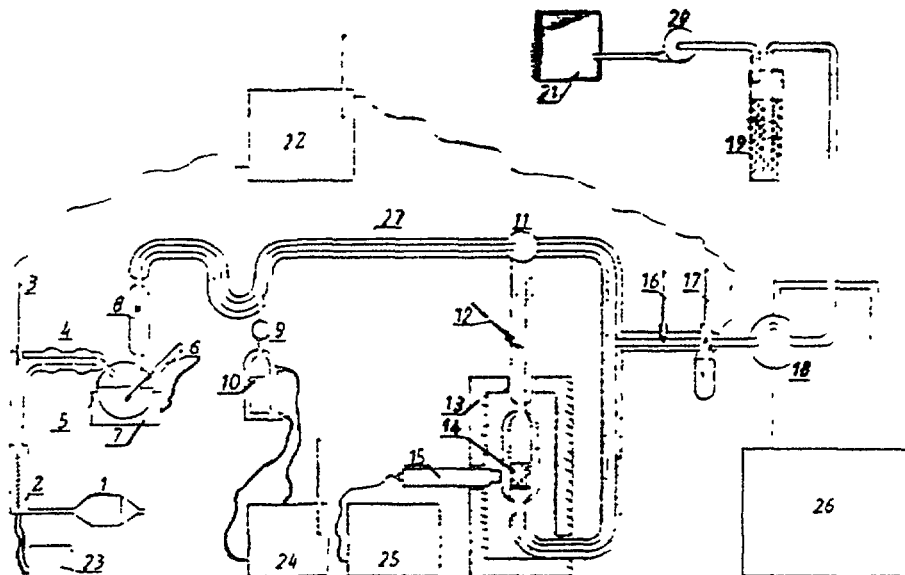


Figure 28. Experimental apparatus for the investigation of the influence of temperature and air humidity on the performance of activated carbon

The air flow is maintained by air pump 20. The inlet air is cleaned by aerosol filter 1. The air is heated by electric heater 2 and the temperature is controlled by thermometer 3. The air flow is adjusted by cock 4, controlled by rotameter 8, humidified by steam generator 5 which is operated by electric heater 7 and contact thermometer 6. The relative humidity is determined by the help of dry and wet thermometers 16 and 17. The vapour of CH_3I is produced by evaporating liquid CH_3I from vessel 10. The CH_3I concentration is determined by the air flow rate and the evaporation rate which is controlled by ultrathermostate 24. Upstream and downstream samples can be taken by two-way cock 11 and can be introduced in the gas-chromatograph 26 by gas-sampler 18. Appropriate mixing and final adjustment of temperature and humidity occurs in joint 27. The temperature of joint 27 and the adsorption bed 14 is controlled by ultrathermostate 22. When using CH_3I labelled with radioactive ^{125}I the accumulation of radioactive CH_3I on the adsorption bed can be measured by scintillation counter 15 in lead shielding 13. Downstream flow is introduced in the ventilation

system through safety charcoal bed 19 and air pump 20. Parameter ranges during the experiments were as follows:

CH ₃ I concentration:	$5 \times 10^{-3} - 10^{-3}$ M/l
temperature:	15 - 90 °C
relative humidity:	10 - 95%

The influence of temperature and relative humidity on the performance of activated carbon

The influence of temperature was investigated in the range of 25 - 80 °C, the inlet concentration of CH₃I was $2,1 \times 10^{-4}$ M/l, relative humidity was 30%. Bed depth was 4 cm, bed diameter 2 cm, face velocity 3 cm/s, the specific surface of the used granulated carbon $1125 \text{ m}^2/\text{g}$ /BET. The temperature dependence of the CH₃I break-through curves is shown in Fig. 29.

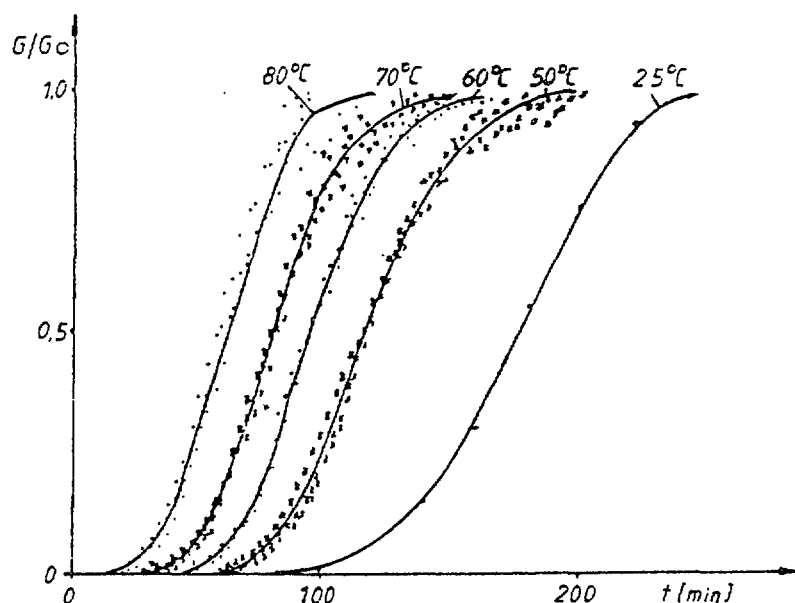


Figure 29. The influence of temperature on the break-through curves. CH₃I concentration $2,1 \times 10^{-4}$ M/l, relative humidity 30 %.

The influence of temperature on the dynamic saturation capacity of the activated carbon is shown in Fig. 30. The adsorption isotherms in Fig. 30 show the maximum mass of CH₃I adsorbed by unit mass of carbon as a function of inlet CH₃I concentration, at 25, 50 and 70 °C and 30% relative humidity.

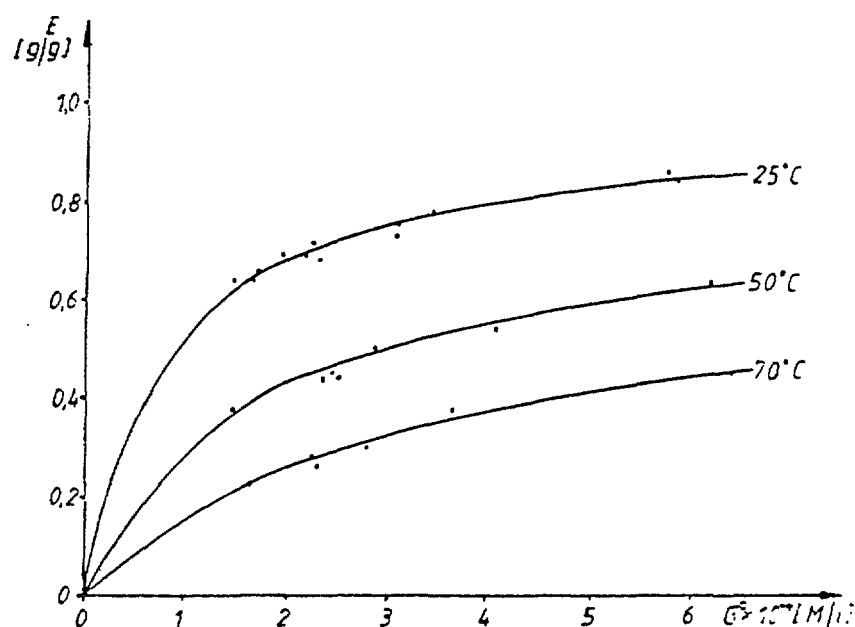


Figure 30. The influence of temperature on the dynamic saturation capacity of activated carbon. E - the maximum mass of CH_3I adsorbed by unit mass of carbon, G^0 - CH_3I concentration upstream

The influence of relative humidity is shown in Figs 31 and 32. The CH_3I break-through curves shown in Fig. 31 were measured at 50°C , 3×10^{-4} M/l CH_3I concentration, the relative humidity was 30 % /curve 1/ and 75 % /curve 2/, the adsorbent was preconditioned for one hour with dry air both cases.

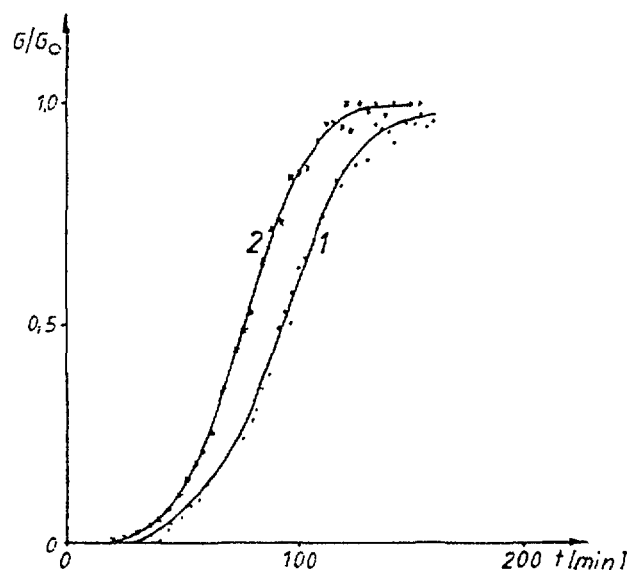


Figure 31. The influence of relative humidity on the break-through curves at 50°C and 3×10^{-4} M/l CH_3I concentration.
1 - relative humidity 30%, 2 - relative humidity 75%

The break-through curves shown in Fig. 32 were measured at 30 °C, 3×10^{-4} M/l CH₃I concentration, the relative humidity was 75 % and preconditioning /1 hour/ with dry air for curve 1 and with humid air (RH = 75 %) for curve 2.

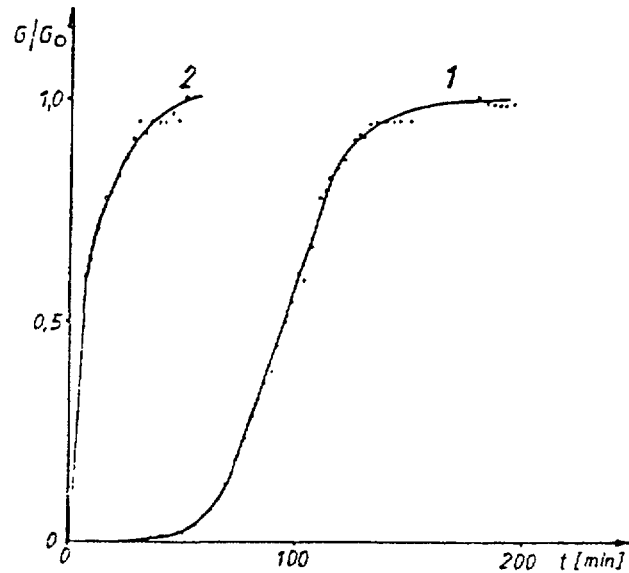


Figure 32. The influence of relative humidity on the break-through curves at 30 °C and 3×10^{-4} M/l CH₃I concentration.
 1 - preconditioning with dry air
 2 - preconditioning with humid air (RH = 75%)

As conclusion it can be established that both increasing temperature and relative humidity decrease the lifetime and useful capacity of the activated carbon. When searching for quantitative description of these effects it seems to be possible to determine the temperature dependence of the physico-chemical constants /adsorption and desorption rate constants, active site concentration/ which are included in the theoretical model.

REFERENCES

1. Friedrich, V.: CRP Progress Report, Budapest, 1986
Contract No. 3723/R1/RB.
2. Hirling, J.: Particle Size Analysis of Submicron Radioactive Aerosols by Centrifugal Spectrometer and High Efficiency Filtration
Dissertation, Budapest, 1976 (in Hungarian).
3. Hirling, J.: Comparison of Some Existing Testing Methods for Particulate Filters with Special Regard to Radioactive Tracer Measures. Final Report. Part of an IAEA Coordinated Research Programme on Particulate Filter Testing Methods 1982, Contract No. 2270/RB.
4. Friedrich, V.: Investigation of the Influence of Accident Conditions on the Performance of HEPA Filters and Iodine Trapping Systems, Progress Report, Part of an IAEA Coordinated Research Programme on Retention of Iodine and Other Airborne Radionuclides in Nuclear Facilities During Abnormal and Accident Conditions, 1984, Contract No. 3723/RB.
5. Wilhelm, J. G.: Removal of Gaseous Radioiodine with Solid Adsorbents, IAEA Seminar on Testing and Operation of Off-Gas Cleaning Systems at Nuclear Facilities, Karlsruhe, 1982.
6. Deitz, V.R.: Charcoal Performance Under Simulated Accident Conditions, 17th DOE Nuclear Air Cleaning Conference Proceedings, Vol. 2, 1982.
7. H. Shiomi, Y. Yuasa, A. Tani, M. Ohki, T. Nakagawa: A Parametric Study on Removal Efficiency of Impregnated Activated Charcoal and Silver Zeolite for Radioactive Methyl Iodide, 17th DOE Nuclear Air Cleaning Conference Proceedings, Vol. 1, 1982.
8. L. A. Jonas, W. J. Svirbely: The Kinetics of Adsorption of Carbon Tetrachloride and Chloroform from Air Mixtures by Activated Carbon, Journal of Catalysis 24, 446-469 /1972/.
9. Friedrich, V., Lux, I.: Theoretical and Experimental Study of the Adsorption of Radioactive Gases on Continuous Flow Columns. I. Radional. Nucl. Chem. Letters 93/5/309-318 (1985).

EVALUATION OF HIGH EFFICIENCY PARTICULATE AIR (HEPA) AND IODINE FILTERS UNDER HIGH TEMPERATURE, HUMIDITY AND RADIATION

K. RAMARATHINAM, S. KUMAR, K.G. GANDHI,
S. RAMACHANDRAN
Bhabha Atomic Research Centre,
Bombay, India

Abstract

Effects of temperature, humidity and gamma irradiation were investigated related to the performance of micro-glass fibre filter media, iodine removal on impregnated activated charcoal and overall performance of HEPA filter and iodine adsorber prototype units.

1 INTRODUCTION

The ventilation and air cleaning systems of Nuclear facilities are equipped with High Efficiency Particulate Air (HEPA) Filters for the ultimate removal and retention of particulates and Iodine filters for the removal and retention of radioiodine, mainly to restrict the release of airborne radioactivity during normal operations and anticipated operational occurrences (1, 2, 3, 4, 5). During the course of anticipated operational occurrences the filters may be exposed to (a) high temperature and humidity, (b) heavy entrained water droplets due to condensation of steam or spray activation, (c) temperature rise due to fire or decay heat of retained activity and (d) high radiation dose due to contaminated stream or due to highly active trapped particulates, vapours or gases. Exposure of these filters under such conditions may result in performance deterioration.

As safety related problem the work on the evaluation of main components, as that of HEPA Filter media, impregnated activated charcoal and prototype HEPA and Iodine filter units assembled using selected filter media and impregnated activated charcoal, under conditions of high temperature, humidity and radiation, was included as the IAEA coordinated research programme of work. (6).

This report details the work carried out on (a) evaluation of micro glass fibre filter media under conditions of high temperature, humidity and gamma radiation, (b) the performance of impregnated activated charcoal in respect of their removal and retention of radioiodine under high temperature, humidity, gamma radiation and washout of impregnants due to bulk condensation of water vapour and (c) evaluation of prototype units of HEPA and iodine filters, to ascertain the overall performance under exposure to air streams of high temperature, humidity.

2 PERFORMANCE EVALUATION OF HEPA FILTER MEDIA

The high efficiency particulate filters are assembled using micro glass fibre filter medium (7). The glass fibre used is to a large extent less than one micron in diameter and the inter fibre space is quite large compared to the fibre diameter. Glass fibre filter papers are formed using additives to provide the required strength and water repellancy to the medium. The basic requirements of the medium is given in Table 1.

TABLE 1. BASIC REQUIREMENTS OF MICRO GLASS FIBRE FILTER MEDIUM

Basis weight	: Not less than 78 gm/m ²
Thickness	: 0.4 to 0.75 mm
Combustible Content	: Not more than 5%
Particle Retention Efficiency	: Not less than 99.97% for the most penetrating submicron size aerosol.
Air Flow Resistance	: Not more than 25 mm at 2.5 mm/sec
Water repellancy	: "0" penetration at 75 cms water column. "0" penetration at 15 cms of water column after irradiation to 6.4×10^7 rads
Dry Bursting strength	: Not less than 26 cms w.g. after exposure to 300 °C

Three different microglass fibre filter media coded A, B and C procured from various sources, were evaluated for their filtration and other physical characteristics after exposure to high temperature, steam air mixture involving high temperature and high humidity and gamma radiation.

2.1 Effect of high temperature and radiation

A number of samples of 15cm x 15cm were exposed to different temperatures upto 350°C in steps of 50°C over a period 8 hours to study the effect of temperature exposure on the characteristics of the media such as, water repellancy, wet and dry bursting strength, flow resistance and particulate removal efficiency. These filter media, after exposure to different temperatures were irradiated to different gamma radiation dose levels upto a cumulative dose level of 2.5×10^8 rads at the rate of 1.1×10^5 rads per hour in the ISOMED gamma irradiation facility (Fig. 1) at Bhabha Atomic Research Centre, Trombay, Bombay.

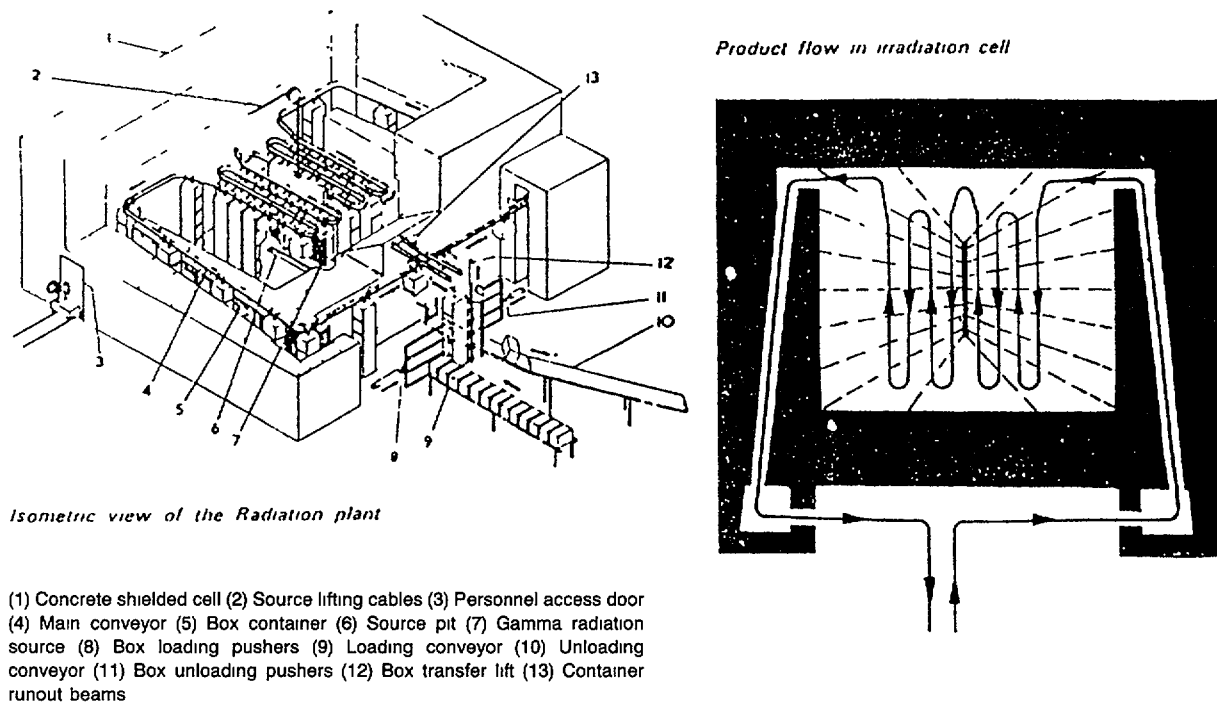


FIG.1 ISOMED: gamma irradiation facility at BARC

Water repellancy of the media was determined using 50mm dia. supported test sample installed between two flanges. The water repellancy of the media was measured in terms of cms. of water head at which the first drop appears within 10 minutes. The wet bursting strength was determined by using 50mm dia of unsupported media and determining the water head at which the media ruptures. The height of the water column is taken as the measure of the wet bursting strength. Dry bursting strength of the media was evaluated by clamping a 50mm dia unsupported sample and increasing the air flow rate through the media. The pressure drop in cms. of w.g. at which the media ruptures was recorded. The flow resistance of the medium was evaluated using the test set up as shown in Figure 2 and the particulate removal efficiency of the filter media was evaluated in the same set up using polydisperse DOP aerosol and single particle counter method (8). The results of such evaluations are summarised in Tables 2, 3 and 4.

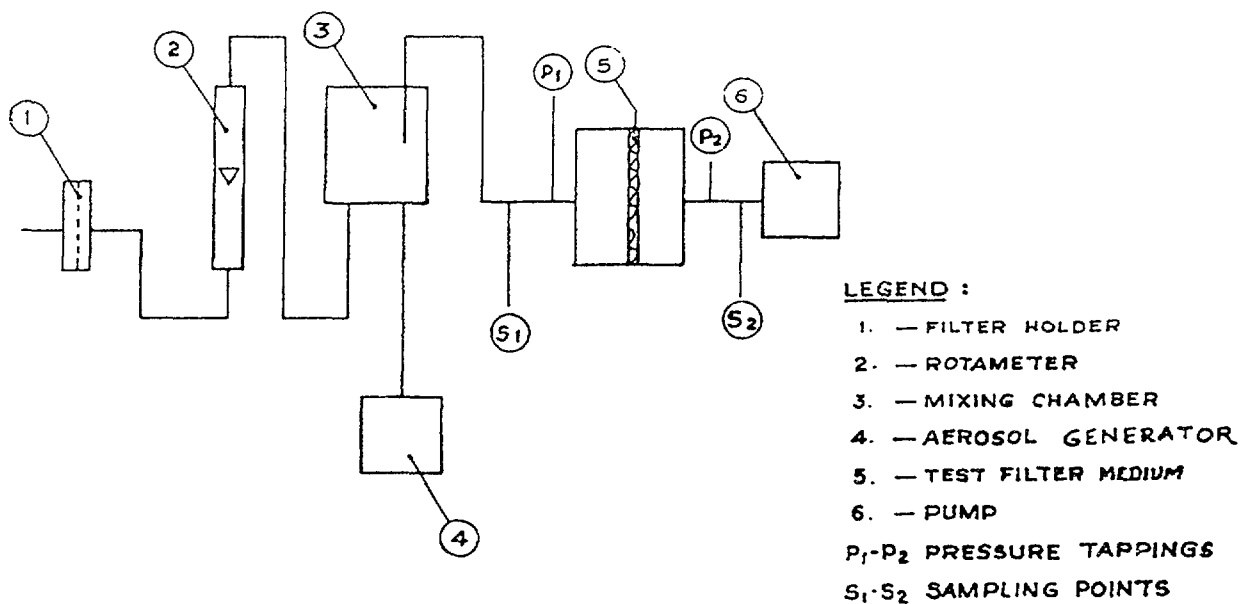


FIG.2. Test assembly for evaluation of filter media.

TABLE 2. EFFECT OF TEMPERATURE AND GAMMA RADIATION ON WATER REPELLENCY OF FILTER MEDIA

Sl No	Dose in Rads	Water Repellency of filter media exposed to Temperatures (cms of v,g)																						
		Room Temp			50°C			100°C			150°C			200°C			250°C			300°C				
		A	B	C	A	B	C	A	B	C	A	B	C	A	B	C	A	B	C	A	B	C		
1.	N11	90+	85	90+	90+	84	90+	90+	83	90+	90+	79	90+	90+	61	90+	90+	0	90+	90+	0	90+	90+	
2.	2.8×10^6	90+	65	90+	90+	53	90+	90+	45	90+	90+	36	90+	90+	5	90+	90+	0	90+	90+	0	90+	90+	
3.	5.6×10^6	90+	50	90+	90+	44	90+	90+	38	90+	90+	26	90+	90+	3	90+	90+	0	90+	90+	0	90+	90+	
4.	8.4×10^6	90+	36	90+	90+	32	90+	90+	23	90+	90+	21	90+	90+	3	90+	90+	0	90+	90+	0	90+	90+	
5.	1.4×10^7	90+	21	90+	90+	14	90+	90+	13	90+	90+	9	90+	90+	2	90+	90+	0	90+	90+	0	90+	90+	
6.	5.5×10^7	90+	5	90+	90+	4	90+	90+	3	90+	90+	3	83	90+	2	79	90+	0	75	90+	0	65	90+	0
7.	1.0×10^8	90+	2	64	90+	0	60	90+	0	46	90+	0	41	90+	0	30	90+	0	28	90+	0	30	90+	0
8.	2.0×10^8	90+	0	60	90+	0	60	90+	0	45	90+	0	40	90+	0	30	80	0	30	83	0	30	80	0
9.	2.5×10^8	90+	0	55	90+	0	50	90+	0	46	90+	0	40	90+	0	32	80	0	32	75	0	30	71	0

NOTE: 1. A,B and C above are the three types of filter media used for the evaluations
 2. + indicates the values above the figure shown
 3. No significant variation in respect of resistance to air flow and particulate removal efficiency was observed for all the media evaluated.

TABLE 3. EFFECT OF TEMPERATURE AND GAMMA RADIATION ON WET BURSTING STRENGTH OF FILTER MEDIA

Sl No	Dose in Rads	Wet Bursting Strength of filter media exposed to Temperatures(cms of v,g)																		350°C					
		Room Temp			50°C			100°C			150°C			200°C			250°C			300°C					
		A	B	C	A	B	C	A	B	C	A	B	C	A	B	C	A	B	C	A	B	C			
1.	N11	88	55	36	88	53	36	88	52	35	46	53	36	36	52	29	20	22	19	27	17	15	27	9	18
2.	2.8×10^6	72	46	35	78	45	34	88	44	33	44	41	24	32	31	26	31	-	12	29	-	12	29	-	11
3.	5.6×10^6	55	43	24	55	39	25	88	38	28	42	35	24	31	29	27	29	-	11	27	-	13	27	-	11
4.	8.4×10^6	52	42	23	53	32	22	87	32	23	39	31	23	31	-	24	26	-	12	27	-	13	27	-	13
5.	1.4×10^7	46	40	22	47	31	19	61	31	22	38	29	22	27	-	22	21	-	10	20	-	13	20	-	14
6.	5.6×10^7	43	-	18	42	-	18	54	-	22	34	-	18	25	-	17	20	-	12	15	-	12	15	-	11
7.	1.0×10^8	28	-	16	32	-	13	37	-	17	32	-	16	22	-	16	19	-	12	13	-	12	13	-	10
8.	2.0×10^8	37	-	15	38	-	14	35	-	17	31	-	15	20	-	16	20	-	13	15	-	13	15	-	10
9.	2.5×10^8	31	-	12	34	-	16	31	-	16	31	-	14	20	-	15	20	-	12	16	-	12	15	-	10

NOTE: 1. A,B and C above are the three types of filter media used for evaluations.
 2. - indicates that water head could not be developed due to total permeability to water.
 3. No significant variation in respect of resistance to air flow and particulate removal efficiency was observed for all the media evaluated.

TABLE 4. EFFECT OF TEMPERATURE AND GAMMA RADIATION ON DRY BURSTING STRENGTH OF FILTER MEDIA

Sl No	Dose in Rads	Dry Bursting strength of filter media exposed to temperatures (cm's of w.g)																							
		Room Temp			50°C			100°C			150°C			200°C			250°C			300°C					
		A	B	C	A	B	C	A	B	C	A	B	C	A	B	C	A	B	C	A	B	C			
1.	N11	39 ⁺	36 ⁺	40 ⁺	39 ⁺	36 ⁺	40 ⁺	39 ⁺	36 ⁺	40	39 ⁺	36 ⁺	40	39 ⁺	36 ⁺	37	24	27	10	36	27	19	33	27	21
2.	2.8x10 ⁶	39 ⁺	36 ⁺	40 ⁺	39 ⁺	36 ⁺	39	39 ⁺	36 ⁺	38	39 ⁺	36 ⁺	37	39 ⁺	36 ⁺	35	34	33	11	34	26	14	36	22	22
3.	5.6x10 ⁶	39 ⁺	36 ⁺	40 ⁺	39 ⁺	36 ⁺	38	39 ⁺	36 ⁺	35	39 ⁺	36 ⁺	34	39 ⁺	35	33	23	32	32	32	25	15	36	22	20
4.	8.4x10 ⁶	39 ⁺	36 ⁺	36	39 ⁺	36 ⁺	34	39 ⁺	36 ⁺	33	38	36	32	37	34	31	24	31	10	26	25	14	35	23	19
5.	1.4x10 ⁷	39 ⁺	36	33	39 ⁺	36	32	37	34	30	36	33	28	35	32	24	21	30	10	25	23	16	33	21	20
6.	5.6x10 ⁷	39	36	26	38	34	24	36	32	25	35	30	24	31	29	20	22	30	11	23	22	17	29	18	21
7.	1.0x10 ⁸	39	33	23	38	29	22	33	28	21	33	27	19	28	22	20	20	22	10	21	21	13	27	19	24
8.	2.0x10 ⁸	38	26	19	36	26	18	35	23	21	35	26	17	28	21	20	26	20	15	25	21	14	25	20	12
9.	2.5x10 ⁸	26	24	11	24	26	16	22	24	21	25	21	17	25	19	17	24	17	14	25	21	11	23	20	12

NOTE:- A, B and C above are the three types of filter media used in the evaluations.

*indicates values above the figure shown

No significant variation in respect of resistance to air flow and particulate removal efficiency was observed for all the media evaluated.

2.2 Effect of steam air mixture

Filter media when exposed to steam and hot air mixture indicated that for the range of temperatures of 50°C to 95°C and near saturation relative humidity, there was initially marginal increase in the pressure drop for all the media. Temperature exposed gamma irradiated filter medium B, having lesser water repellency, when exposed to droplets, as a result of bulk condensation the pressure drop increased rapidly resulting in rupture even after very short exposure. The filter medium having higher water repellency, however, did not rupture even after extended exposures and the performance of the medium was found to be satisfactory when tested thereafter.

3 PERFORMANCE EVALUATION OF IMPREGNATED ACTIVATED CHARCOAL

Iodine adsorber in the combined particulate iodine filter are in the form of trays of 2" thick, suitably assembled to provide the desired residence time of

0.24 sec. (Fig. 3). For the removal and retention of elemental iodine and methyl iodide, the selected activated charcoal was impregnated with reactive chemicals to provide high and consistent removal efficiency and low desorption of adsorbed iodine (9, 10, 11). The specifications of the impregnated activated charcoal currently used in the assembly of iodine filters are shown in Table 5.

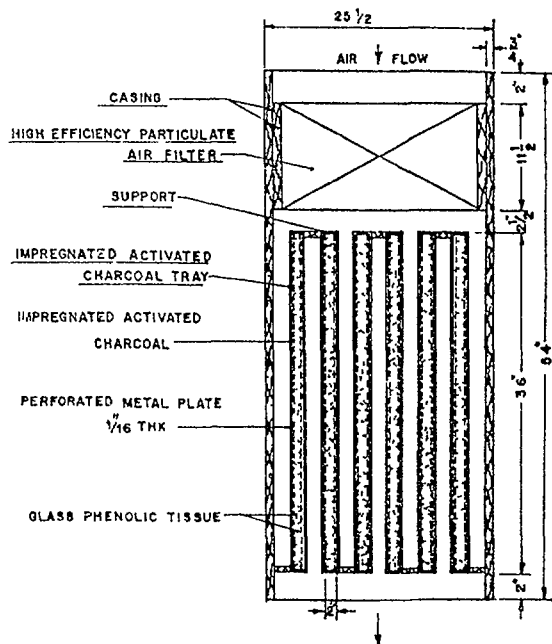


FIG 3 Iodine filter of 1000 CFM capacity

Selected activated charcoal, impregnated with 2% KI + 1% KOH were evaluated for the performance effectiveness at high temperature, high humidity and radiation. The bed of 5cm and a stay time of 0.24 sec was employed for this investigation.

3.1 Evaluation at high temperature and high humidity

The experimental set up used to study the behaviour of impregnated activated charcoal for the removal of methyliodide under high temperature and high humidity is shown in Fig. 4. In the set up, the temperature and relative humidity of the air stream can be maintained at a constant predetermined value, during the single test. Before introducing activity into the stream, the air was permitted to flow over the charcoal beds for atleast an hour to equilibriate the beds.

TABLE 5. SPECIFICATIONS OF IMPREGNATED ACTIVATED CHARCOAL CURRENTLY IN USE
IN IODINE FILTERS

1.	Base material	:	Coconut shell
2.	Activation agent	:	Steam - air
3.	Mesh size	:	8/16 B.S.S. mesh
4.	Ash content	:	2% or less
5.	B.E.T. surface area	:	$1050 \pm 50 \text{ m}^2/\text{g}$
6.	Hardness number	:	97 ± 2
7.	Moisture content	:	5% (wt/wt)
8.	Carbontetra chloride activity	:	$62 \pm 2\%$
9.	Iodine number	:	1000
10.	Ignition tempera- ture	:	350°C min.
11.	Apparent density	:	$0.5 \pm 0.02 \text{ g/ml.}$
12.	Impregnants	:	2% KI 1% KOH wt/wt

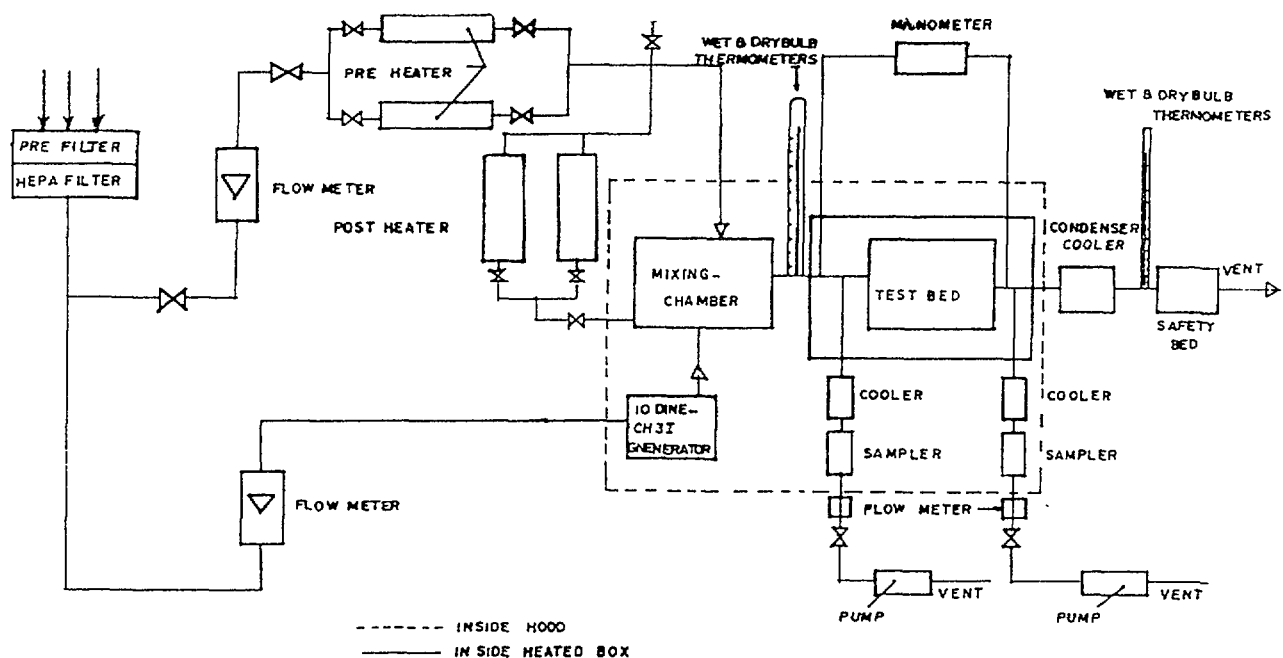


FIG.4. Set-up for evaluation under high humidity and high temperature.

3.2 Effect of high temperature

The effect of high temperature on the removal effectiveness of methyl iodide by impregnated activated charcoal was studied in detail by controlling the air flow temperature from ambient to 100°C at very low humidity. The results are shown in Fig. 5.

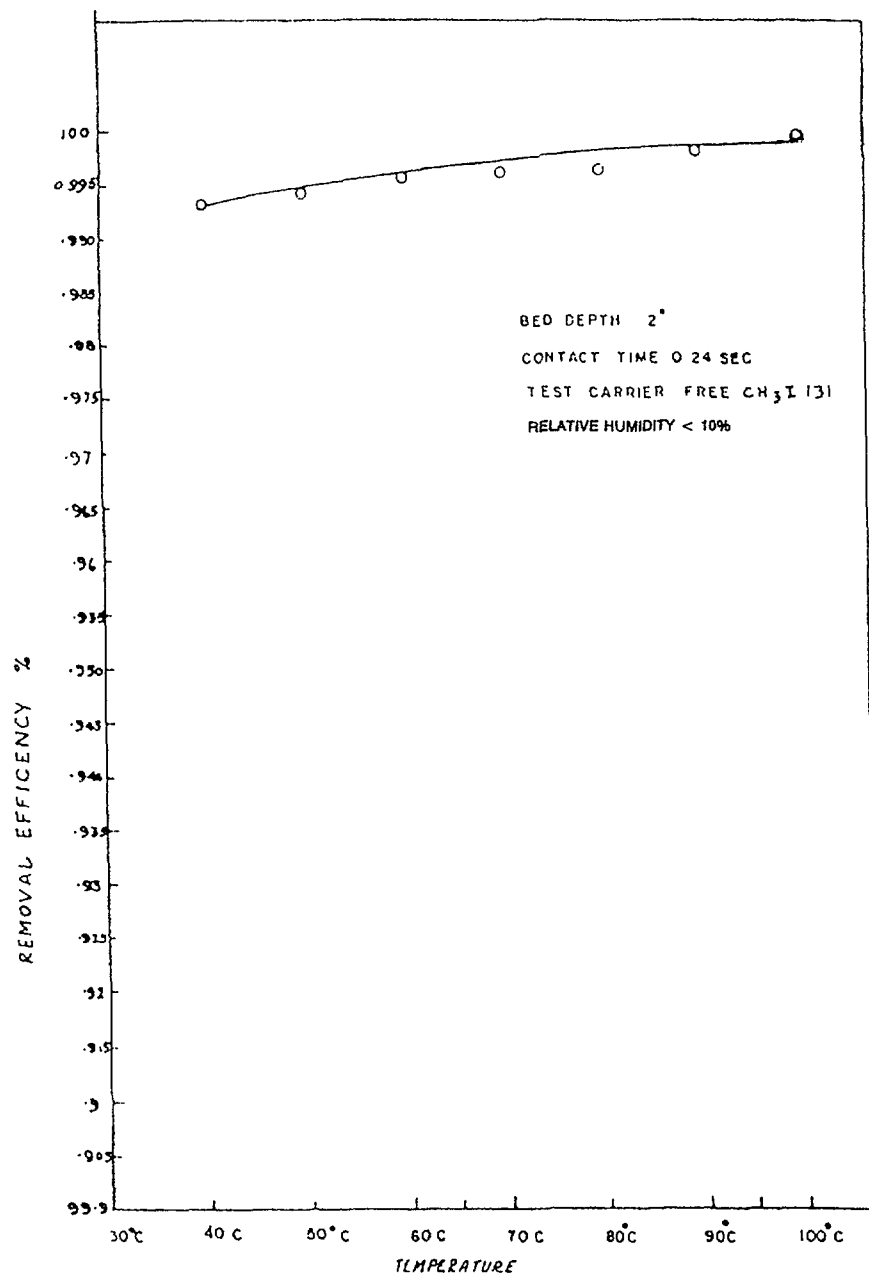


FIG.5. Efficiency of impregnated activated charcoal at different temperatures.

3.3 Effect of relative humidity

The effect of relative humidity was studied using the streams at three different temperatures. The results of the evaluations are shown in Fig. 6.

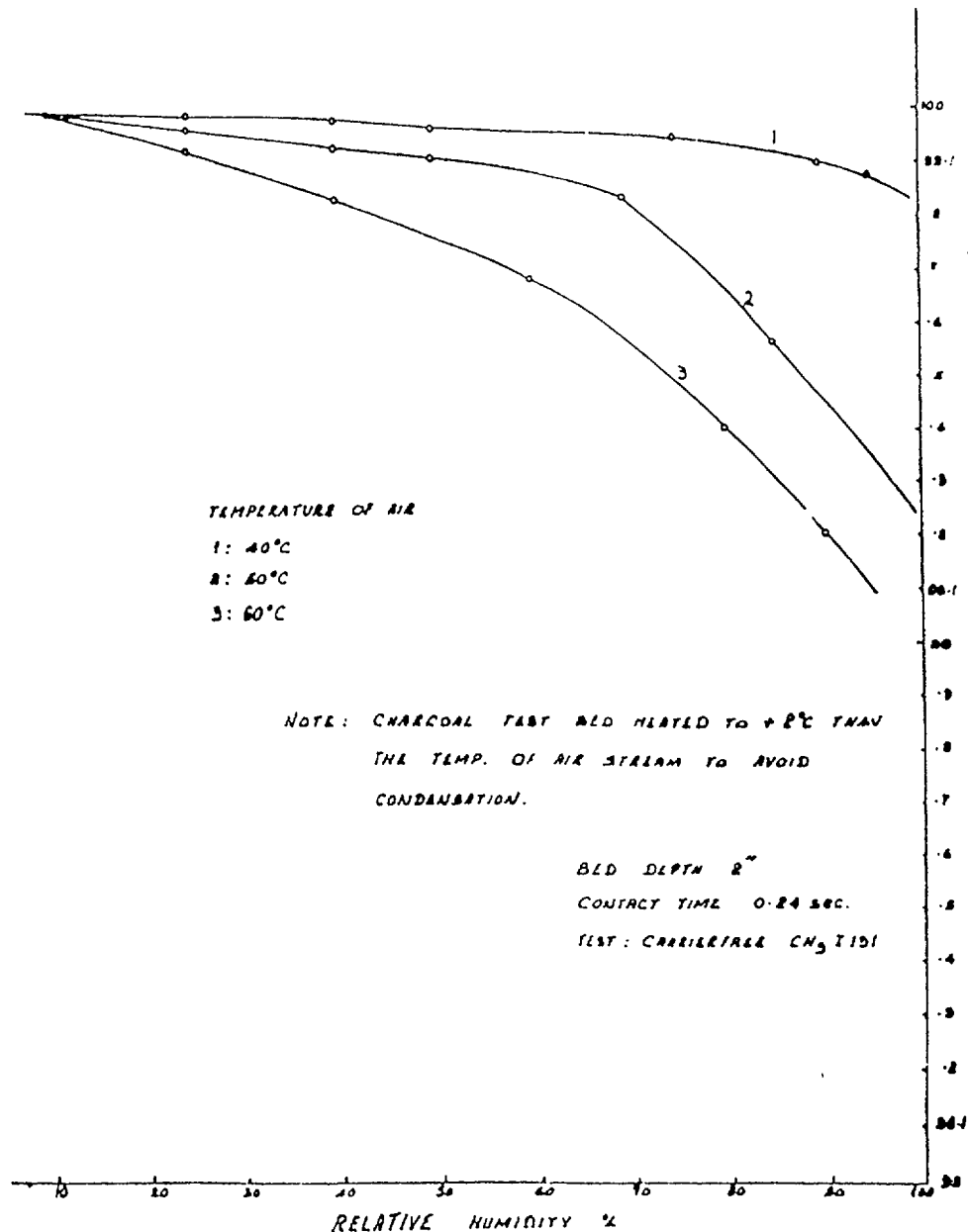


FIG.6. Removal efficiency of impregnated activated charcoal at different temperatures and relative humidity.

3.4 Effect of high temperature and high humidity

The combined effect of high temperature and high humidity on the removal effectiveness of impregnated charcoal for methyl iodide was studied and the results are shown in Fig. 7.

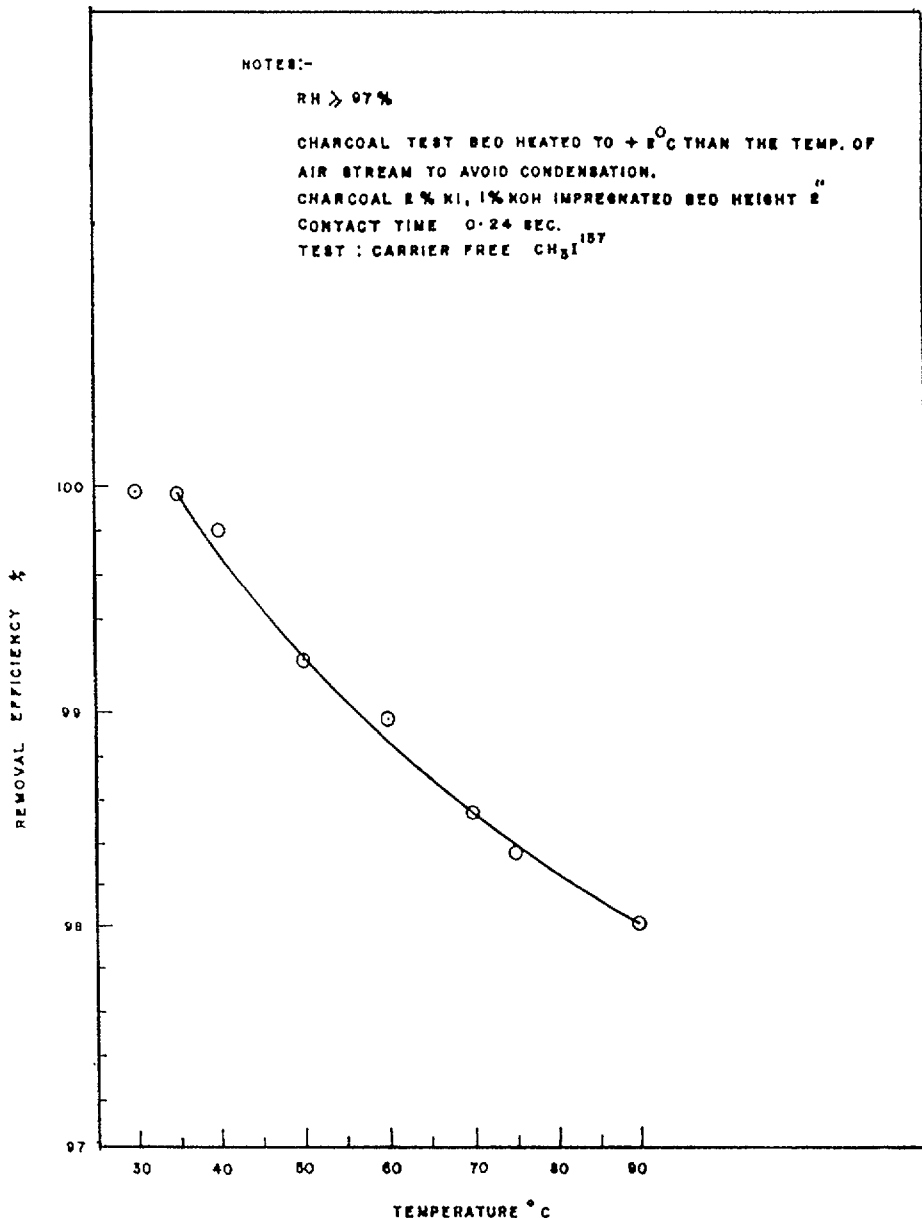


FIG.7. Removal efficiency of impregnated activated charcoal with temperature.

3.5 Effect of Condensation of Water Vapour on the performance of impregnated activated charcoal

The performance of the impregnated charcoal with different moisture loading due to up-take of condensed water have been carried out to estimate the extent of performance deterioration. Table 6 summarises the results of such evaluations using an experimental set up as shown in Fig. 8.

TABLE 6. METHYL IODIDE REMOVAL EFFICIENCY OF IMPREGNATED ACTIVATED CHARCOALS HAVING DIFFERENT MOISTURE CONTENTS

Mesh Size : 1-8 + 16 BSS mesh
 Impregnation : 2% KI, 1% KOH
 Contact time : 0.24 Sec
 Temperature : 28°C
 Humidity : Near saturation
 Bed thickness : 50mm

Sl.No.	Moisture content % (Wt/Wt)	$\text{CH}_3\text{I}^{131}$ Removal Efficiency (%)
1.	7.50	99.85
2.	10.00	99.60
3.	15.05	99.30
4.	20.00	98.07
5.	25.07	96.02
6.	26.07	95.83
7.	29.05	93.54
8.	31.00	93.10
9.	34.01	91.24
10.	35.04 (Wet)	83.00*

* Results were erratic ranging from 80 to 86%

1	NEEDLE VALVE	11	$\text{CH}_3\text{I}^{131}$ GENERATOR *
2	FLOW METER	12	$(\text{CH}_3)_2\text{SO}_4 + \text{NaI}$ *
3	WATER	13	3 WAY VALVE
4	HEATER	14	SORBENT UNDER TEST
5	ENERGY REGULATOR	15	BACKUP BEDS
6	CONDENSER	16	STEAM GENERATOR
7	I_2 GENERATOR *	17	STEAM AIR HEATER
8	$\text{H}_2\text{O}_2/\text{NaNO}_2 + \text{NaI}$	18	HOT AIR OVEN
9	H_2SO_4	19	THERMO-COUPLE
10		20	CONDENSATE COLLECTOR

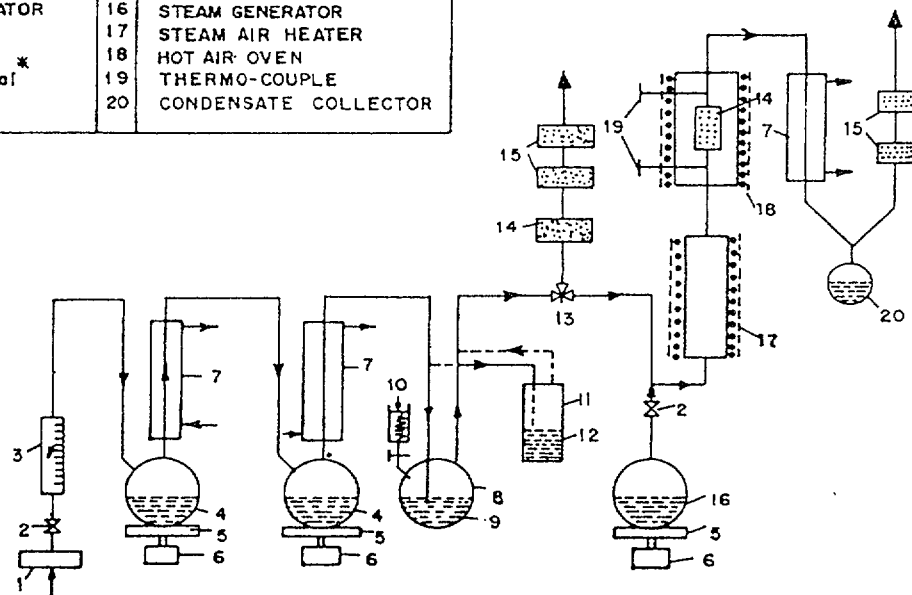


FIG.8. Experimental set-up for $\text{I}_2/\text{CH}_3\text{I}$ removal studies.

Continued condensation of the moisture on the adsorbent bed results in the draining of condensed water from the bed containing the impregnant resulting in its washout which depends on the extent of condensed water and the amount of impregnant on the adsorbent bed. The average amount of impregnant retained on the adsorbent in relation to the ratio of volume of the condensed water to that of the bed volume was estimated using the experimental set up shown in Fig. 9, which ensures constant rate of distillation of water on to the top of the adsorbent bed of 50mm thickness. The extent of impregnant retained on the charcoal by the washout due to the condensing steam is arrived at by estimating the amount of impregnant in the drained liquid. The extent of impregnant retained on the adsorbent in relation to the amount of liquid condensed is shown in Fig. 10. Table 7

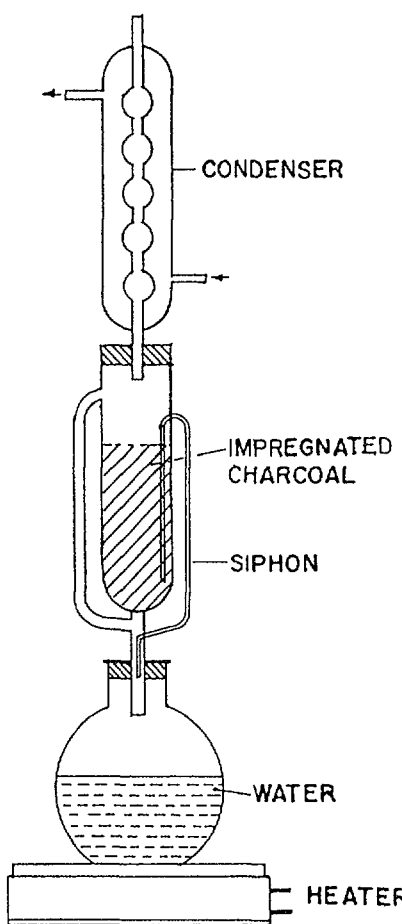


FIG.9. Experimental set-up to study the washout of impregnant.

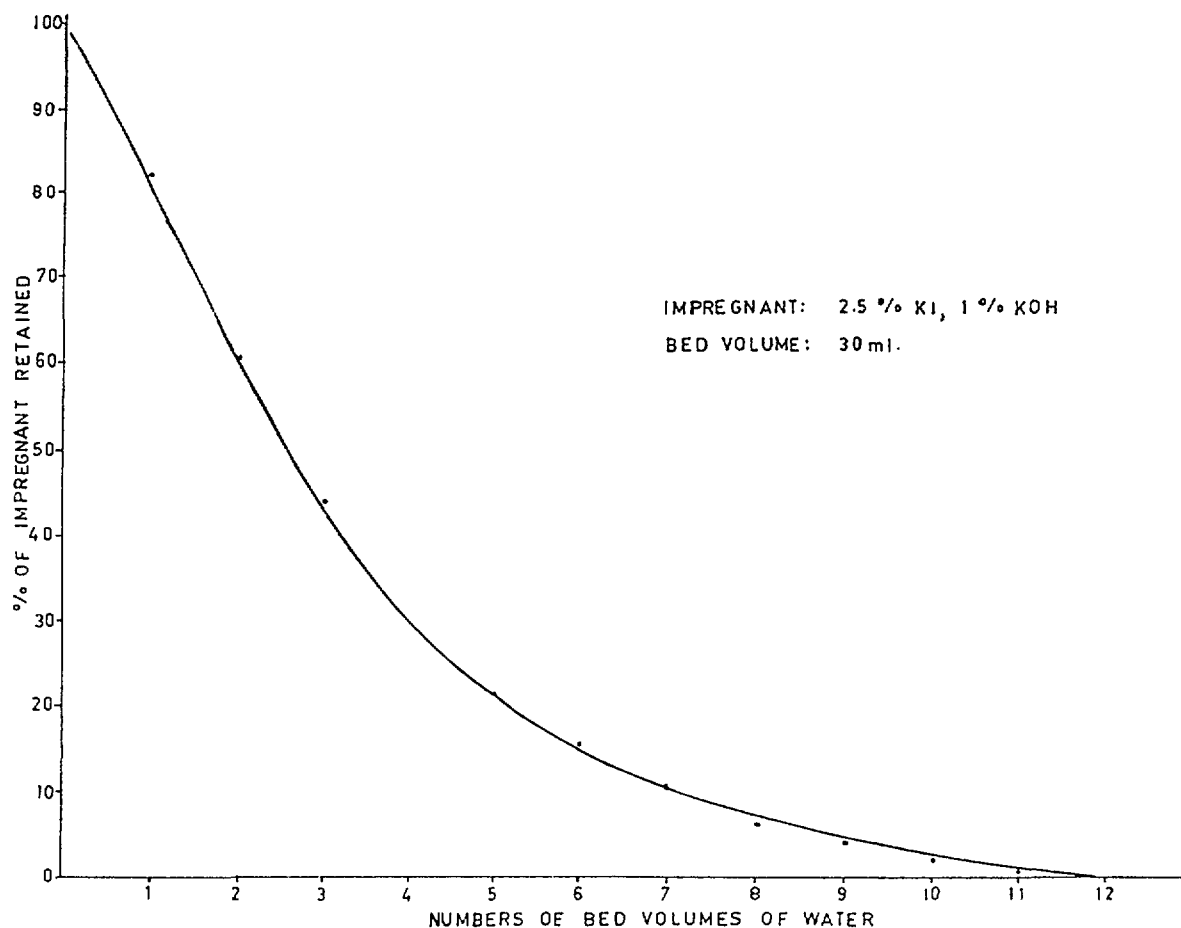


FIG.10. Washout of impregnant due to moisture condensation.

TABLE 7. $\text{CH}_3\text{I}^{131}$ REMOVAL EFFICIENCY OF IMPREGNATED ACTIVATED CHARCOAL

Bed thickness : 50mm
 Contact time : 0.24 Sec
 Temperature : 28°C
 Relative Humidity : Near saturation
 Test Source : Carrier free $\text{CH}_3\text{I}^{131}$
 Moisture Content : 7.5% (W/W)

S1. No	Impregnation (Wt%)		$\text{CH}_3\text{I}^{131}$ Removal Efficiency (%)
	KI	KOH	
1.	-	-	95.156
2.	0.5	0.25	98.461
3.	1.0	0.50	99.389
4.	1.5	0.75	99.548
5.	2.0	1.00	99.874
6.	2.5	1.25	99.990
7.	3.0	1.50	99.964

summarises the results of evaluation of charcoals containing different quantity of impregnants which may result after washout and subsequent drying up of the charcoal due to flow of air.

3.6 Effect of gamma irradiation on the performance of impregnated activated charcoal

Sample trays of 50 mm thickness containing activated charcoal were exposed to gamma radiation in the ISOMED gamma irradiation facility at BARC to a cumulative dose levels from 2.8×10^6 rads to 8.4×10^7 rads. The gamma exposed charcoals were evaluated for their surface area using the BET method and the results are given in Table 8. Methyl iodide removal efficiency of the irradiated charcoals were evaluated and the results are given in Table 9.

TABLE 8. BET SURFACE AREA MEASUREMENT OF IMPREGNATED ACTIVATED CHARCOAL AFTER EXPOSURE TO GAMMA RADIATION

Unimpregnated Charcoal : $940 \text{ m}^2/\text{gm}$

Impregnated Charcoal : $894 \text{ m}^2/\text{gm}$

Sl. No.	Cumulative Exposure dose (Rads)	BET Surface Area m^2/gm
1	2.8×10^6	868
2	8.4×10^6	876
3	2.0×10^7	878
4	5.0×10^7	880
5	6.5×10^7	859
6	8.4×10^7	864

TABLE 9. $\text{CH}_3\text{I}^{131}$ REMOVAL EFFICIENCY OF IMPREGNATED ACTIVATED CHARCOALS EXPOSED TO GAMMA RADIATION

Impregnants : 2% KI, 1% KOH
 Bed thickness : 50mm
 Contact time : 0.24 Sec
 Temperature : 90°C
 Relative Humidity : 90%
 Test Source : Carrier free $\text{CH}_3\text{I}^{131}$

S1 No	Cumulative Exposed dose (rads)	$\text{CH}_3\text{I}^{131}$	Removal Efficiency (%)
1.	2.8×10^6		99.478
2.	2.0×10^7		99.464
3.	6.5×10^7		99.470

3.7 Ignition temperature and desorption of adsorbed iodine

Ignition temperature of impregnated activated carbon was investigated in details. The details of such an evaluation is given in the Figure - 11. The desorption of adsorbed iodine was studied by subjecting the loaded adsorbent at 180°C for a period of 5 hours and the amount of desorption was estimated to be less than 1 percent for elemental iodine and methyl iodide.

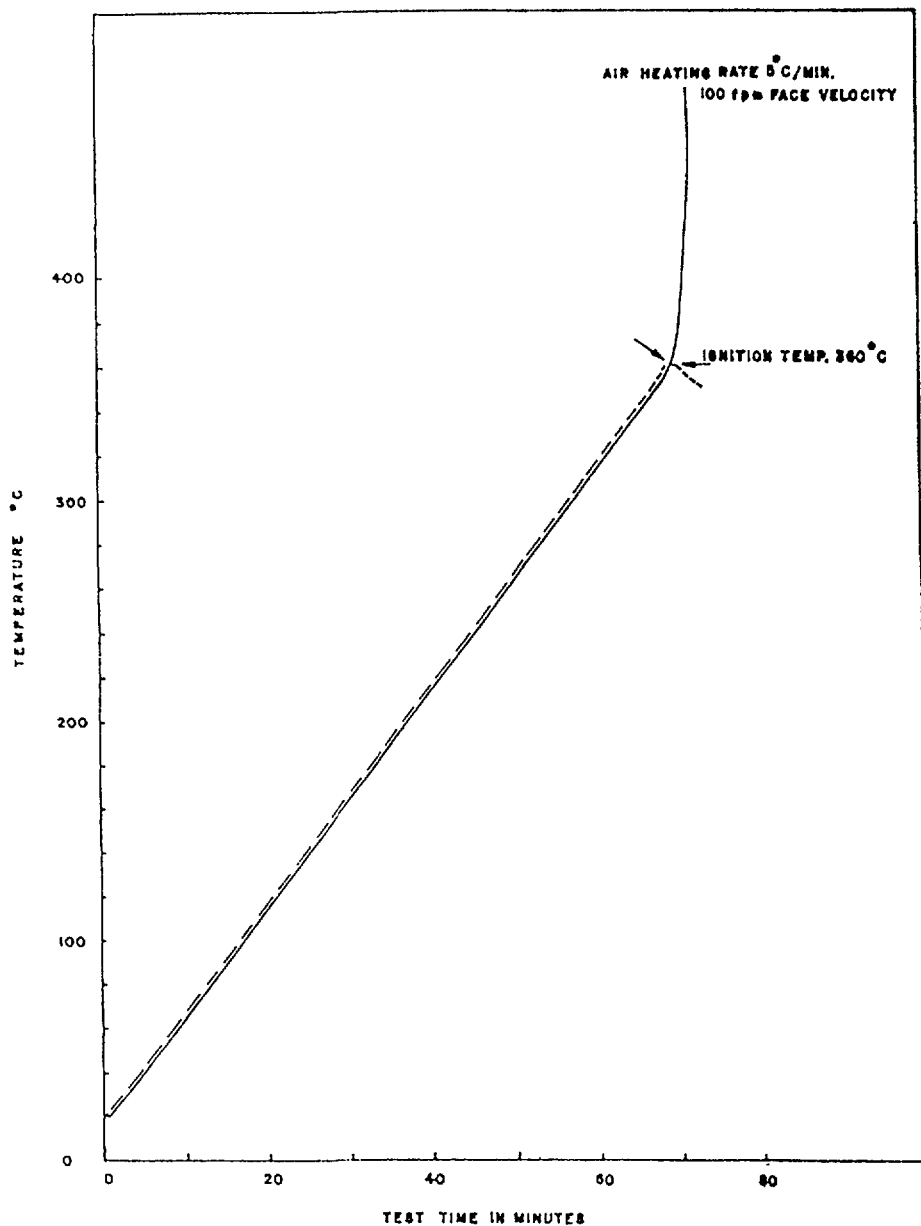


FIG.11. Typical ignition temperature curve.

4

PERFORMANCE EVALUATION OF PROTOTYPE HEPA AND IODINE FILTER UNITS AT HIGH TEMPERATURE, HUMIDITY AND RADIATION

4. 1 Evaluation of prototype HEPA filters

4.1.1 Prototype HEPA filter unit

Prototype units of HEPA filters of designed capacity of 15 cfm (filtering velocity of 2.5 cms/sec) were assembled using the filter medium-A, selected based on

our detailed studies covered during this work, which has shown better characteristics to withstand the conditions of high temperature, humidity and radiation than the other filter media. The specifications of the filter assembled using the selected media and other selected materials of construction are given in Table 10.

TABLE 10. SPECIFICATIONS OF PROTOTYPE HEPA FILTERS USED FOR EVALUATION

1.	Capacity	: 15 cfm
2.	Overall dimension	: 160mm x 160mm x 92mm including 6mm gaskets on both faces
3.	Pressure drop	: Not more than 25mm w.g at the rated capacity of 15 cfm
4.	Efficiency	: Not less than 99.97% for DOP aerosol down to 0.3 micron
5.	Temperature Resistance	: 120°C
6.	Humidity Resistance	: 100% RH
7.	<u>Materials of Construction</u>	
	Filter casing	: Mild Steel (epoxy coated)
	Filter medium	: 100% micro glass fibre filter medium designated as A in this report
	Separator	: Corrugated Aluminium Foil
	Gasket	: Neoprene/glass fibre pad
	Sealant	: Commercially available PVA based adhesive

4.1.2 Test rig for evaluations at high temperature and humidity
Considering certain difficulties experienced in the test rig earlier set up, the same was modified. The test rig used for the evaluation of the prototype units is given in Fig. 12.

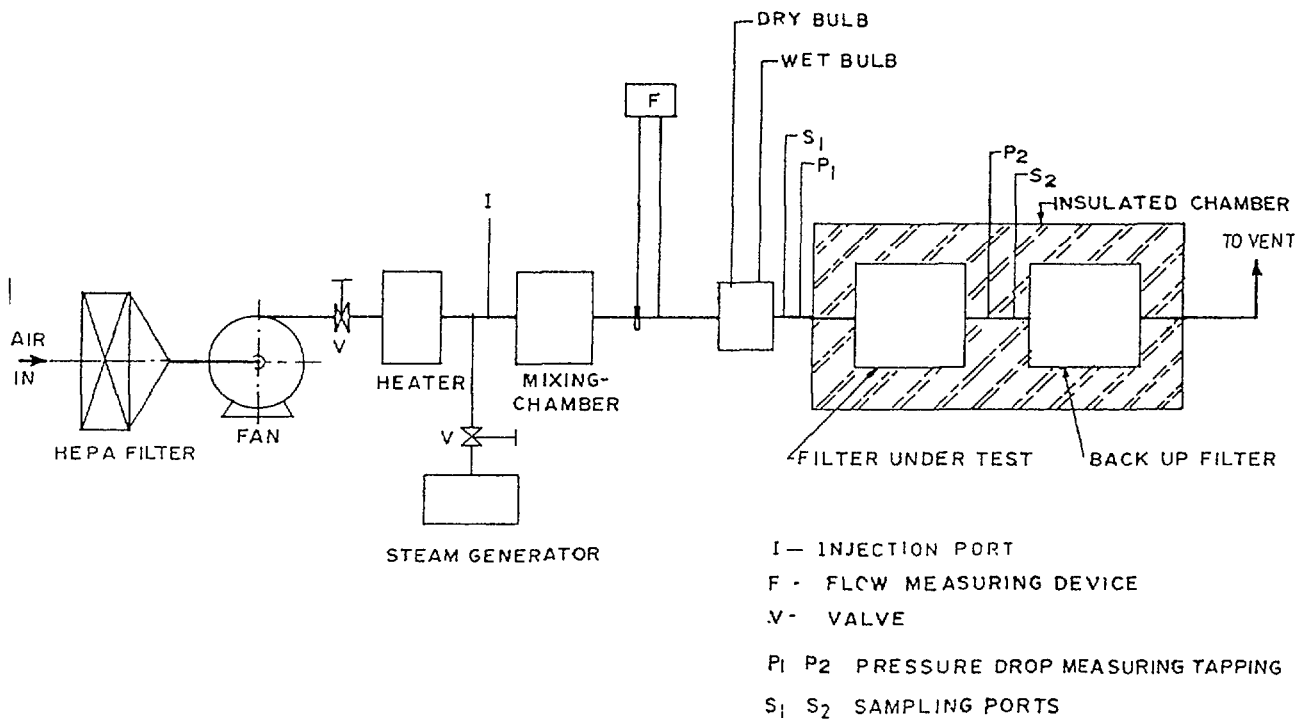


FIG.12. Schematic diagram of filter test rig for evaluation of filters under high temperature and humidity.

The filter testing rig essentially consists of a blower, heater, point for injection of steam from a steam generator, mixing chamber for adequate mixing of steam and hot air, a device for measuring the flow through the duct, wet and dry bulb thermometers for humidity measurement, a filter holder for installation of the test filter, sampling points both upstream and downstream of the filter and pressure tappings to measure the pressure drop across the filter. The whole duct line including the filter housing was well insulated to prevent the loss of heat and to prevent bulk condensation on to the filter under test. By appropriate control over the heater and the steam supply, the desired conditions of the temperature and humidity could be maintained during the experiments.

4.1.3. Evaluation of HEPA filter at high temperature under conditions of static exposure

The prototype HEPA filter units were exposed to varying temperatures from 50°C to 225°C for a period of 4 and 8 hours in a hot air oven. The filters were allowed to cool to room temperature and evaluated for their overall performance in

TABLE 11. PARTICULATE REMOVAL EFFICIENCY OF HEPA FILTERS AFTER EXPOSURE TO ELEVATED TEMPERATURES UNDER STATIC CONDITIONS

Sl No	Temperature of exposure °C	PARTICULATE REMOVAL EFFICIENCY (%)		
		Initial	After 4 hrs	After 8 hrs
1.	38	99.997	99.996	99.991
2.	50	99.994	99.992	99.990
3.	100	99.990	99.990	99.990
4.	125	99.992	99.990	99.980
5.	150	99.990	99.990	99.990
6.	200	99.992	99.990	99.990
7.	225	99.992	97.000	92.70

* By DOP method using polydisperse DOP aerosol and size selective particle counter.

Note: No variation in the pressure drop across the filters was observed when tested at the rated capacity.

respect of their particulate removal efficiency and pressure drop. The particulate removal efficiency of the filters were evaluated using test method standardised employing polydisperse DOP and size selective particle counter (8) in the test rig described in section 4.1.2. The results of evaluation are shown in Table 11.

4.1.4. Evaluation of HEPA filters at elevated temperatures under dynamic conditions.

a) Prototype filter units were exposed to streams of different temperatures of 80°C, 100°C and 120°C in the test set up by selecting heaters of different capacities. During the test no steam was introduced into the set up. After exposure the filters were cooled to room temperature and evaluated for their performance. The results of such evaluations are summarised in Table 12.

TABLE 12. PARTICULATE REMOVAL EFFICIENCY OF HEPA FILTERS AFTER EXPOSURE TO STREAMS OF ELEVATED TEMPERATURES

Sl No	Temp. of stream °C	Hours of exposure	Particulate Removal Efficiency* (%)	
			INITIAL	AFTER exposure
1.	80	8	99.998	99.996
2.	100	8	99.999	99.998
3.	120	8	99 .998	99.998

* By DOP method using Poly-disperse DOP aerosol and size selective single particle counter.

Note: No variation in the pressure drop across the filters was observed when tested at the rated capacity,

b) The filter units were also subjected to flow streams at high temperature and the performance in respect of their removal efficiency was evaluated insitu using uranine(sodium fluoresceinate) method. The method involves atomisation of two percent solution of uranine, using a Laskin type atomiser, as test aerosol and measurement of concentration of the aerosol, upstream and down stream, by sampling onto a millipore filter paper and analysing the concentration using a photofluorimeter set to measure uranine (8). The results of such an evaluation are given in Table 13.

4.1.5. Evaluation of HEPA filters at high temperature and humidity

The filters were exposed to high temperature and high humidity by controlled introduction of steam into the hot air stream. The stream flowing through the filter was maintained at near saturation humidities at 60°C, 90°C and 100°C for 4 and 8 hours. In the absence of a suitable method for measuring the particulate removal efficiency(in-situ), the filters were cooled to room temperature and evaluated for their collection efficiency by DOP method. The results of such evaluations are given in Table 14.

TABLE 13. PARTICULATE REMOVAL EFFICIENCY OF HEPA FILTERS (IN SITU) DURING EXPOSURE TO STREAMS OF ELEVATED TEMPERATURES FOR VARIOUS DURATIONS

Sl No.	Temperature of Exposure °C	<u>PARTICULATE REMOVAL EFFICIENCY (%)</u>		
		After 0 hrs	After 4 hrs	After 8 hrs
1.	80 °C	99.983	99.987	99.988
2.	100 °C	99.982	99.981	99.988
3.	120 °C	99.974	99.988	99.988

* For Uranine (Sodium Fluoreceinate) aerosol of specific size distribution.

Note No Variation in pressure drop across the filters at rated flow was observed during exposures.

TABLE 14. PARTICULATE REMOVAL EFFICIENCY OF HEPA FILTERS AFTER EXPOSURE TO STREAMS OF DIFFERENT TEMPERATURES AT NEAR SATURATION HUMIDITY (RH = 95%)

Sl No	Temperature of Exposure °C	<u>Particulate Removal Efficiency* (%)</u>		
		After 0 hrs	After 4 hrs	After 8 hrs
1.	60	99.998	99.999	99.999
2.	90	99.999	99.999	99.998
3.	100	99.998	99.998	99.998

* By DOP method using polydisperse DOP aerosol and size selective particle counter.

Note: No variations in the pressure drop across the filters was observed when tested at the rated capacity.

4.1.6. Evaluation of HEPA filters exposed to high gamma radiation

The filter units were sealed in polythene bags and irradiated to a cumulative dose from 2.8×10^6 rads to 8.4×10^7 rads. The filters were drawn out at different periods to provide the desired exposure and the filters were tested for their performance using DOP test method. The results of such evaluation are summarised in Table 15.

TABLE 15 PARTICULATE REMOVAL EFFICIENCY OF HEPA FILTERS EXPOSED TO GAMMA RADIATION

S.No	CUMULATIVE DOSE OF EXPOSURE (rads)	PARTICULATE REMOVAL EFFICIENCY	
		<u>BEFORE EXPOSURE</u>	<u>AFTER EXPOSURE</u>
1.	2.8×10^6	99.999	99.999
2.	8.4×10^6	99.998	99.998
3.	2.0×10^7	99.999	99.999
4.	5.0×10^7	99.999	99.999
5.	6.5×10^7	99.999	99.998
6.	8.4×10^7	99.981	99.971

* By DOP method using polydisperse DOP aerosol and size selective particle counter.

Note: No variation in the pressure drop across the filters was observed when tested at the rated capacity.

4.1.7. Evaluation of irradiated HEPA filters after exposure to high temperature and humidity

The gamma irradiated filters were exposed to near saturated air stream at 100°C for a period of 4 and 8 hours. The filters after exposure were cooled and evaluated for their performance by DOP test method. The results of such evaluations are given in Table 16.

TABLE 16. PARTICULATE REMOVAL EFFICIENCY OF IRRADIATED HEPA FILTERS AFTER EXPOSURE TO STREAMS OF ELEVATED TEMPERATURE AND HUMIDITY

S.No	Cumulative dose of Radiation exposure (Rads)	* PARTICULATE REMOVAL EFFICIENCY (%)	
		Before exposure to elevated temperature and humidity	After exposure to elevated temperature and humidity
1.	2.8×10^6	99.999	99.998
2.	8.4×10^6	99.998	99.999
3.	2.0×10^7	99.999	-
4.	5.0×10^7	99.999	99.999
5.	6.5×10^7	99.998	99.998
6.	8.4×10^7	99.972	99.961

* By DOP method using poly disperse DOP aerosol and size selective particle counter

Note: No variation in the pressure drop across the filters was observed when tested at the rated capacity

4.2 Evaluation of prototype Iodine filters

4.2.1 Prototype iodine filters

Prototype iodine filters (15 cfm) were assembled using the impregnated activated charcoals, keeping the bed depth 50mm and a residence time of 0.24sec. in the adsorber tray. A single tray of size 183mm x 183mm x50mm was installed in a casing for evaluation.

4.2.2 Evaluation of Iodine filters

Prototype iodine filters of 15 cfm rated capacity were evaluated using the test rig described in section 4.1.2 of this report. The filters were exposed to 90°C, 90% RH air streams for a duration of 8 hrs during which evaluations for $\text{CH}_3\text{I}^{131}$ removal efficiency were carried out at the end of 4 hrs and 6 hrs. The results of these evaluations are given in Table 17.

TABLE 17. $\text{CH}_3\text{I}^{131}$ REMOVAL EFFICIENCY OF PROTOTYPE IODINE FILTERS AFTER EXPOSURE TO ELEVATED TEMPERATURE AND HUMIDITY

FILTER No	<u>$\text{CH}_3\text{I}^{131}$ Removal Efficiency</u> (%)		
	After 0 Hrs	After 4 Hrs	After 8 Hrs
I	99.96	99.24	99.24
II	99.97	99.24	99.26

5 RESULTS AND DISCUSSIONS

5.1 HEPA filter media

- i) Water repellency of the media coded 'A' and 'C' were unaffected upto 350°C exposure whereas media coded 'B' showed complete loss at 250°C . The studies on the effect of gamma radiation on the water repellency of filter media coded A, B and C, preexposed to different temperatures have shown that: (a) The filter media A exposed to a temperature of 150°C and radiation level of 2.5×10^8 rads does not show any decrease in water repellency. However at temperature 200°C to 350°C the water repellency values steeply decrease due to degradation of additives, (b) The filter medium B shows steady degradation of water repellency due to irradiation with steep decrease of water repellency for a cummulative dose level of 5.6×10^7 rads. The same media exposed to high temperatures and gamma irradiation has much pronounced effect on water repellency and (c) the medium C is stable upto a cumulative dose of 1.4×10^7 rads. However, the media starts degrading at higher temperatures and radiations.

- ii) Wet bursting strength of all the media showed steady decrease with increase in temperatures. The studies on the wet bursting strength of the medium A under combined effect of temperature and radiation shows steady decrease from 88.0 cms to 15cms of water head. For medium coded 'B', for samples exposed to a level of 5.6×10^7 rads and above there is a complete loss in the wet bursting strength at room temperature. In medium C the wet bursting strength decreases from 36 cms to 10 cms of water head, when exposed to a temperature of 350°C and irradiations to a cumulative gamma dose of 2.5×10^8 rads.
- iii) Dry bursting strength of all the media decrease with increasing temperature. Further when the preheated media were exposed to gamma radiations, show enhanced deteriorations.

The deterioration in physical properties as above is attributed to the loss of organic additives at different temperatures which is also reflected in the loss of weight of media at elevated temperatures. Also all the organic additives are known to degrade when exposed to high gamma radiations.

The studies on the effect of steam air mixture on the filter media have shown that for extended operation of HEPA filters for steam air mixture with possible condensation, the main contributing factor is water repellancy of the filter media.

It was also found that there is no significant change in the filtration characteristics of filter media i.e. the resistance to air flow and collection efficiency against submicron particles due to exposure to temperatures upto 350°C and radiations upto 2.5×10^8 rads and due to combined effect of the two parameters.

The above studies on the evaluation of different filter media has shown that filter medium A of imported origin, presently used in the assembly of HEPA filters in India,

has better performance characteristics compared to filter media B and C.

5.2 Impregnated activated charcoal

The evaluation of 2% KI + 1% KOH impregnated activated charcoal for methyl iodide under high temperature and humidity has shown:

- i) the removal efficiency of the charcoal increases with increasing temperature of the air stream at low relative humidities. This is due to increase in the velocity of nearly all the reaction steps (12).
- ii) at constant temperature the removal efficiency of charcoal decreases with relative humidity, which is due to reduced diffusion velocity in the macropores.
- iii) the combined effect of high temperature and high humidity has shown that there is a net decrease in the overall performance indicating that with the increased humidity the rate of fall of efficiency is much higher than that of the temperature, with no condensation on the adsorbent bed. The reduced performance of activated charcoal is due to loading of the charcoal surface with water and the reduced diffusion velocity in the macropores.
- iv) Performance evaluation of impregnated activated charcoal due to bulk condensation has shown that $\text{CH}_3\text{I}^{131}$ removal efficiency steadily decreases from 99.85 to 91.24% with increase in moisture uptake by activated charcoal upto 34% (wt/wt). Above 34% the surface wetting starts blocking almost all the pores available resulting in erratic performance ranging between 80 to 86%. Investigation on the wash out of impregnants has shown that maximum amount of the impregnant gets washed out in the first four bed volume washings upto 70%. Such loss of impregnants may lead to steep decrease in the performance.

- v) Effect of irradiation on impregnated activated charcoal in the cumulative gamma radiation dose ranges from 2.8×10^6 rads to 8.4×10^7 rads has shown that there is no significant change in surface area of all the samples thus indicating that there is no structural damage to the charcoal. Further the removal efficiency for $\text{CH}_3\text{I}^{131}$ is also found to be consistent.
- vi) The ignition temperature of the charcoal was found to be 350°C with the desorption rate less than 1% for both elemental and methyl iodide when subjected to 180°C for five hours.

5.3 HEPA Filter

Evaluation of prototype HEPA filters assembled with materials of construction similar to the one being presently used and exposed to high temperature, humidity and radiation has shown that:

- i) No change in resistance to air flow and collection efficiency was observed when exposed to a temperature of 200°C under static conditions. However around 225°C the collection efficiency decreases sharply due to decomposition of poly vinyl acetate based adhesive.
- ii) Filters exposed to air stream upto a temperature of 120°C for 8 hours were found to maintain their filtration properties when evaluated after cooling.
- iii) Filters when tested, in-situ, under dynamic exposure to heated air at 80°C , 100°C and 120°C for different time interval upto 8 hours have shown that there was no change in the filtration properties.
- iv) Filters exposed at near saturation humidities for different time intervals have shown no deterioration in the filtration properties when evaluated after cooling.

- v) The filters after exposure to gamma radiations and also exposed to hot air stream at near saturation relative humidity have shown no change in resistance to air flow and collection efficiency.

5.4 Iodine adsorber

Evaluation of prototype iodine filters at 90°C and 90% RH indicated a drop in removal efficiency initially which remained constant over a period of 8 hrs. The initial loss in removal efficiency from 99.96% to 99.2% was due to increase in moisture content of charcoal, initially due to exposure to high humidity airstreams.

REFERENCES

1. Air filters for use at Nuclear facilities: IAEA Tech report series no. 122, IAEA, Vienna(1970)
2. Design of off gas and Air cleaning systems at Nuclear power plants : IAEA Tech reports series No. 274, IAEA, Vienna (1987)
3. Radioiodine Removal in Nuclear facilities : IAEA Tech report series No. 201 IAEA, Vienna (1980)
4. Burchsted C.A. et al: Nuclear air cleaning Handbook Rep ERDA-76-21, ERDA, Washington DC (1976)
5. Testing and monitoring of off gas clean up system at Nuclear facilities : IAEA Tech report series No. 243, IAEA, Vienna (1984)
6. Ramarathinam K. et al : Evaluation of HEPA and Iodine filters under high temperatures, high humidity and radiation - First IAEA CRP meeting on "Removal and retention of iodine and other airborne radionuclides in nuclear facilities during abnormal and accidental conditions - Mol, Belgium (1984)

7. High efficiency Air filters : Indian patent No. 129682 - Controller of Patents, India (1974)
8. Ramarathinam K. et al : Comparison of High efficiency particulate filter testing methods : IAEA - TECDOC-355 IAEA, Vienna (1985)
9. Khan A.A. et al : "Studies on removal of methyl iodide by activated charcoal" - BARC - 796 (1975)
10. Khan A.A. et al. : "Development of combined particulate and iodine filters" -BARC - 817 (1975)
11. "Design, testing and maintenance criteris for atmospheric clean up system" Air filtration and adsorption system units of light water cooled nuclear power plant" - USNRC 1-52 June (1953)
12. Ramarathinam K. et al: Evaluation of HEPA and Iodine filters under high temperature, humidity and radiation - 2nd Year -IAEA CRP progress report BARC (1986)

**EXPERIMENTAL, ANALYTICAL AND NUMERICAL STUDY
ON THE REMOVAL EFFICIENCY OF A CHARCOAL BED
FOR METHYL-IODIDE UNDER HUMID CONDITIONS**

(Summary)

Soon Heung CHANG
Korea Advanced Institute of Science
and Technology,
Seoul, Republic of Korea

Scientific Background and Scope of Project

=====

The removal efficiency of charcoal beds for removal of fission gases varies with the operation time, operating conditions and the number of adsorbable components.

This project consists of two major part for the study of the removal efficiency of charcoal bed. First, this research will express the removal efficiency of methyliodide by a TEDA-impregnated charcoal bed as a function of the time and operating conditions and analyze quantitatively the influence of relative humidity in the efficiency of a charcoal bed. The second part of this study is to develop a mathematical and numerical model for the dynamics of a charcoal bed systems with multi-component fission gases and analyze the time-dependent removal efficiency of charcoal beds in nuclear power plants.

Experiment and Numerical Method

Activated charcoal (10 to 12 mesh) was impregnated with 6% TEDA. The experimental conditions are as follows : bed depth. 3.5, and 7 cm : $\text{CH}_3^{127}\text{I}$ concentration. 7.8×10^{-8} to 1.52×10^{-7} mol/cm³ velocity 10 to 45 cm/s : relative humidity, o 50 70% : temperature of bed, 50°C.

Air from the air cylinder was dehumidified in the dryer and the humidity and concentration of $\text{CH}_3^{127}\text{I}$ were controlled by a humidifier and methyliodide saturator.

The air was introduced into the charcoal bed at 50°C. Inlet and outlet concentration of $\text{CH}_3^{127}\text{I}$ and humidity were measured by a gas chromatograph and hygrometer, respectively.

Obtained Results

Adsorption isotherm of $\text{CH}_3^{127}\text{I}$ by impregnated charcoal is the Langmuir favorable isotherm, and adsorption wave fronts show constant pattern behavior. Adsorption mechanism of methyliodide controlling the overall removal rate is the pore diffusion when air velocity is 20 cm/s and both pore diffusion and external mass transfer contribute to adsorption resistance in the case of air-velocity 10 cm/s as shown in Fig.1.

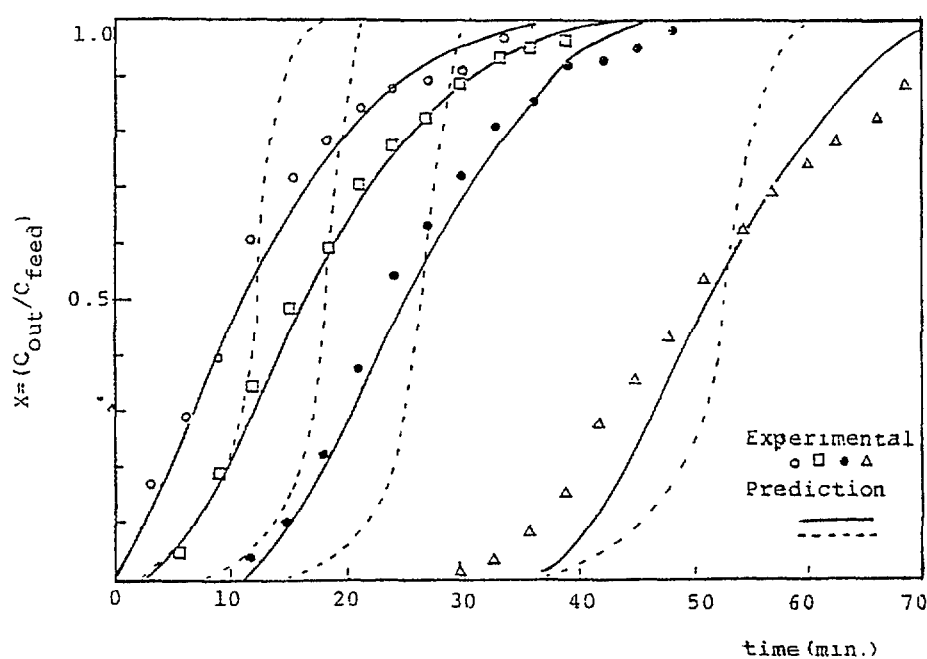


Fig.1 Variation of breakthrough curves for the adsorption of methyliodide due to the change of superficial velocity at 50°C (bed depth : 5cm, feed concentration ; 1.10×10^{-7} g mole/cm³, superficial velocity, Δ : 10 cm sec, \bullet ; 20 cm/sec, \square ; 30 cm/sec, \circ ; 45 cm/sec, - pore diffusion control case, ---- ; external mass transfer control case)

Effective pore diffusivity (D_{pore}) is 0.0060 cm²/s and it is nearly constant in the range of experimental condition.

In the humid condition, poor removal efficiency is explained through the reduction of the adsorption capacity of the charcoal and effective pore diffusivity of CH₃¹²⁷I.

When the relative humidity is 0, 30, 50, and 70%, the adsorption capacities of charcoal are 1.597x10⁻³, 7.073x10⁻⁴, 6.487x10⁻⁴ gmol/g, respectively, and D_{pore} are 0.0060, 0.0054, 0.0046, and 0.0034 cm²/s, respectively. These values are used to obtain the time-dependent CH₃I removal efficiency of the charcoal bed. The predicted breakthrough curves and experimental results agree well as shown in Fig.2.

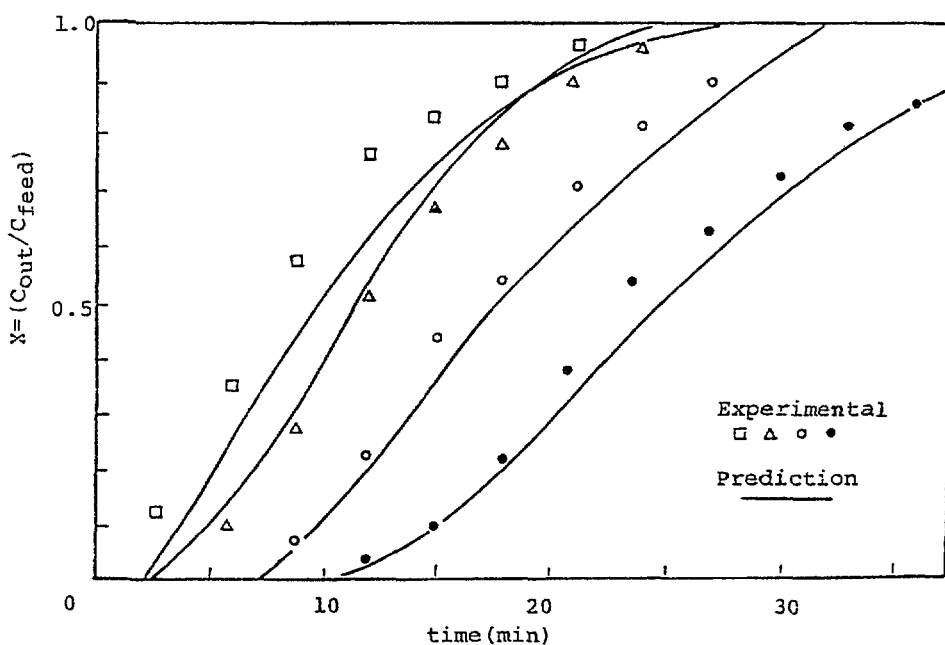
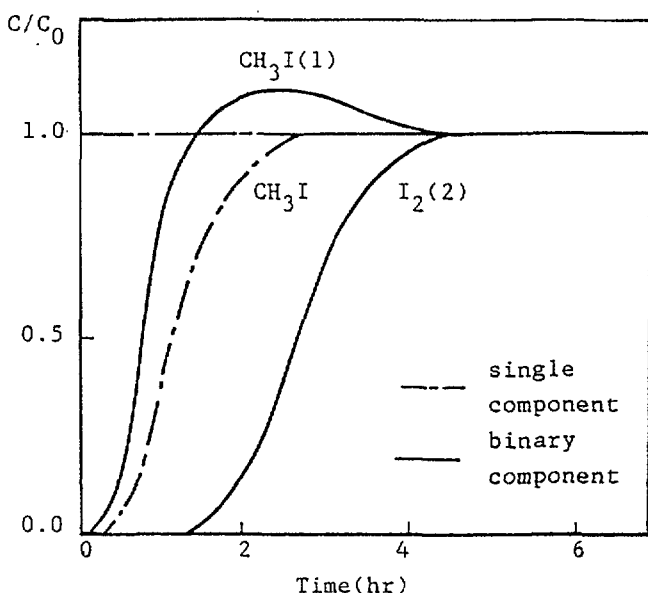


Fig.2 Effect of relative humidity on the breakthrough curves for the adsorption of methyl iodide at 50°C (bed depth : 5cm, superficial velocity ; 20cm/sec, feed concentration ; 1.10x10⁻⁷ gmole/cm³, relative humidity ● ; 0%, ○ ; 30%, △ ; 50%, □ ; 70%)

The breakthrough curves of multicomponent adsorption are entirely different from that of a single-component system. The peak in Fig. 3 arises from competitive adsorption between methyl-

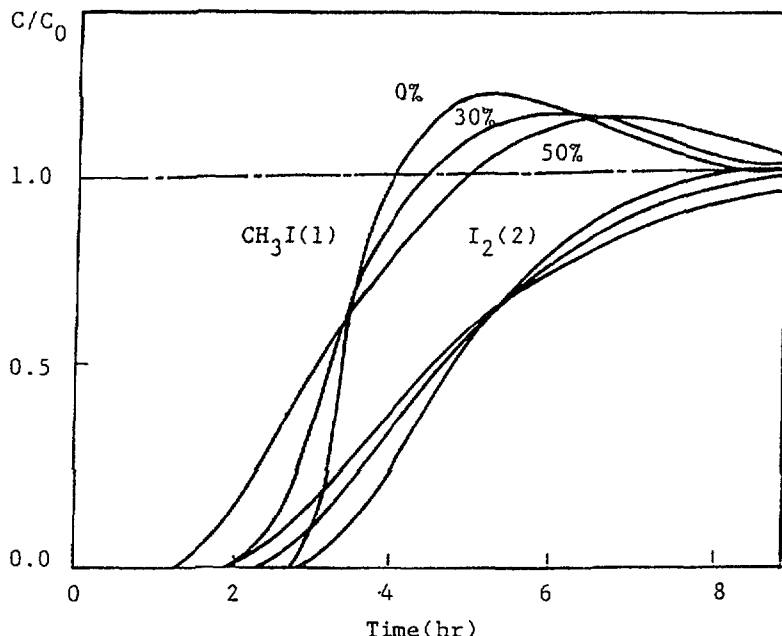


$$\begin{aligned}
 L &= 20.0 \text{ cm} & U &= 10.0 \text{ m/hr} \\
 \rho &= 542.0 \text{ g/cm}^3 & \epsilon &= 0.24 \\
 C_0(1) &= C_0(2) = 0.5 \times 10^{-9} \text{ gmole/cm}^3 \\
 K_{s1} &= 11.0 \text{ hr}^{-1} & K_{s2} &= 9.0 \text{ hr}^{-1} \\
 a_1 &= 0.1743 \text{ l/g} & a_2 &= 1.0 \text{ l/g} \\
 b_1 &= 0.1 \text{ l}/\mu\text{mole} & b_2 &= 0.5 \text{ l}/\mu\text{mole}
 \end{aligned}$$

Fig.3 Breakthrough curves for binary component adsorption of $\text{CH}_3\text{I}(1)$ and $\text{I}_2(2)$ systems

iodide and elemental iodine. In earlier stages of adsorption, both CH_3I and I_2 are adsorbed on activated carbon. Later, since the I_2 has the stronger affinity, it replaces the CH_3I . Therefore, the effluent concentration profile (breakthrough curve) shows a peak, indicating a higher concentration than the inlet concentration. Conclusively, it can be said that the breakthrough time in multicomponent adsorption is faster and the corresponding peak is higher than that of the single-component adsorption.

The humid conditions, the breakthrough time is decreased with increasing relative humidity. The effect of relative humidity on the breakthrough curves is shown in Fig.4. The decrease of breakthrough time is associated with the reduction of adsorption capacity and effective pore diffusivity.



$$\begin{aligned}
 L &= 15.0 \text{ cm} & U &= 10.0 \text{ m/hr} & \rho &= 542.0 \text{ g/cm}^3 \\
 \epsilon &= 0.24 & C_0(1) = C_0(2) &= 0.5 \times 10^{-9} \text{ gmole/cm}^3 \\
 K_{s1} &= 2.0 \text{ hr}^{-1} & K_{s2} &= 1.0 \text{ hr}^{-1} (\text{at } 0\% \text{ humidity}) \\
 a_1 &= 1.743 \text{ } \mu\text{g} & a_2 &= 3.0 \text{ } \mu\text{g} \\
 b_1 &= 1.0 \text{ } \mu\text{mole} & b_2 &= 1.5 \text{ } \mu\text{mole}
 \end{aligned}$$

Figure 4. Effects of relative humidity on breakthrough curves

Conclusion

The adsorption model to describe the performance of impregnated charcoal bed is proposed. The analysis of experimental data indicates that pore diffusion is the controlling step when gas velocity is over 20cm/sec, and both pore diffusion and external mass transfer resistance are contributed to the overall resistance when the gas velocity is 10cm/sec.

The reduction of removal efficiency under humid condition should be considered in view of the reduction of equilibrium adsorption capacity and the decrease of effective pore diffusivity.

The mathematical model for multicomponent adsorption to describe the performance of a charcoal beds and the corresponding numerical solution is proposed.

RELATED PAPERS PUBLISHED

1. Time-Dependent Removal Efficiency of a Charcoal Bed for Methyl iodide, ANS Transactions, 46, 523-525, 1984.
2. Experimental and Analytical Study on the Removal Efficiency of Methyl iodide by a Impregnated Charcoal Bed," Nuclear Technology, 68, 242, (1985).

THE AGEING AND POISONING OF CHARCOAL USED IN NUCLEAR POWER PLANT AIR CLEANING SYSTEMS*

(Abstract)

D. BROADBENT

Scientific Services Department,
Central Electricity Generating Board,
North Western Region,
Withenshawe, Manchester,
United Kingdom

This paper describes an investigation aimed at identifying the relative importance of oxidative ageing and hydrocarbon poisoning in the overall weathering of both potassium iodide (KI) and triethylene diamine (TEDA) impregnated charcoal used in filters on air cleaning systems.

Preliminary results on oxidative ageing show a marked dependence of the KI material on relative humidities above 40% and to a lesser extent on temperature. The TEDA material on the otherhand showed no such dependence at least up to 50 °C. Hydrocarbon poisoning is shown to affect both impregnant types to the same extent but the TEDA material due to its higher initial performance shows the greater resistance to poisoning. No one type of hydrocarbon species appeared to be significantly more deleterious than the rest and even with loadings up to 5% hydrocarbon some useful methyl iodide adsorption capability is retained. A laboratory investigation of the combined effect of oxidation and poisoning up to 2000 hours showed the superior performance of TEDA charcoal. However translating these results to operating plant and extrapolating to an operating time of one year it is clear that even TEDA charcoal filters would require the use of a guard bed designed to remove airborne organic species.

The work has shown that the observed deterioration of charcoal filters on air cleaning systems can be accounted for by the combined effect of oxidative ageing and hydrocarbon poisoning in the case of both KI and TEDA impregnated charcoals.

* An account of the work can be found in Gaseous Effluent Treatment in Nuclear Installations (Proc. Eur. Conf. Luxembourg, 1985), EUR 10580 (Commission of the European Communities), Graham & Trotman, London (1986).

THE EFFECTS OF TEMPERATURE AND HUMIDITY ON THE AGEING OF TEDA IMPREGNATED CHARCOALS

B.H.M. BILLINGE

Central Electricity Research Laboratories,
Central Electricity Generating Board,
Leatherhead, Surrey

D. BROADBENT

Scientific Services Department,
Central Electricity Generating Board,
North Western Region,
Withenshawe, Manchester

United Kingdom

Abstract

Samples of triethylene diamine (TEDA) impregnated 207B carbon have been aged for up to 1000 hours at temperatures in the range 40° to 70° and relative humidities of 50% and 90%. The rate of ageing (in terms of methyl iodide-131 trapping efficiency) increases progressively as the temperature is raised above 50°C and also as the relative humidity is increased; below 50°C however the ageing rate is relatively low, even at 90% RH.

A parallel examination by temperature programmed desorption of the growth of surface oxygen groups with ageing indicates that, unlike KI impregnated carbons, the groups formed on the TEDA carbons are not linked to the decline in performance. Also, the presence of an amine, which, as a group, are generally regarded as anti-oxidants, does not reduce the rate of surface oxidation.

Since the rate of ageing of TEDA carbons has been shown to follow the increase in the partial pressure of water above the sample it is proposed that TEDA carbon ageing could be caused by loss of TEDA either by a process akin to steam distillation, or by reaction with or catalysis by water, to form a less efficient impregnant.

1. INTRODUCTION

It has been found that KI impregnated charcoals, which are very effective at trapping radio-iodine compounds in CO₂ cooled systems, rapidly lose efficiency when exposed to high humidity air (Broadbent, 1985).

Research showed that this deterioration was mainly caused by oxidative ageing of the carbon surface and that the more acidic groups formed, e.g. carboxylic acid groups, were particularly deleterious (Billinge, Docherty and Bevan, 1984). The rate of oxidative ageing also increases with increasing humidity of the air (Billinge and Evans, 1984), while additional deterioration is caused by adsorption of trace organics which poison active surface sites (Broadbent, 1985).

Similar carbons impregnated with the amine triethylene diamine (TEDA) show a much reduced rate of ageing under ambient conditions and are consequently becoming more widely used in this application (Broadbent, 1985). The ageing rate is still appreciable, however, but for reasons which are not, as yet, clear.

Amines are a class of compounds well-known for their anti-oxidant properties so TEDA carbon may age more slowly than KI material because the rate of formation of organo-oxygen surface groups is reduced; a second possibility is that the basic properties of the amine neutralize any surface acidity formed. A separate problem with TEDA is its comparatively high vapour pressure which may result in an increasing loss of impregnant as operating temperatures rise above ambient. The work reported here examines the effect of exposure of TEDA impregnated carbons at various times, temperatures and relative humidities on (1) the K value (or methyl iodide trapping efficiency factor), measured under standard conditions; (2) the level of surface oxygen groups, measured by temperature programmed desorption of the surface groups as CO₂ and CO into a flow of helium.

2. EXPERIMENTAL

2.1 Materials

Samples of Sutcliffe-Speakman Ltd. 207B coal based carbon (8-12 BS mesh) impregnated to a nominal 5% TEDA were taken from a single batch held at NWR SSD).

2.2 Ageing - Description of Apparatus and Method

A dynamic ageing rig (Fig. 1) has been constructed to study ageing at temperatures up to 100°C and relative humidities up to 100%.

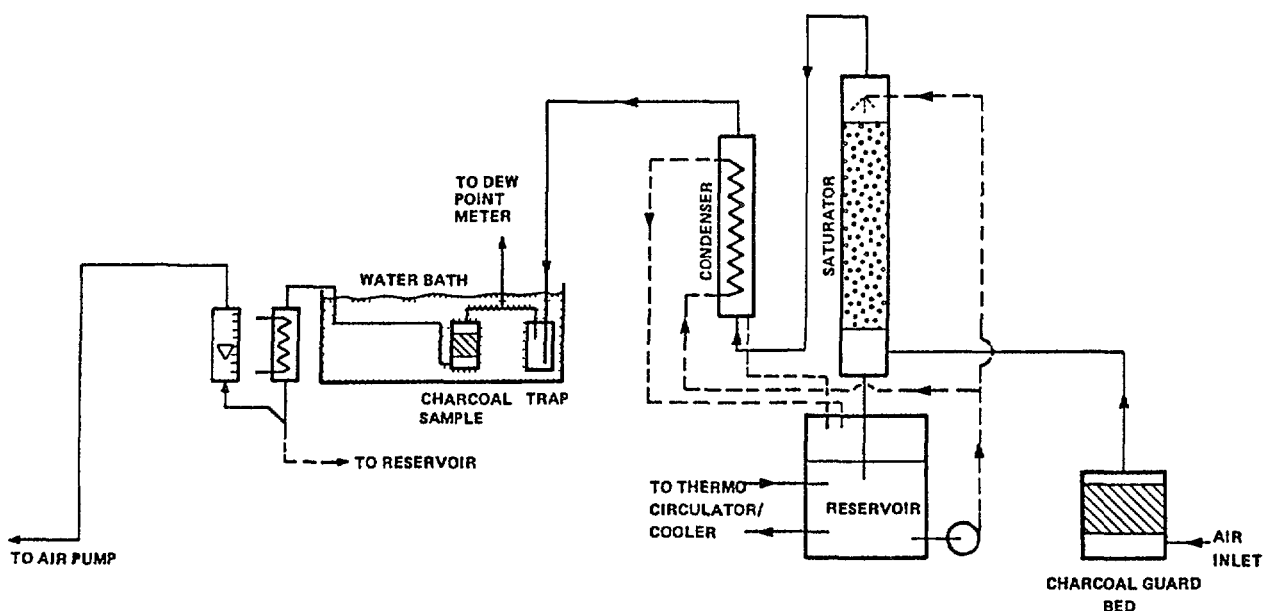


FIG. 1 DYNAMIC ACCELERATED AGEING RIG

Four charcoal samples of approximately 100 ml each can be accommodated in parallel in the rig. The relative humidity of the air flowing through the samples for a given bath temperature is controlled by the temperature of the water cascading down the saturator column against the upward air flow, mist and water droplets being effectively removed by a double coiled condenser. At dew points above ambient, condensation is avoided by using trace heating on the air flow line between the saturator column and the water bath. Relative humidity is measured by a heated cell dew point hydrometer (EG&G mirror condensation type). The airflow of about 5 litres per minute per sample is measured on a GAP meter after removal of excess

moisture in a cold water condenser. This flow is induced by an extraction pump drawing from a manifold connected to the outlets of each flow meter. The inlet air is cleaned by passing through an activated charcoal bed.

Ageing runs were carried out for periods of up to 1000 hours for each set of conditions of temperature and RH. These conditions were set up at the start of each run when about 100 ml of "as received" charcoal is loaded into specially designed sample vessels (Fig. 2) and then attached to the rig via flexible tubing. Samples were removed from the rig at predetermined intervals up to the end of the run. Test conditions were then changed and a further run started. Once removed from the rig the charcoal samples were quickly transferred to air tight polythene bottles (125 ml) and stored for K factor determination, which was carried out within a few days to minimise the chance of any further ageing.

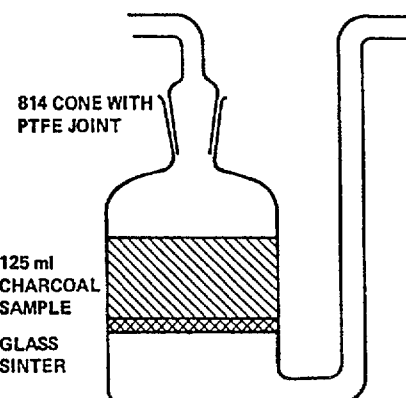


FIG. 2 CHARCOAL SAMPLE VESSEL—AGEING RIG

2.3 Rig for the Measurement of the Index of Performance (K factor) of Charcoal

The Index of Performance of charcoal is a measure of the efficiency of a charcoal bed for the adsorption of methyl iodide vapour contained in a flowing stream of air under standard conditions of sample size, air flow, temperature and relative humidity. These standard conditions have been established by the UKAEA at Sellafield and have been used in a rig developed by them.

The relative humidity is controlled in the range 97%-99%. The methyl iodide (traced with I-131) is loaded onto the sample by deposition from the vapour phase, over a 10 minute period, to yield a loading of 50 micrograms per gram of charcoal. Following the injection of the methyl iodide, the airflow is continued for a further two hour period. Any methyl iodide penetrating the test bed is collected on two traps containing small grain size charcoal. The overall decontamination factor for the sample is determined by counting the I131 activity on the sample and in the traps. The K factor or index of performance is then calculated from the expression

$$K = \frac{\log_{10} DF}{t}$$

when DF is the decontamination factor, which is the ratio of the initial methyl iodide charge to that released from the bed and t is the gas residence time in the carbon bed (in seconds).

The rig constructed for the present study (see Figure 3) was originally designed for a dual purpose and differs in a number of ways from the standard rig developed by the AEA. It was intended to be used as a standard K factor rig and also as a rig on which the dependence of K factor on relative humidity, temperature and gas residence time could be determined.

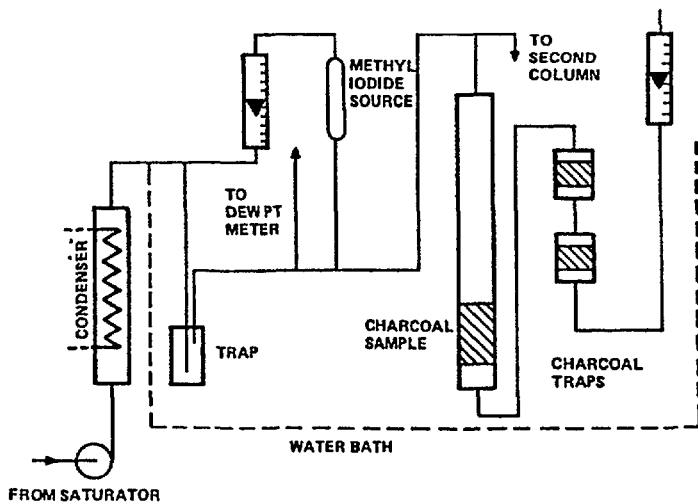


FIG. 3 CHARCOAL K FACTOR RIG

A saturator system similar to that used for the ageing rig provides air to the sample at a relative humidity in the range 97%-99%. The sample temperature is controlled at 20°C by the use of a water bath. Normally duplicate samples are measured together. Although there are slight deviations from standard conditions, the K factors determined for three reference charcoals agreed very well with the determinations from other laboratories taking part in an inter-laboratory comparison exercise and using the AEA rig design (see Taylor and Billinge (1985)).

2.4 Measurement of Surface Oxygen by Temperature Programmed Desorption

Samples were dried for 2 hours at 373 K and were then crushed and sieved to the range 211-600 µm. About 0.5 g was packed into a silica U tube and retained in place with a silica wool plug. The tube was placed in an electric furnace and the temperature held at 423 K overnight in a controlled flow of purified helium to remove as much of the TEDA impregnant as possible and thus reduce interference with the gas chromatography of CO and CO₂.

The sample temperature was then raised at a linearly programmed rate of 5 K min⁻¹. The helium carrier gas, together with any desorbed gases, passed through the sample loop of a gas chromatograph fitted with a katharometer detector. The sample valve was actuated automatically every 213 seconds and the levels of desorbed carbon dioxide and monoxide were determined using a 2 m "Porapak Q" column held at 313 K. The evolution of these two gases, as vpm, was plotted against temperature to give a characteristic desorption pattern. The total oxygen desorbed in carbon dioxide, designated [O(CO₂)] and in carbon monoxide [O(CO)] was evaluated by integration.

3. RESULTS

3.1 Effect of Ageing on K Values

Samples of TEDA carbon were exposed at two levels of humidity, 50% RH and 90% RH, and three temperatures, 40°C, 60°C, 70°C for periods up to 1000 hours. A plot of K value against exposure time (Fig. 4) shows that, at 50% RH, ageing increases with temperature, e.g. 1000 hr K value at 60°C is $>11\text{ s}^{-1}$, at 70° is $\sim 9\text{ s}^{-1}$. However, the effect of humidity is more significant; at 90% RH, the 1000 hr K value at 60°C is $\sim 6.0\text{ s}^{-1}$, the 70°C figure is $\sim 4.5\text{ s}^{-1}$. In contrast, the 40°C/90% RH material remained at $K \sim 11.0\text{ s}^{-1}$ from 200 to 1000 hours, which is consistent with previous results (Broadbent, 1985) where humidity was found to have only a small effect on K up to 50°C.

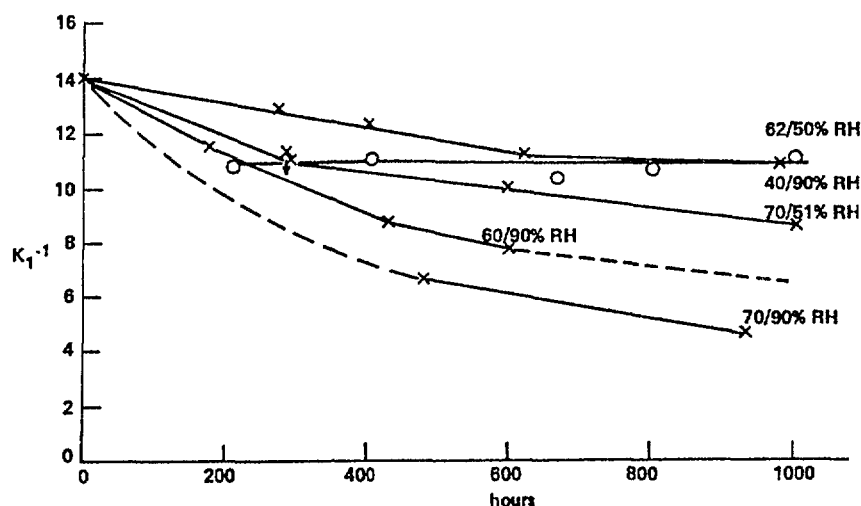


FIG. 4 DECLINE IN K WITH EXPOSURE TIME

In summary, at 40°C even relative humidities as high as 90% have little effect on the ageing of TEDA carbons. At temperatures above 50°C humidity has a considerable and progressive effect i.e. at any given temperature 90% RH ages much faster than 50%.

3.2 Effect of Ageing on Surface Oxide Growth from Temperature

Programmed Desorption

A typical desorption pattern from a fresh TEDA/207B carbon is shown in Fig. 5a with that from an aged sample (Fig. 5b). Patterns from an unimpregnated carbon and a KI-carbon are included for comparison (Fig. 5c and 5d). The characteristics of the TEDA curves are close to those of the unimpregnated charcoal, differing mainly in the low temperature evolution (<773 K) of CO in the TEDA case. In contrast KI impregnation (Fig. 5d) causes a change in shape of the second CO_2 peak and the creation of a new CO peak at ~ 1023 K. These points indicate less interaction between TEDA and the support carbon than is the case with KI.

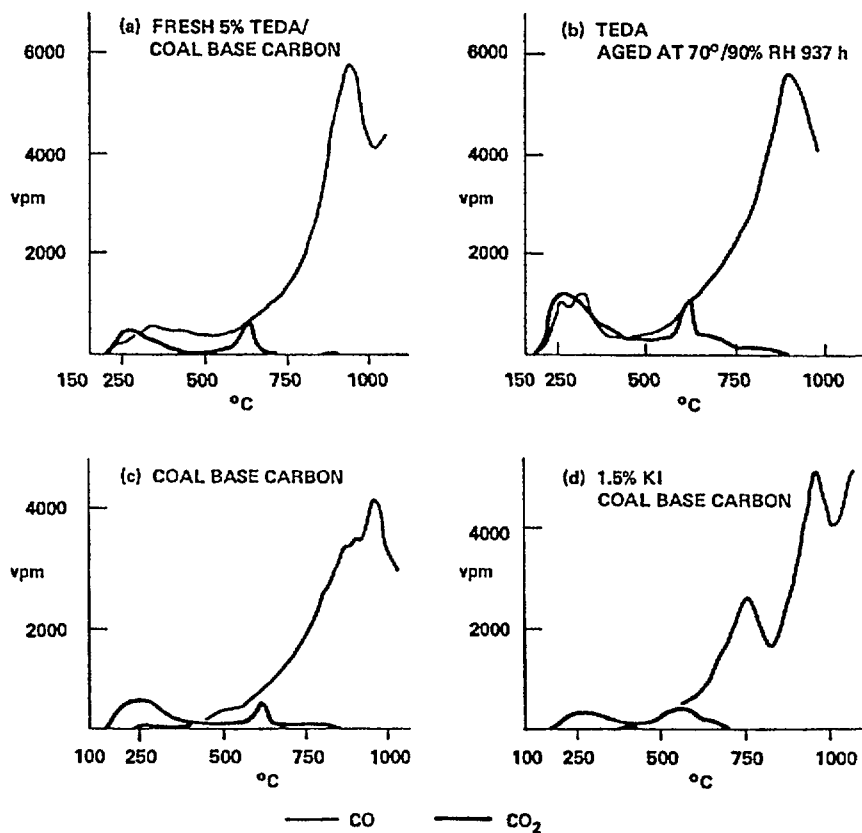


FIG. 5 TEMPERATURE PROGRAMMED DESCRIPTION PATTERNS

The desorption pattern from the aged sample (Fig. 5b) shows how the peaks grow with ageing. The quantities of oxygen evolved from the surfaces of fresh and aged TEDA carbons are presented in Table 1, columns

Table 1: TPD Results: Total and Decremental Surface Oxygen Desorption Values

1 Sample	2 Time hrs	3 *OCO ₂ (1)	4 *OCO ₂ (2)	5 *OCO(1)	6 *OCO(2)	7 K	8 ΔOCO ₂ (1)	9 ΔOCO ₂ (2)	10 ΔOCO(1)	11 ΔOCO(2)
Fresh A60C/50%RH	0	0.12	0.09	0.07	0.96	14.05				
	272	0.18	0.10	0.15	1.00	12.89	0.06	0.01	0.08	0.04
	400	0.18	0.11	0.14	1.09	12.33	0.06	0.02	0.07	0.13
	619	0.21	0.14	0.14	1.12	11.11	0.09	0.05	0.07	0.16
	985	0.22	0.12	0.18		10.84	0.10	0.03	0.11	-
A70C/50%RH	290	0.22	0.12	0.18	0.97	11.00	0.10	0.03	0.11	0.01
	597	0.23	0.16	0.18	1.07	10.00	0.11	0.07	0.11	0.11
	1004	0.28	0.19	0.22	1.16	8.63	0.16	0.10	0.15	0.20
A60C/90%RH	175	0.26	0.12	0.13	1.01	11.59	0.14	0.03	0.06	0.05
	285	0.32	0.20	0.14	1.11	11.32	0.20	0.11	0.07	0.15
	430	0.43	0.32	0.15	1.16	8.74	0.31	0.23	0.08	0.20
	600	0.45	0.33	0.16	1.10	7.76	0.33	0.24	0.09	0.14
A70C/90%RH	480	0.45	0.32	0.24	1.35	6.70	0.33	0.23	0.17	0.39
	937	0.55	0.46	0.25	1.23	4.56	0.43	0.37	0.18	0.27
A40C/90%RH	213	0.28	0.17	0.13	1.01	10.87	0.16	0.08	0.06	0.05
	405	0.34	0.24	0.14	1.15	11.00	0.22	0.15	0.07	0.19
	667	0.38	0.26	0.15	1.24	10.32	0.26	0.17	0.08	0.28
	800	0.39	0.28	0.16	1.24	10.73	0.27	0.19	0.09	0.28
	1000	0.27	0.25	0.12	1.22	11.05	0.15	0.16	0.05	0.26

* OCO₂(1) and (2) - % oxygen evolved in CO₂ from dry, ash-free carbon

+ OCO(1) and (2) - % oxygen evolved in CO from dry, ash-free carbon

three to six, for the first CO_2 peak, ($\text{OCO}_2(1)$) up to 728 K; the second CO_2 peak from 728 K to completion ($\text{OCO}_2(2)$); the first CO peak also to 728 K ($\text{OCO}(1)$); the second CO peak from 728 K to peak maximum ($\text{OCO}(2)$).

In columns 8 to 11 the increases in size of each peak over that of the fresh material are given (Δ).

The Δ values for the two CO_2 peaks are shown in Fig. 6. Considering the 60°C and 70°C results only, the graphs fall into two groups with the 90% RH runs showing a far greater increase in surface oxygen than the 50% RH runs, which show little change over the 1000 hours ageing period. This is a parallel trend to the effect of ageing on K value (3.1. above) where the higher humidity causes a faster decline in K. The 40°C/90% RH results show an intermediate pattern. The K value shows little change over the ageing period of these runs but the increase in surface O(CO_2) lies between that for the higher temperatures at 50% RH and 90% RH.

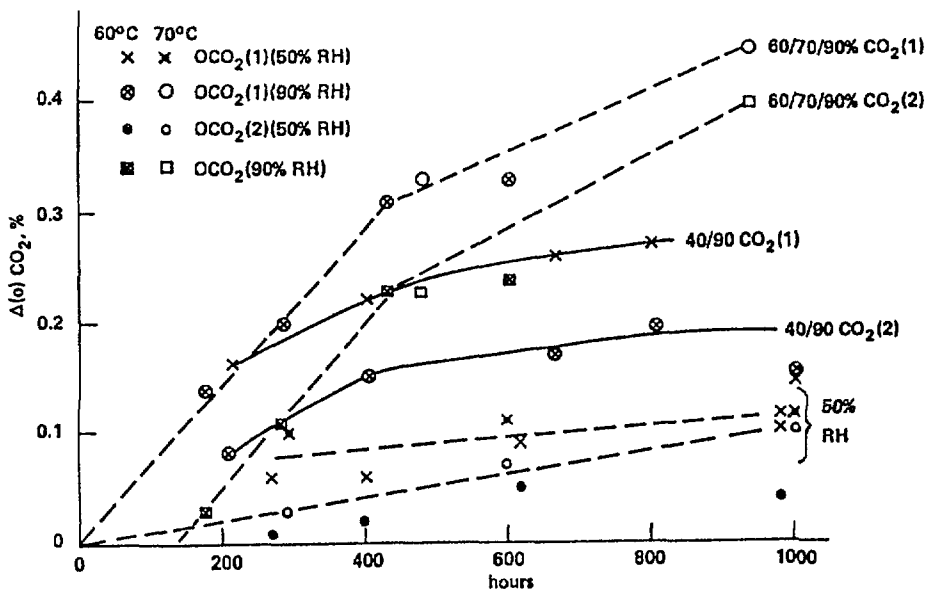


FIG. 6 INCREASE IN CO_2 EVOLVED vs. AGEING TIME

The ΔO values for the CO peaks are shown in Fig. 7 and 8. The first CO peak points (Fig. 7) while exhibiting some scatter, do not vary very greatly for all the humidities and temperatures examined. Variation of RH and temperature has no appreciable effect on the growth of the first

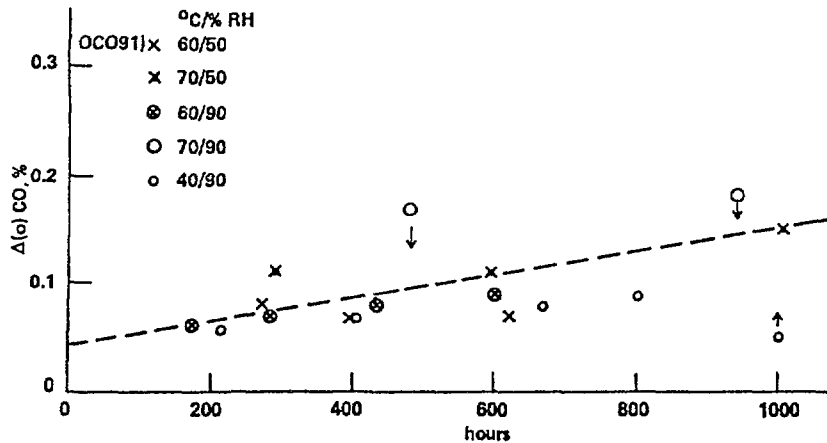


FIG. 7 INCREASE IN CO EVOLVED vs. AGEING TIME FOR 1st CO PEAK

CO peak, although it does increase slowly with ageing. The second CO peak (Fig. 8) shows a qualitatively similar pattern of behaviour to CO_2 ; the 90% RH results show a greater increase than the 50% RH results. The 40°C/90% RH results fall in with the general trend, the first CO peak following the same curve as the 60°C/70°C, 50% RH results, the second CO peak falling close to the 60°C/70°C 90% RH results. In summary, the growth of all peaks except the first CO peak is very sensitive to RH.

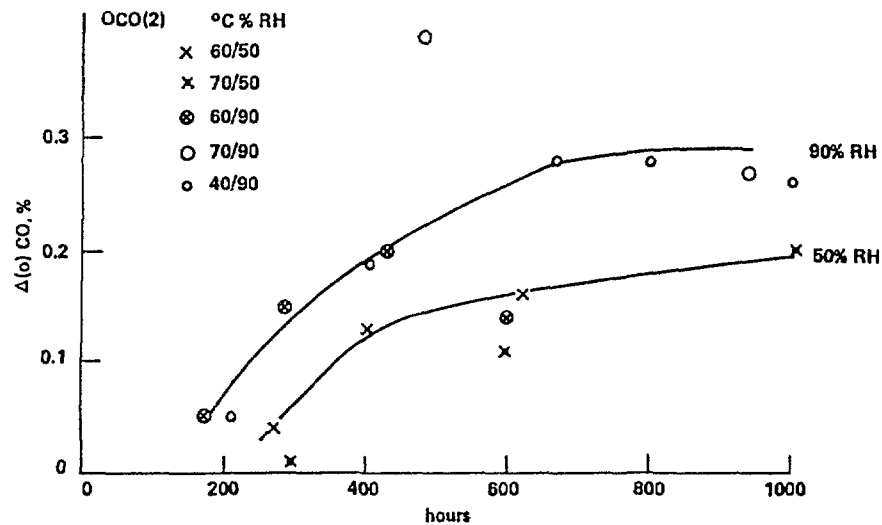
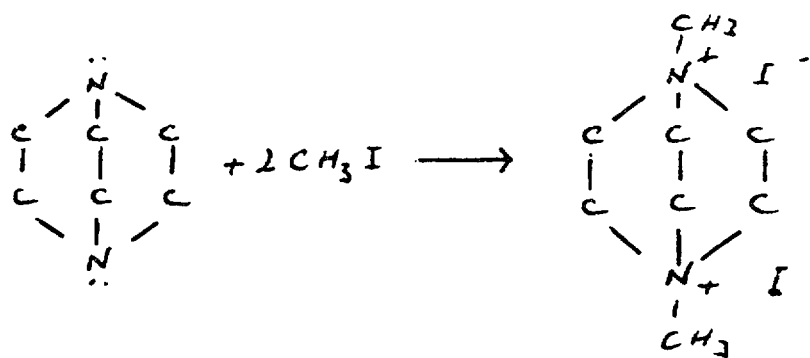


FIG. 8 INCREASE IN CO EVOLVED vs. AGEING TIME FOR 2nd CO PEAK

4. DISCUSSION

For KI impregnated carbons previous work (Billinge et al., 1984, Billinge and Evans, 1984) clearly demonstrated at temperatures below 50°C links between (1) the rate of oxidative ageing of the carbon surface and relative humidity and (2) the increase in acidic surface groups and the deterioration in methyl iodide retention efficiency (K values). In contrast, other work (Broadbent, 1985) found that below 50°C/90% RH, similar carbons impregnated with triethylene diamine (TEDA) showed only a small decline in performance with time compared with KI carbons and no relationship between this decline and temperature or humidity.

Explanations can be offered in terms of the difference in chemistry of the two systems: in the KI/carbon system, adsorption of CH₃I initially requires scission of the C-I¹³¹ bond followed by isotopic exchange with I¹²⁷ from the KI impregnant. The coal carbon surface catalyses the C-I scission step and acidification of the surface by oxidation to carboxyl or lactone groups inhibits this step, causing a fall in the rate of reaction; on the other hand TEDA is a cage-structure tertiary diamine, the stereochemistry of which makes the lone pair electrons on each nitrogen atom very accessible. CH₃I-131 is trapped by the formation of quaternary groups.



The chemistry is not totally divorced from that of the underlying carbon surface, however, as demonstrated by UKAEA workers (Evans and Hillary) who showed that TEDA on low ash coconut shell carbon has a K value of only 6.7, compared with 12.7 for the same quantity of impregnant on a coal-based carbon. Whether this difference can be equated with variations in mineral

content or surface oxidation state remains to be seen but the latter is a less likely explanation since (1) amines in general have anti-oxidant properties which may inhibit carbon surface oxidation and (2) the basicity of the amine impregnant may neutralize any acidic groups formed and so reduce their effect.

4.1 Growth in Surface Oxides and the Decline in K Factor

Examination of the desorption patterns (Fig. 5) of TEDA and KI carbons shows that the major similarity is in the first CO₂ peak, which reaches a maximum ~523 K in both cases. It has previously been found that, for KI carbons this peak is due to acidic oxy-groups which are a major cause of ageing. It is therefore informative to consider this peak in relation to TEDA ageing.

Results obtained previously up to 50°C/90% RH (Broadbent, 1985) and those reported here at 40°C/90% RH show only a small fall in K value up to 1000 hours ageing but the TPD results at 40°C/90% (Table 1, Fig. 6) show there has been a considerable increase in the quantity of CO₂-forming groups in that time ($\Delta OCO_2(1)$ maximum value is 0.27%). There are no comparable figures for KI carbon under these conditions but it appears that the presence of amine is not significantly suppressing the formation of surface carboxyl groups and, conversely, on TEDA carbon these groups are not greatly affecting the K value.

The results at 60°C/50% RH and 70°C/50% RH show a greater decline in K value than do the 40°C/90% RH results (Fig. 4 and Table 1) but the maximum increase in first peak O(CO₂), 0.16%, (70°C/50% RH, 1004 h) is a factor of 1.7 less than that for the maximum 40°C/90% RH sample (800 h 0.27%), i.e. the samples showing the greater increase in surface oxygen show the lesser decline in K factor. This indicates no linkage between K value and acidic surface oxygen groups in TEDA carbons.

The results at 60°C/90% RH and 70°C/90% RH show the largest decline in K and the greatest increase in the first CO₂ peak (Fig. 6). One comparable result on KI carbon is available at 60°C/85% RH. After 400 h the first CO₂ peak oxygen increased by 0.31% which agrees well with the TEDA figure at 60°C/90% RH/430 h of 0.31%. This is confirmation that the presence of TEDA is not interfering appreciably with the rate of growth of oxy-acidic groups on the surface and, coupled with the 40°C/90% results, confirms that combined surface oxygen is not the primary cause of ageing in TEDA carbons.

At a given temperature, the rate of growth of surface oxygen groups increases with increasing relative humidity on KI carbons (Billinge and Evans, 1986). Assuming TEDA carbons behave similarly, the expected order of increasing surface oxygen would be 60°C/50% RH < 70°C/50% RH < 60°C/90% RH < 70°C/90% RH for the samples examined here, with the position of the 40°C/90% RH samples depending on the relative effects of temperature and humidity. By comparison of the 60°C/50% RH with 60°C/90% RH or 70°C/50% RH with 70°C/90% RH it is clear that this increase in relative humidity has a much greater effect than the 10° temperature change. Therefore the position of the 40°C/90% RH surface oxygen levels between 70/50 and 60/90% is not anomalous. This is consistent with the formation rate of surface oxygen-groups being dependent on the quantity of water absorbed on the surface which itself is governed by relative humidity. As it has already been argued that no relationship exists between the rate of TEDA carbon ageing and surface oxygen level, the cause of ageing is still an open question. The most probable answer is a loss of the impregnant itself or its conversion to a less active entity.

Further examination of Fig. 4 shows that the rate of decline in the K value with ageing time follows the sequence 40/90% < 60/50% < 70/50% < 60/90% < 70/90%. It can be seen, from Table 2, that this order is coincident with one of increasing water vapour partial pressure. The

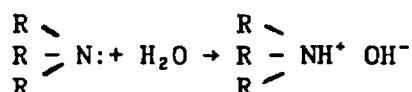
vapour pressure of TEDA impregnated on activated carbon is not known but values for the pure compound at 298 and 323 K have been reported by Deitz (1981) as 0.6 and 2.9 torr respectively. Using the simplified Clausius-Clapeyron equation and plotting log p against 1/TK enables values of 1.6, 5.3 and 8.5 torr to be deduced at 313, 333 and 343 K. Thus the combined TEDA and water vapour pressures also maintain the same order of increase (Table 2).

TABLE 2: Absolute Partial Pressure of Water
at Various Temperature/Relative Humidity Conditions
and Vapour Pressure of TEDA

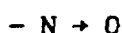
Expt.	Condition	P _{H₂O} mm Hg	P _{TEDA} mm Hg
T°C	RH%		T°C
40	90	49.8	25 0.6
60	50	74.7	40* 1.6
70	50	116.9	50 2.9
60	90	134.4	60* 5.3
70	90	210.3	70* 8.5

* Deduced from the Clausius-Clapeyron equation

It is therefore possible that a mechanism of TEDA removal, similar to that of steam distillation, is in operation with the rate of TEDA removal dependent on the combined partial pressure of TEDA and water vapour above the carbon surface. An alternative possibility is that a direct reaction between TEDA and water occurs to form another component, or that water catalyses the oxidation of TEDA by air, as it does the carbon surface. Such reactions could result in the formation of a quaternary hydroxide:



or an amine oxide, i.e.



either of which may be less effective than TEDA itself for trapping methyl iodide.

Further work is required to substantiate which of these mechanisms is important but it is clear that a mechanism dependent on water vapour pressure only should cause a similar decline in performance of TEDA carbon in wet inert gas as in wet air. Minimal decline in K value in humidified inert gas would indicate that chemical reactions of the TEDA molecule itself were the more important. Total nitrogen analysis on aged samples would show whether TEDA conversion to another N-compound was important. These investigations will be the subject of a later report.

4.2 The First CO Peak

The major difference in the TPD pattern of TEDA carbon compared with those of KI or unimpregnated carbon is the appearance of a CO peak over the same temperature range as the first CO_2 peak (Fig. 5). This near coincidence might suggest that the two emanate from the same source and some interaction between TEDA and the carbon surface offers a possible explanation. However, the behaviour of the two peaks under ageing conditions is very different. The first CO peak (Fig. 7) shows only slow growth over 1000 hours which is insensitive to changes in humidity and temperature; the first CO_2 peak also shows low growth at low (50%) humidity (Fig. 6) but raising the humidity causes a large increase as also happens with KI carbons, so the temperature coincidence of the two peaks seems fortuitous. Even so the fact that this CO peak is present only on TEDA carbons does indicate that it is linked to the TEDA impregnant in some way and may be due to the slow degradation of that compound with time.

5. CONCLUSIONS

- (1) The decline in methyl iodide trapping efficiency (K) of TEDA impregnated carbons in moist air is low below 50°C and relatively unaffected by humidity.

- (2) At 50°C and above K declines with temperature but is more susceptible to increasing relative humidity from 50 to 90%.
- (3) The rate of growth of surface oxygen groups with ageing increases with relative humidity throughout the temperature range so that the level of surface oxygen at 40/90% RH exceeds that formed at 70/50% in spite of which the K values at 40/90% exceed those at 70/50%.
- (4) Thus there is no relationship between the ageing rate of TEDA carbon and surface oxygen group growth. Furthermore, there is no indication that the presence of this base inhibits the formation of acid surface oxygen groups.

(5) The K value declines in the sequence of increasing partial pressure of water which indicates one of two possible ageing mechanisms.

- (a) Removal of TEDA by a physical 'steam distillation' mechanism related to the combined water + TEDA vapour pressure over the surface.
- (b) Chemical reaction either by hydroxylation of TEDA or oxidation of TEDA catalysed by water to form a less efficient product.

REFERENCES

- Billinge, B.H.M., Docherty, J.B. and Bevan, M.J., 1984, 'Carbon', 22(1), 83-89
- Billinge, B.H.M. and Evans, M.G., 1982, J de Chimie Physique 81, (11/12), 779-784
- Broadbent, D., 1985, European Conference on Gaseous Effluent Treatment in Nuclear Installations, Luxembourg, Paper 43
- Deitz, V.R., 1981, US Nuclear Regulatory Commission Report NUREG/CR 2112
- Evans, M.G. and Hillary, J..J., 1986, UKAEA Report No. ND-R-1198(W)
- Taylor, M.R. and Billinge, B.H.M., 1985, European Conf. on Gaseous Effluent Treatment in Nuclear Installations, Luxembourg, Paper 58

REMOVAL OF ^{131}I FROM OFF-GAS STREAM AT KRŠKO NUCLEAR POWER PLANT

L. VUJISIĆ

Department of Chemistry,
Boris Kidrič Institute of Nuclear Sciences,
Belgrade, Yugoslavia

Abstract

The concentrations and forms of radioiodine species were determined throughout the air cleaning systems of Krško Nuclear Power Plant. The performances of the new fibrous carbon material (FCM) and a TEDA impregnated version were investigated showing good results in laboratory experiments under high temperature and relative humidity conditions.

INTRODUCTION

In nuclear power plants impregnated activated charcoal is used almost exclusively for removal of airborne radioiodine species from off-gas streams.

It is well known that the airborne radioiodine consists of molecular iodide, and organic iodine which can be divided in easy to trap species, such as methyl iodine and much penetrating iodine species. Problem in filtration is organic iodine species that in accidental high humidity conditions can cause troubles.

Our investigation on the off-gas systems of NPP Krško and laboratory were divided in two parts:

-the first to determine content of molecular and organic species,
-the second to investigate a new filter material for iodine trapping because of well known drawbacks of carbon (decreasing of efficiency on very high relative humidity, fire hazard, etc.)

RESULTS AND DISCUSSION

The first group of experiments were carried out on NPP Krško on two systems which are continuously in operation: the first system which covers chemical laboratories, workshops and decontamination area; the second system which covers the pool for waste storage.

Experimental canister was attached in the front of the filter train on air inlet. Flow rate through the adsorber beds was 0.2 s.

Experimental canister for iodine trapping was sectioned to allow selective adsorption of iodine species. Experimental adsorption beds preceded by a particulate filter in direction of flow were:

- two beds of DMS 11 for retention of molecular iodine,
- two beds of activated carbon impregnated with 5 w% of TEDA for retention easy-to-trap organic species such as CH_3I and more penetrating iodine species.

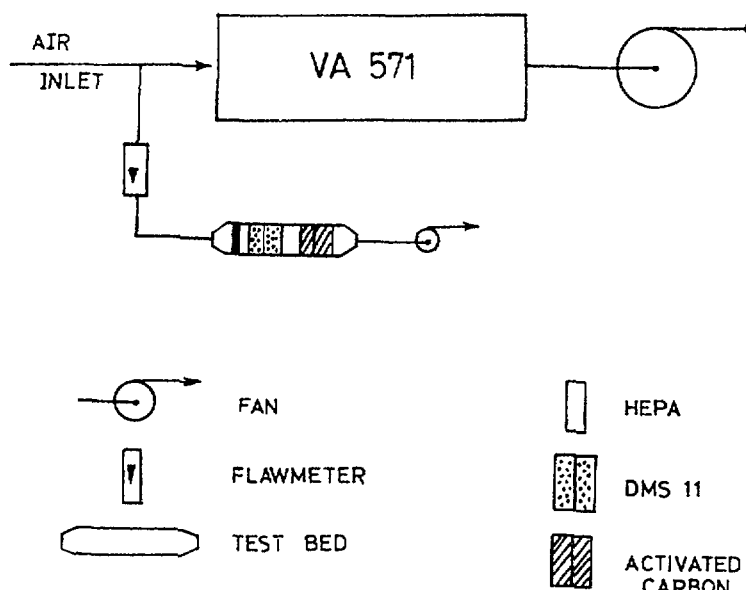


Figure 1. Schematic diagram of experimental facility.

Bed depth was 5 cm and dia 5cm. Temperature and relative humidity during experiments were working conditions of NPP filtration system, about 25°C . Duration of the experiments were 8 days (192 h).

Experiments were carried out from April 1985. to October 1986 year. During this period 14 experiments were done on the first system which covers laboratories, workshops and decontamination area and 5 on the second system which covers waste storage.

From 14 experiments obtained average content was 37.9% of molecular iodine and 62.1% of organic iodine species. Content of organic iodine species varied from 40 to 66%. The content of organic iodine species depends of work done in treated area. It increases when welding or painting were done, as it was expected.

Experiments on the system which covers pool for waste storage was done: 1) a month before the fuel was put in the pool, 2) on the day when the fuel was put in the pool, 3) one month after. In the first and the third experiments no iodine was detected, while in the second 70.1% of molecular iodine and 29.9% of organic iodine was detected (3.58 pCi/s, 11.96 pCi/s).

Because of the high contents of organic iodine species even in a normal operating conditions we decided to investigate a new filter material for iodine trapping. We have chosen the activated fibrous carbon material which is almost pure carbon.

The fibrous carbon material investigated in laboratory and on NPP Krško is new product with performances which follow high requirements of nuclear technology. The complete results of investigation are given in the paper: Lj.Vujisić, M.Todorović, Lj.Đuričić and M.Polovina, New Filter Material for Iodine Trapping, Gaseous Effluent Treatment in Nuclear Installations, p. 701, Graham and Trotman,1986, (see Appendix).From the experiments in laboratory and on NPP Krško it can be concluded:

1. Oxidation stability of the fibrous carbon material shows that the carbon textile is very stable in oxidative atmosphere. That makes possible to use this material in extreme conditions (accidental).
2. Under the same experimental conditions, relative humidity of air stream 95% and testing temperature 30°C , water loading on the fibrous carbon material is only 5% comparing to 20% for impregnated activated charcoals. So, it can be used with good results under very high relative humidity.
3. Dusting during the experiments due to the compact textile structure of fibrous material did not occur. If this performance is sustainable in a real filtration system back up HEPA filters could be avoided.
4. Apparent density of fibrous carbon (0.13 g cm^{-3}) is about four times less than the bulk density of granular activated charcoals. It means that the filter of the same bed depth is lower weight in a case of fibrous carbon.
5. In comparison with a granular activated carbon, advantages of the fibrous carbon material are: very easy handling, cutting in desired forms, easy placing in filters and transportation. Also, its volume can be reduced and that characteristics could be important for radioactive waste management.
6. Adsorption properties of the investigated fibrous carbon material are equal or better than the same properties of impregnated activated charcoals used on NPP Krško.

After these two groups of experiments : 1. on NPP Krško with impregnated carbon and 2. investigation of the impregnated fibrous carbon material, parallel experiments of iodine trapping were done on both materials.

The question was is 5 cm layer of a impregnated activated carbon or the impregnated fibrous carbon material enough for complete trapping of the airborne radioiodine species. Fact that the water loading on impregnated fibrous carbon material is four time less (5%) compared with a impregnated activated carbon can be neglected if for iodine trapping we need much deeper layer of the impregnated fibrous carbon material.

To solve this problem new group of experiments on ventilation system of NPP Krško were done. Standard system, which covers laboratories, workshops and decontamination area, have been chosen. In these rooms a lot of iodine is liberated due to the nature of work done (material from primary cycle) and the most of these iodine species are organic.

Experiments with impregnated activated carbon

Experimental colon was devided in eight beds 3 cm depth and 5 cm dia, that means 24 cm long. Stay time of exusted air was 0.2 s for each bed.

Adsorbents were activated carbon impregnated with: 1.5 w% of KI (used in NPP Krško) and in second case 5 w% of TEDA. Adsorption period was ten days (240 h) for each experiment. After disconnecciton of colons gama spectroscopic measurements of carbon samples (beds) were done.

Results of measurements for activated carbon impregnated with 1.5 w% of KI show that for complete iodine trapping 9 cm of carbon is used, Fig. 2. It can be assumed that on the first adsorption bed (3 cm) molecular iodine is adsorbed and on the second and the third adsorption beds organic species of iodine are adsorbed. This assumption is allowed by the inspection of the curve on the Fig. 2.

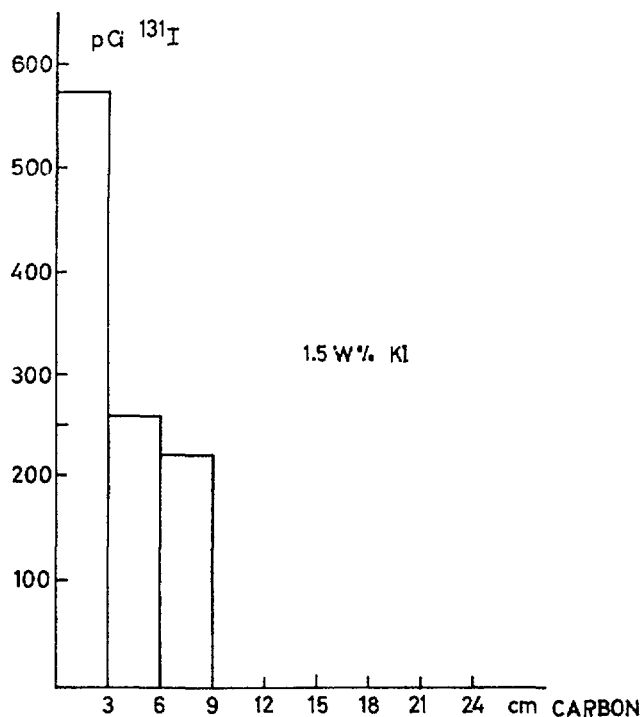


Figure 2. Adsorption of ^{131}I on KI impregnated activated carbon.

Same results were obtained by the experimental colon filled with 5 w% of TEDA impregnated activated carbon (Fig.3.). Experimental results presented on the Fig.3. show that complete iodine is adsorbed on the 9 cm of carbon.

On the same time on KI impregnated carbon ^{133}Xe was adsorbed from the first to the eighth layer (24 cm).

Fig. 4. It is well known that ^{133}Xe in adsorption processes competes with ^{131}I . In the case of accident, when large quantity of ^{133}Xe expels from the reactor, it might cause trouble.

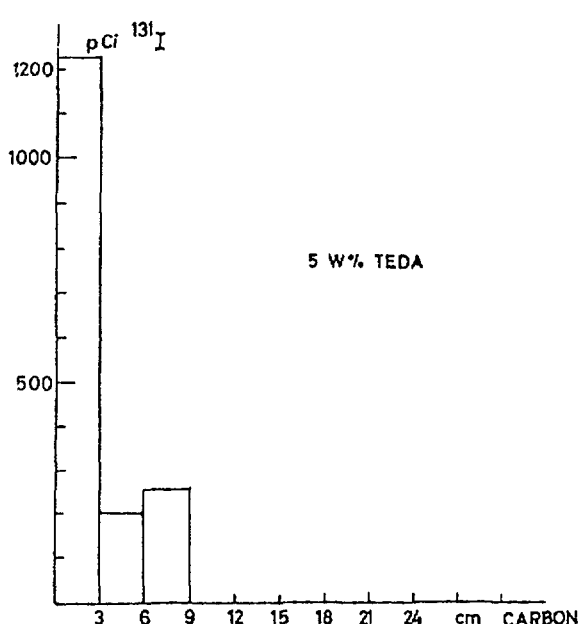


Figure 3.

Adsorption of ^{131}I on TEDA impregnated carbon.

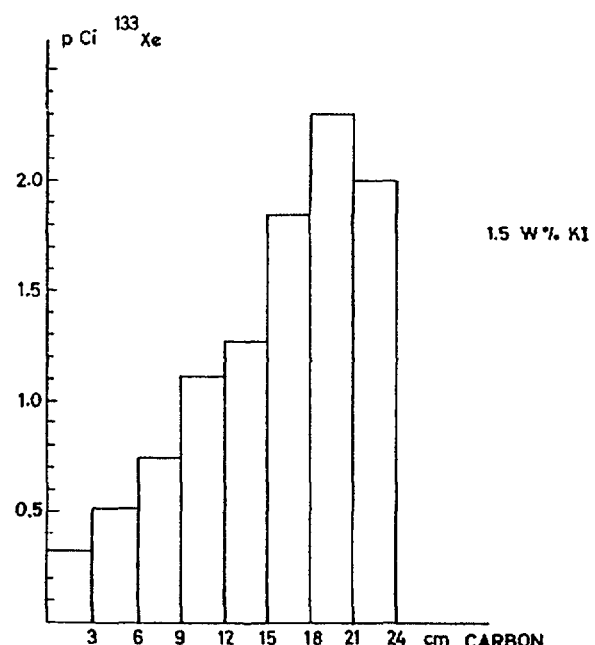


Figure 4.

Adsorption of ^{133}Xe on KI impregnated carbon.

Experiments with the impregnated fibrous carbon material

To compare adsorption of ^{131}I and ^{133}Xe on activated carbon and fibrous carbon material, fibrous carbon material was impregnated with 1.5 w% of KI. Experimental colon was 9.8 cm long divided in 14 beds 0.7 cm depth dia 5 cm. Stay time for 3 cm layer was 0.2 s, that means that the experimental conditions were the same as in experiments with impregnated activated carbon. Adsorption period was 14 days (336 h). After disconnection of colon gamma spectroscopic measurements of samples were done.

Experimental results of adsorption are presented on Fig. 5. From the Fig. 5. it can be seen that complete iodine is adsorbed after 6 beds i.e. 4.2 cm. Also, it can be assumed that molecular iodine is adsorbed on the first layer and on the other layers are adsorbed organic iodine species.

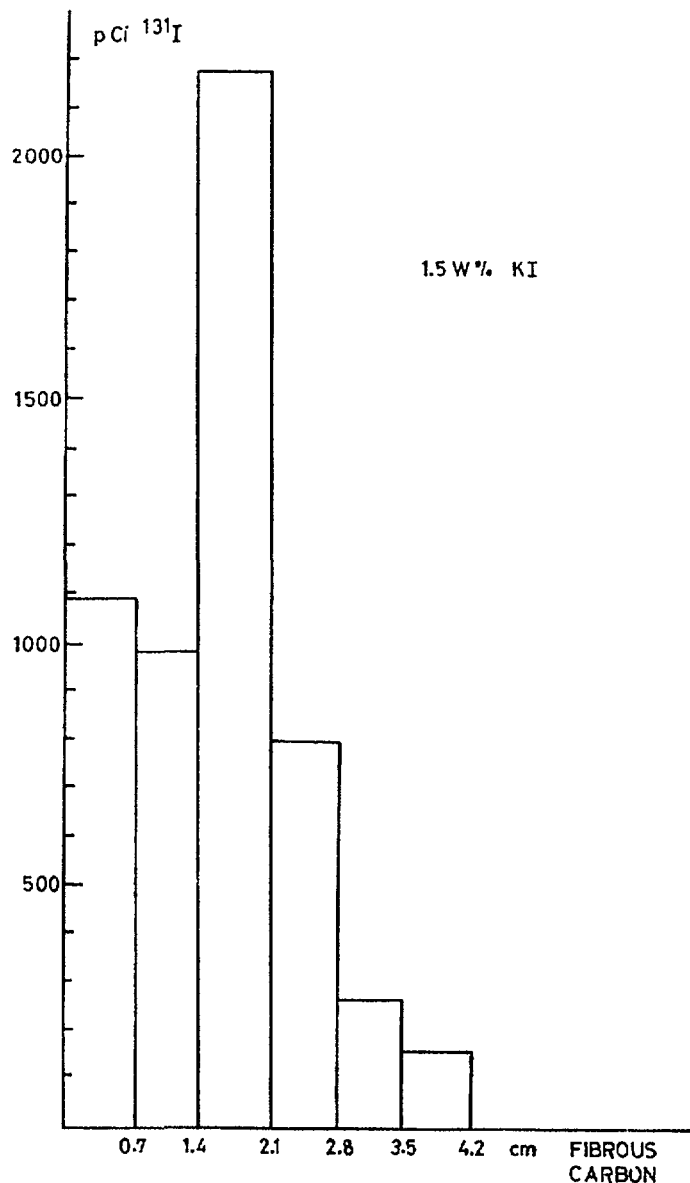


Figure 5. Adsorption of ^{131}I on KI impregnated fibrous carbon material.

Nc ^{133}Xe was detected. Having in mind these results it can be assumed that impregnated fibrous carbon material is promising for nuclear use.

Conclusion

Experimental results are summarized in Table I. From the Table I it can be seen that main percent of iodine, 92%, is adsorbed at the first 3 cm of the impregnated fibrous carbon material, while only 54.4% is adsorbed on the KI impregnated carbon, and 72.9% on TEDA impregnated carbon on the first 3 cm.

Table I. Results of adsorption of ^{131}I on various adsorbers.

Bed Depth (mm)	Retention of ^{131}I (%)
impregnated carbon 1.5 w% KI	
30	54.4
60	24.4
90	21.2
impregnated carbon 5 w% TEDA	
30	72.9
60	11.7
90	15.4
impregnated fibrous carbon material, 1.5 w% KI	
7	20.5
14	18.4
21	40.7
28	13.0
35	4.7
42	2.7

Total amount of iodine on KI impregnated carbon was 1055.5 pCi i.e. 6.2 pCi/s; on TEDA impregnated carbon total amount of iodine was 1682.9 pCi i.e. 9.2 pCi/s; while for impregnated fibrous carbon material it was 5354.9 pCi i.e. 21.9 pCi/s.

In spite of fact that the amount of iodine was 3.5 time greater in the experiments with the impregnated fibrous carbon material then in the experiments with KI impregnated carbon, and 2.2 times greater compared with TEDA impregnated carbon results are better.

INVESTIGATION OF MECHANISM OF ADSORPTION OF METHYL IODIDE AND n-HEXANE ON THE FIBROUS CARBON MATERIAL

Good results of adsorption of methyl iodide on fibrous carbon material impregnated with TEDA under normal operating conditions initiated investigation of adsorption of methyl iodide on higher temperature and relative humidity.

Chosen experimental coditions were:

- bed dept 49.8 mm, dia 50 mm,
- temperature 80°C,
- relative humidity 70 %,
- linear velocity 25 cm s⁻¹,
- feed period 2 h,
- eluation period 4 h.

Adsorption bed, of fibrous carbon material impregnated with 5 % w/w TEDA, was devided into six parts each 8.3 mm dept. Retention of methyl iodide through complete bed was 99.97 %, and of each separate part is given in Table II.

Table II. Retention of CH₃¹³¹I through the adsorption bed of fibrous carbon matherial, impregnated with 5 % w/w TEDA. Each layre 8.3 mm dept.

number of layer	1	2	3	4	5	6
retention (%)	72.44	24.33	2.10	0.58	0.42	0.10

These results together with the results of previous investigations of adsorption of methyl iodide on the fibrous carbon matherial (FCM) and fibrous carbon material impregnated with TEDA (FCM-TEDA) indicate that temperature and humidita does not influence significant, but the question is if non polar organics adsorbed on FCM and FCM-TEDA. To get better insight in the FCM and FCM-TEDA adsorption abilities of non polar organics n-hexane was chosen as a representative.

To evaluated possible competition in adsorption among methyl iodide and n-hexane on FCM and FCM-TEDA mechanism of adsorption has been investigated. These investigations were done by gas chromatographic method in the stream of dry hidrogen on the temperatures from 30°C to 75°C. Adsorbents were FCM and FCM impregnated with 5 % w/w TEDA, and adsorbates were methyl iodide and n-hexane. Complete results and details of investigation are given in

the paper: M.M.Kopečni, J.F.Čomor, M.Todorović, Lj.Vujisić and D.Lj.Vučković, Adsorption of methyl iodide and n-hexane on fibrous carbon material, (Appendix II), and here we give the conclusion.

Adsorption properties of FCM are strongly altered by the TEDA deposition on the adsorption on the adsorbent surface. Adsorption capacity is almost doubled on the modified FCM for methyl iodide adsorbate. Adsorption of n-hexane is increasing with the FCM modification, although to somewhat less extend, a fact regarded as a undesirable effect from the point of practical use of the studied adsorbents.

Adsorption isothermes obtained for the two adsorbates clearly indicated the action of the two adsorption mechanisms, i.e. adsorption on bare FCM and simultaneously on TEDA that monolayer capacity for n-hexane

cannot be evaluated. All the thermodynamics value of adsorption supports the existence of monolayer (exception is system FCM-TEDA - n-hexane). At the higher surface loading, thermodynamics parameters of adsorption approaches the values for the pure liquid adsorbate.

LIST OF PARTICIPANTS

RESEARCH CO-ORDINATION MEETINGS

Mol, Belgium (1)
24-28 September 1984

Toronto, Canada (2)
2-6 June 1986

Budapest, Hungary (3)
25-29 April 1988

Billinge, B. (3)	CEGB/CERL Cleeve Road Leatherhead, Surrey United Kingdom
Broadbent, D. (2)	Central Electricity Generating Board Scientific Services Department Wythenshawe, Manchester M23 9LL United Kingdom
Brown, A. (2) (Observer)	Nuclear Studies Ontario Hydro 757 McKay Road Pickering, Ontario, Canada
Chalupa, G. (1) (Observer)	Oesterreichisches Forschungszentrum Seibersdorf GmbH Lenaugasse 10 A-1082 Vienna, Austria
Chang, S. H. (1, 2, 3)	Dept. of Nuclear Engineering Korea Advanced Institute of Science and Technology P. O. Box 131 Cheongrayang Seoul, Republic of Korea
Deuber, H. (1)	Laboratorium für Aerosolphysik und Filtertechnik Kernforschungszentrum Karlsruhe Postfach 3640 D-7500 Karlsruhe 1 Federal Republic of Germany
Deworm, J. P. (1, 2)	Belgian Nuclear Research Centre Radiation Protection Section Boeretang 200 B-2400 Mol, Belgium
Friedrich V (1, 2, 3)	Institute of Isotopes of the Hungarian Academy of Sciences P.O. Box 77 H-1525 Budapest, Hungary

Gandhi, K. (2)	Bhabha Atomic Research Centre Waste Management Division Trombay Bombay 400 085, India
(Scientific Secretaries, IAEA)	
Gorbunov, S. (1)	Division of Nuclear Fuel Cycle
Baehr, W. (2)	International Atomic Energy Agency
Friedrich, V. (3)	P. O. Box 100 A-1400 Vienna, Austria
Kabat, M. J. (2)	Hazardous Agents Control Health and Safety Ontario Hydro 757 McKay Road Pickering, Ontario L1W 3C8, Canada
Koppány, Zs. (3)	Institute of Isotopes of the Hungarian Academy of Sciences P.O. Box 77 H. 1525 Budapest, Hungary
Patek, P.R.M. (1)	Oesterreichisches Forschungszentrum Seibersdorf GmbH Lenaugasse 10 A-1082 Vienna, Austria
Ramarathinam, K. (1, 3)	Bhabha Atomic Research Centre Waste Management Division Trombay Bombay 400 085, India
Slegers, W. (3)	Belgian Nuclear Research Centre Radiation Protection Section Boeretang 200 B-2400 Mol, Belgium
Thorgerson, D. F. (2) (Observer)	Atomic Energy of Canada Ltd. Whiteshell Nuclear Research Est. Pinawa, Manitoba ROE 1LO, Canada
Ullmann, W. (1, 2, 3)	Board of Nuclear Safety and Radiation Protection Waldowalle 117 1157 Berlin German Democratic Republic
Vujisic, L. (2, 3)	Boris Kidric Institute of Nuclear Sciences Department of Chemistry P. O. Box 522 YU-11001 Belgrade, Yugoslavia